وزارة التعليم العالي و البحث العلمي

BADJI MOKHTAR–ANNABA UNIVERSITY
UNIVERSITE BA DJI MOKHTAR-ANNABA

جامعة باجي مختار - عنابة

Faculté des sciences de l'ingénieur Année : 2009

Département de Génie Civil

T H E S E

Présentée en vue de l'obtention du diplôme de DOCTORAT Es-Science

THE USE OF FILLED STEEL STRUCTURE IN ARCHITECTURAL DESIGN AN EXPERIMENTAL AND THEORETICAL CONTRIBUTION TO THE DEVELOPMENT OF THE DESIGN OF SLAG STONE FILLED THIN WELDED COLD FORMED STEEL STUBS.

Présentée par :

Djamel BEGGAS

DIRECTEUR DE THESE : Jahid ZEGHICHE Maitre de conférence Université d'Annaba

DEVANT LE JURY

PRESIDENT : Dr. Mohamed Faouzi HABITA Professeur Université d'Annaba

EXAMINATEURS : Dr. Med Cherif ADAD M.C C.U Oum El Bouaghi
Dr. Djamel ALKAMA M.C Université de Biskra
Dr. Brahim BOUSSALM M.C Université de Constantine

To the Memory of My Beloved Father

Acknowledgements.

I would like to express my gratitude to all those who have so friendly given their assistance over the duration of this work, in particular, my supervisor Dr Jahid ZEGHICHE, for his expert, help, guidance and encouragement throughout the work, my gratitude to Dr A.J. Wilson for his help, all the team of laboratory TREFLE of the INSA Bordeaux in particular Pr J.C Batsal, and Dr R Bellouatar for his help in the experimental work at the UBMA laboratory.

Finally I wish also to thanks my wife and my daughters for their encouragement and moral support and all my family and friends.

Djamel BEGGAS

Table of Contents

Abstract

The objective of this work is to increase the understanding of how light steel structure construction should be designed to ensure that buildings using this technology can achieve optimum resistance compared to conventional system and excellent comfort conditions and, be used in an energy efficient manner.

Results of tests conducted on thin welded rectangular steel-concrete stubs are presented. The stub section was made from two U shaped cold formed steel plates welded to form box whose dimensions were: 100x70x2mm. The main parameters studied were: stub height (50-500mm), effect of the concrete infill and the weld fillet location. The tests were carried out 28 days after the date of casting the concrete infill under axial compression up to failure. A total of 28 stubs were tested, 14 were empty and 14 filled with concrete made with crushed crystallized slag aggregate. The object of the study was to investigate the failure load of composite sections and the use of crushed slag instead of conventional aggregate. From test results it was confirmed that the length of stubs had a drastic effect on the failure load and resulted from local buckling. It appeared that the location of weld fillets had only a slight effect on the failure load for empty steel stubs and was insignificant for composite stubs.

Methods of measuring and calculating thermal resistance in light steel framing are reviewed and the effect of detail design decisions on thermal performance and condensation risk are considered. The importance of air infiltration and thermal mass are also discussed, and methods of achieving good air tightness and integrating thermal mass into light steel frame construction are presented. A variety of alternative ways of avoiding thermal bridging through the steel are reviewed.

The work also reviews computer simulation design tools and identify how these can be used in the detail design of light steel framing. Thus, chapter 6 discusses the most appropriate computer simulation tools that can provide a detailed analysis of the thermal and hydroscopic performance of building envelopes using light steel framing.

These tools provide the opportunity to optimise the location and thickness of insulation and vapour control layers to avoid excessive thermal bridging and the risk of condensation. They also allow the assessment of the impact of alternative strategies for incorporating more thermal capacity into buildings. They can be used to optimise the thermal characteristics of the whole building to provide comfort, durability and energy efficient performance.

ملخـــــــص

تقدم تقنيات استعمال مواد البناء العصرية في مجال العمارة وكدا الطلب المتزايد على السكنات في الآونة الأخيرة دفع الباحثين على تكثيف الجهود من اجل ابتكار تقنيات جديدة في استعمال مواد البناء التي تستجيب لهده المتطلبات و التي يمكن حصرها في السرعة في الانجاز الصلابة إلى جانب قلت استهلاك الطاقة و خاصة بناءات غير ملوثة للبيئة آو بالأحرى بناءات تدخل في إطار التطور المستديم.

هدا البحث يخص استعمال الهياكل المعدنية الخفيفة في مجال تصميم العمارة يهدف البحث بشكل خاص إلى تقوية فهم استعمال هدا النوع من الهياكل عند المهندسين المعماريين و يتطرق إلي الموضوع من جانبين: جانب ميكانيكي بحت يخص كل ما يتعلق بالصلابة و جانب حراري أي كل ما يتعلق بأنجع الطرق المؤدية إلى تخفيض استهلاك الطاقة في العمارات المستعملة لهدا النوع من الهياكل.

البحث مقسم إلى خمسة أبواب : الباب الأول يتطرق إلى أهم الانجازات عبر التاريخ إلي الانجازات المعاصرة لهدا النوع من الهياكل.

الباب الثاني: التعريف بخبث فرن العالي المصنع الحجار للحديد و استعماله في الخرسانة يطرق كذلك إلى أهم الأبحاث المنجزة في هدا المجال.

الباب الثالث يتطرق الجانب الميكانيكي وببدء بإعطاء نبذة على أهم الأبحاث المنجزة في هدا المجال، ويليه تجارب أنجزت على ثمانية و عشرون عمود مصغر نصفها فارغ و النصف الأخر معبئ بخرسانة مصنوعة من خبث الفرن.

الباب الثالث يتطرق الجانب العزل الحراري للهياكل المعدنية الخفيفة من الناحية التجريبية و النظرية فمن الناحية التجريبية تم أجاء تجارب على عيينات من الخرسانة المصنوعة من خبث الفرن و أظهرت التجارب بان هدا استعمال هدا النوع من الخرسانة يرفع بحوالي 48 في المائة من مقاومته الحرارية. و تتطرق الدراسة النظرية إلى حساب المقومة الحرارية باستعمال طريقة العناصر المنتهية و التي في الواقع تعتمد على البرمجة، و كدا الطرف المبسطة في حساب المقاومة الحرارية.

الباب الخامس عبارة عن جملت استنتاجات عامة و كدا بعض التوصيات فيما يخص الأعمال المستقبلية.

GENERAL INTRODUCTION

INTRODUCTION

Light steel structure is being used successfully for construction especially housing in many countries. In the USA, Japan, Canada, Sweden, and Australia, increasing numbers of light steel structured houses are being built. Actually several systems are now available and significant numbers of schemes are being built. The reasons for this are the inherent quality and durability of light steel structure when compared to the alternatives, and its suitability for the design of well insulated dwellings. Concerns about the volatility of the timber market, the declining quality of structural timber, environmental issues such as sustainable forestry practices and quarrying for clay used for bricks and aggregates used in concrete blocks, have affected the use of these materials. The American Institute of Architects [1], in its Environmental Resource Guide, recommends that steel may be considered less environmentally harmful than many other alternatives because many steel products are made totally or partially from recycled scrap.

Light steel structures typically comprise of C, U and Z shaped, galvanised cold-formed steel sections, usually 0.9 mm to 3.2 mm thick that are produced by roll forming. The technology has developed from specific applications such as purling and lintels to the wider building market. Construction on site can use individual light steel components or sub frames; often prefabricated welded, bolted or riveted panels are assembled on site using self tapping screws to create whole building structures. Increasingly, there is interest in volumetric production using whole room or even whole house pods with internal finishes and services fitted in the factory.

Steel is manufactured to tight specifications and does not suffer from twisting, warping or movement due to changes in moisture content. This results in easier fixing of linings and higher quality finishes, avoiding problems such as opening up of cracks around architraves around doors due to movement. Steel components are lightweight and easy to lift and carry. Wall panels can be moved around by two men; only about 2.5 to 3 tonnes of steel is required for a typical house. There is little waste in production, fabrication or assembly and benefits can be gained from off-site prefabrication in controlled conditions in a workshop. This minimises inefficient and disruptive work on site and improves quality control. Useable roof spaces and clear span internal spaces can be easily created without the need for internal load bearing walls, allowing for future adaptability and change.

There are increasing demands for improvements in standards of construction quality, comfort and performance in building internationally. The building industries in many countries are looking for new and improved methods for construction.

Increasingly, energy efficiency issues have come much more important in the assessment of a construction system. In particular, the ability to provide the required thermal performance so that excessive heating or cooling are avoided, and comfort is maintained. Furthermore, concerns over global warming have led to an international commitment to reduce emissions of global warming gases.

Light Steel structure for buildings has become a competitive alternative to traditional building systems in over the world and in particular in Annaba (Algeria) which is known as potential steel producer. Future trends are the use of Light Steel structure in new applications. The applications are residential housing with in-situ and pre cast concrete structures, office buildings, schools and there is a big potential of further prefabrication of structural elements to hotels.

The repetition of standard elements is big. Room modules or parts of rooms can be prefabricated for export as well as domestic use. There are also great possibilities to use Light Steel structure in casual buildings.

Building systems based on cold-formed steel profiles, is gaining ground in many countries. It started in the US and the inspiration came from timber framed buildings. In the US and also in Australia and Japan light steel structure has substantial shares of the residential market. The most common systems have load-bearing walls and the floors may be of lightweight steel profiles or concrete. The load-bearing studs are lipped channels typically of thickness 1–3 mm. In the US, it is common to assemble the building on site (stick building) usually by welding. This system is used for as tall buildings as eight storeys.

The aim of the present work is to increase the understanding of how light steel structure (tube) construction should be designed to ensure that buildings using this technology can achieve excellent comfort conditions and be used in an energy efficient manner with special reference is given to cold formed steel stubs filled with slag stone concrete. This concept is totally in concordance with the sustainable development as the aim is to design light steel structure buildings which are comfortable to live in, achieve energy efficiency requirements, and result in low greenhouse gas emissions.

The thesis is divided into six chapters; **chapter one** gives a review of the steel in the architectural design with a historical background, **chapter two** provides an overview on the use of the slag in concrete, **chapter three** deals with mechanical part or resistance issue of the filled stubs results of test on twenty eight samples empty and filled tubes tested is then presented present.

Chapter four deals with experimental thermal aspect of light steel structure, method of thermal parameters measuring are presented then an experimental programme of measuring the thermal proprieties of slag stone samples is presented with discussion and conclusion.

Chapter five deals with the theoretical Thermal aspect of light steel structure, simplified methods for the calculation of the thermal resistance are presented, comparison then conclusion, this chapter provides also some design envelope consideration as thermal capacitance and condensation issue.

Chapter six is a general conclusion followed by recommendations for further work.

CHAPTER 1.
REVIEW OF THE USE OF STEEL IN THE ARCHITECTURAL DESIGN.

The Metal in Architecture

1.1 History background

The symbiosis between metal and architecture has evolved over centuries, with successive areas opening up new technical and aesthetic possibilities through the development of different types of metals.

The use of metals is as old as human civilization. Our ancestors knew of just seven metals: gold, silver, copper, iron, tin, lead and mercury. Historically, metals occupied the mysterious realm of alchemy, with its mixtures and secret formulations, and were little understood by those who worked with them. A century ago, aluminium was considered more precious than gold or silver (Napoleon treated his most favoured dinner guests to aluminium cutlery), and the notion that metals could resist nature (for instance, as stainless steel does) was considered fanciful speculation. Yet each era has brought about the discovery of new types of metal, chiefly through the process of alloying (which has its roots in alchemy), whereby a new material is formed from the combination of various constituents. The Ancients experimented with alloys, mixing copper and tin to produce a new metal, bronze, with a lower melting temperature and improved casting properties. (Zinc was also added to copper to produce brass, a gold-like material which could fool the unsuspecting until it eventually and inevitably became tarnished.)

The Romans were the first to use metal as a major building material. The Pantheon had a bronze roof, parts of which survived until the middle of this century; Hagia Sophia originally had a lead roof that lasted 1400 years. Because of their malleability and relative ease of working, copper and lead became synonymous with the complexities of Gothic architecture. Endowed with the rich green patina of age, weathered copper spires and roofs still enliven the skylines of northern European cities. Improved techniques of pre-patination can now bestow an instant, uniform illusion of maturity; Jean Nouvel's new cultural centre in Lucerne is crowned by a vast, overhanging roof clad in sheets of prepatinated copper. Sheltering a new urban square in its oversailing embrace, the emerald green structure forms a powerful horizontal datum in the lakeside landscape.

Fig 1.1 Hagia Sophia (532-537 AD during the **Emperor Justinian I**

(Designed by Anthemios of Tralles and Isidoros from Miletos)

But it is iron and steel that has had the most radical influence on architecture. The skeletal structural frame effectively liberated buildings from the inhibitions of the load bearing wall and tabulated construction. Cast iron, the great material of the Industrial Revolution, revolutionized Georgian and Victorian buildings. Ideally suited to repetition and standardization, the metal's ubiquity defined the British Empire; cast iron bandstands, ornamental gates, fountains, and entire prefabricated buildings (Victorian 'tin tabernacles') were simply plucked from manufacturers' pattern books and energetically exported around the Imperial world, from Durban to Bombay.

FIG 1.2 Crystal Palace built in Hyde Park by sir Joseph Paxton for Exposition the universal Exposition, held in London on 1851. Destroyed by fire on 1936.

In 1851, Paxton's Crystal Palace marked a defining moment in the history of metal and architecture. Employing 3300 columns and 2220 girders prefabricated from molded cast iron, it set the tone for iron buildings for the next 50 years. In Europe, seminal buildings such as Labrouste's Bibiliotheque de Saint-Genevieve pioneered the use of cast iron internally in Gothicized barrel vaults of prefabricated sections. Yet the metal's associations with mass production and popular taste provoked ambivalence and even abhorrence among the architectural establishment. Frantz Jourdain wrote 'The Institut treated iron with a pious terror that might have been appropriate for a shameful disease'. Ruskin also loathed it - 'No ornaments are so cold, clumsy and vulgar, so essentially incapable of a fine line or shadow as those of cast iron.

The evolution of iron and steel frames made it possible to build upwards; the heroic scale of American cities was determined by steel-framed skyscrapers. The development of stainless steel at the turn of the century provided an environmentally stable metal that could sustain a polished, lustrous appearance. The Chrysler Building in New York was one of the first buildings to use stainless steel externally, on its sleek, hypodermic pinnacle roof.

Fig 1.3; Chrysler Building Designed by Willian Van Allen and opened on *27th May 1930.*

After the war, the transfer of technology from military and aeronautical industries generated new metal forms. Reductionist structures composed of steel channels, angles, I-beams and H-columns were tautly elegant expressions of a new minimalist aesthetic. Jean Prouve's refinement of industrial detailing and use of lightweight sheet metal have been exhaustively explored by the recent generation of High-Tech architects.

Fig 1.4 ING-House, Amsterdam High-Tech , the Netherlands Architect(s) : Meyer en van Schooten Architecten BV, Amsterdam Engineer(s) : Aronsohn Raadgevende Ingenieurs bv, Rotterdam

Unlike other building materials, metals yield to the entropic nature of the environment, but can be recovered and reformed. This capacity for recycling gives them some tentative credentials to sustainability. Aluminium, for instance, is very expensive to refine, in terms of energy used to extract the metal from its abundant ore (and the ravaging of the earth's

surface to obtain the bauxite in the first place), but can be usefully recycled at a fraction of the original cost. Metal recovered from scrap accounts for around a third of the world's aluminium supply and should play a greater role in future production. Around 75 per cent of copper used in buildings comes from recycled sources. Steel too is becoming greener, with potential for re-use as a structural material. It can be recycled many times, without any loss of its structural strength and although a mass market for used steel has not yet emerged, architects have a potentially influential part to play in selecting and specifying used material if available.

New appropriations of metal continue to evolve. A few decades ago, titanium was considered to be a weak and brittle material only fit for creating pigments in paints. Yet roiled into very thin sheets, its light weight and resistance to corrosion makes it an excellent cladding and roofing material.

Fig1.5 The new Guggenheim Museum in Bilbao by Frank Gehry (AR December 1997)

The new Guggenheim Museum in Bilbao by Frank Gehry (AR December 1997) is clad in an extraordinary shimmering skin of very thin titanium scales. Sophisticated CATIA software, developed by the French aerospace industry, was used to rationalize the metal surfaces of the building established by manual mock-ups, so that even with such complex

surfaces, only four standard panel sizes were needed for 80 per cent of the vast surface area. Gehry's imaginative exploitation of the potential of metal generates new paradigms based on the capabilities of electronics rather than mechanics (although ironically the construction of Bilbao relied on the manual metal-bashing skills of workers schooled in the region's traditional shipbuilding industries) and takes its place in architecture's long history of metal alchemy and invention.

FIG 1.6 SWISS RE HEADQUARTERS BUILDING, LONDON - UK - 1997-2004

Owner(s) : Swiss Re Investments Ltd, London Architect(s) : Foster and Partners, London
Engineer(s) : Ove Arup & Partners, London

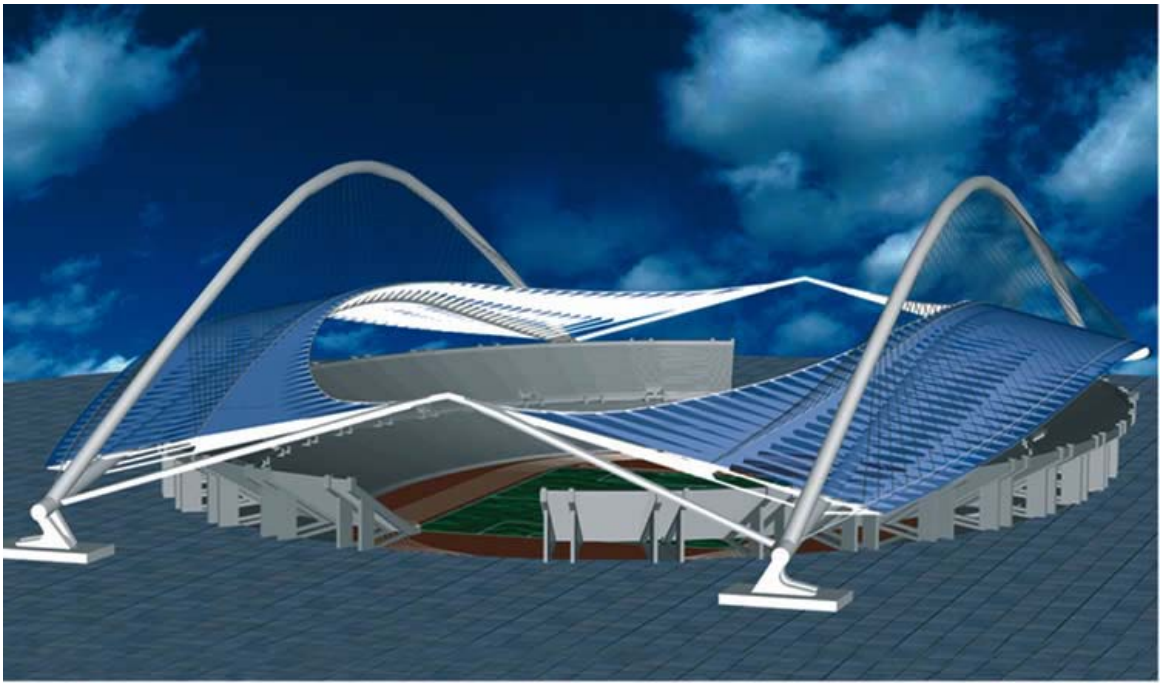

FIG 1.7 OLYMPIC STADIUM "OAKA", ATHENS - GREECE (JUNE 2004)

FIG 1.8 CARGOLIFTER HANGAR, BRAND, GERMANY – 2001 Arch.: SIAT Architektur & Technik; - Eng.: Arup GmbH

CHAPTER 2

SLAG STONE FOR THE FABRICATION OF THE FILLED CONCRETE

2.1 Introduction

Concrete is one of the major construction materials being used worldwide. Aggregate, besides cement and water, forms one of the main constituent materials of concrete since it occupies nearly 55%–80% of concrete volume. The aggregate types utilized are either coarse aggregates (with particle size more than 4.75 mm) or fine aggregates (with particle size less than 4.75 mm). Aggregates which are used in concrete are obtained either from natural sources or by crushing large size rocks. Coarse aggregates are bound with cement paste during the hydration process to form cement concrete whereas fine aggregates are utilized to fill the gaps between the coarse aggregate particles. The rapid increase in the natural aggregates consumption every year due to the increase in the construction industry worldwide means that the aggregate reserves are being depleted rapidly,. It has been reported that,
without proper alternative aggregates being utilized in the near future, the concrete industry globally will consume 8–12 billion tons annually of natural aggregates after the year 2010 [5]. Such large consumption of natural aggregates will cause destruction of the environment. Therefore there is an urgent need to find and supply alternative substitutes for natural aggregates by exploring the possibility of utilization of industrial by-products and waste materials in making concrete. This will lead to sustainable concrete design and greener environment.

Slags are by-products of the metallurgical industry and consist mainly of lime and calcium–magnesium aluminosilicates. The most common slags produced are from the iron and steel industry, called blast-furnace slag [5], which is defined as the glassy granular material formed when molten blast-furnace slag is rapidly chilled as by immersion in water [23–10]. Fast cooling results in minimum crystallisation and converts the molten slag into fine aggregate sized particles (smaller than 4 mm), composed of predominantly no crystalline material [23].
Due to its high content of silica and alumina in an amorphous state, ground blast-furnace slag shows pozzolanic and binding properties in an alkaline medium [23]. Blast-furnace slag has been widely utilized as an ingredient in cement or concrete [52].

2.2 The Blast-furnace slag of Annaba.

Steel slag is a by-product making up a portion of 15–20% of iron output in an integrated steel mill. Most of them are deposited in slag storing yards and thus results in many serious environment problems in Annaba. Few researches explored the feasibility of utilizing steel slag as aggregates in stone concrete.

The blast furnace slag at the beginning of its development on an industrial level was considered as an industrial waste to be stored in heaps. This has also happened in the 1970s, the year of the beginning of the steel complex of El HADJAR, not by ignorance but by lack of opportunities.

Since the 1980s, despite the large annual fluctuations (Table 1) of El Hadjar slag, this by-product is partially recovered in cement (for granulated slag obtained by a sudden cooling by quenching in water) and in some road foundations works.

Generally two types of industrial waste are generated by the steel complex of EL HADJAR:

- Waste not suitable and that are land filled.
- Recoverable waste, known as – by-products such as slag.

The main steel wastes are blast furnace slag. According to the method of cooling two types of slag can be obtained: granulated and crystallized. The production capacity of crystalline and granulated slag from EL HADJAR blast furnaces is about 600 000 tonnes per year with an average of 430 000 tons of granulated slag and 170 000 tonnes of slag crystallized.

The production of the Granulated slag is not automatic but it should be scheduled according to the demand in granulated slag. This restriction is due to water shortages, Algeria having experienced a severe drought during the past ten years.

Fig 2.1 The granulated and crystallized slag production by the blast furnaces of EL HADJAR (Ref [44]).

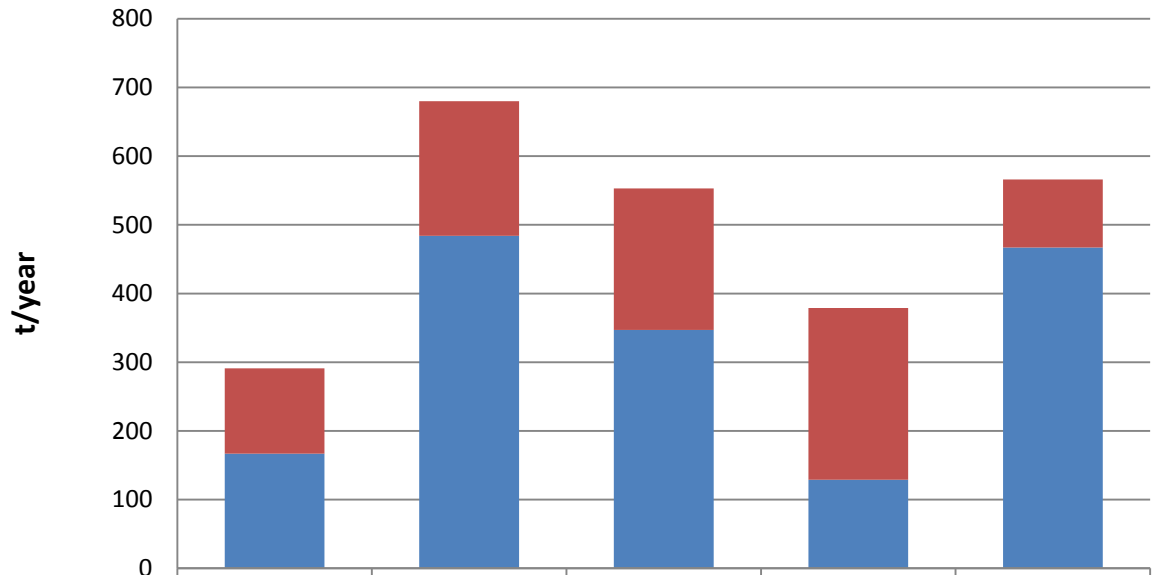

	1987	1988	1989	1995	2002
Crystallized	124	196	206	250	99
Granulated	167	484	347	129	467

-

The production of granulated slag from the steel complex of El HADJAR has experienced three periods:

- The first production period (the 1970s): the production of granulated and crystallized slag was not used but stored in landfills which led to the formation of two heaps, now unused because of their solidification.
- The second period in the 1980s: attempts at industrial level were carried out for the use of slag in the construction of roads foundations and cement, however, only small quantities from the product were used which does absorb all the production.
- The third period (the current): if the use of slag for the construction of road foundation was significantly reduced for economic recession reasons, its employment in cement is always constant, around 20% in addition to clinker (Table 2), leading to a greater production of granulated then crystallized slag, especially in 2002 (Table 1).

The first uses of slag in civil engineering concern three areas:

2.2.1 Realisation of roads foundations:

The good results obtained from the tests carried out on sections of national roads (RN 44 and RN 16) in the 1970s, using granulated slag from the first blast furnace in the form of aggregate - and sand slag - have led to the realisation of the expressway East – West section (Annaba - Tlemcen), connecting the cities of Annaba and Berrahal, with a mixture of ground granulated slag, lime and cement.

The steel complex was then recovered with a production of slag that could not be used, especially after the entry into production of the second blast furnace.

Indeed, the cement of the East, including HAMMA BOUZIANE and especially HADJR Essoud could not absorb all the potential production of granulated slag from blast furnaces EL HADJAR as only (15%) was used in cement.

2.2.2 Cement compound (CPJ)

Since the beginning of the century, VICAT [44] had discovered the power and hydraulic slag and thought to use it to make cement. As soon as the wet form exists, the German steel industry developed its own manufacturing of hydraulic binders made of a mixture of lime and ground granulated slag in accordance with the discovery of LANGEN [44].

PRUSSING [6] from 1882 introduced the granulated slag in cement, the slag is mixed with clinker in proportion varying from 5 to 90 (%), giving the range of today standard slag cement.

• It was only in 1890 that produced the first slag cements in France. In Algeria, the use of slag in cement is very recent and dates back to the 1980s, when was produced the cement type CPJ resulting from a simultaneous mixture of clinker (70 to 80)%, granulated slag (15 to 25%) and natural gypsum (5%) [44].

• The real integration of EL HADJAR granulated slag in the manufacture of cement has been made for the first time in 1982 by the cement manufactory HADJR SOUD after satisfactory laboratory tests validated later by another study [44], followed by tests on an industrial scale. However, the ratio adopted which was 15%, fails to absorb the granulated slag production and even less the stored slag. Today the amount of slag stored inside the steel complex is estimated to 2 million tonnes.

The integration of granulated slag in the cement has been a problem for cement because its water content is too high, an average of 14%, which requires its drying. The cement manufactory of HADJR SOUD has a special dryer to dry the granulated slag. The % of granulated slag in cement type CPJ fluctuates between 15 and 25% depending on the quality of the clinker product.

Table 2 shows the dosages of granulated slag used by the cement plant HADJR WELDING from 1994 to 2002 [6].

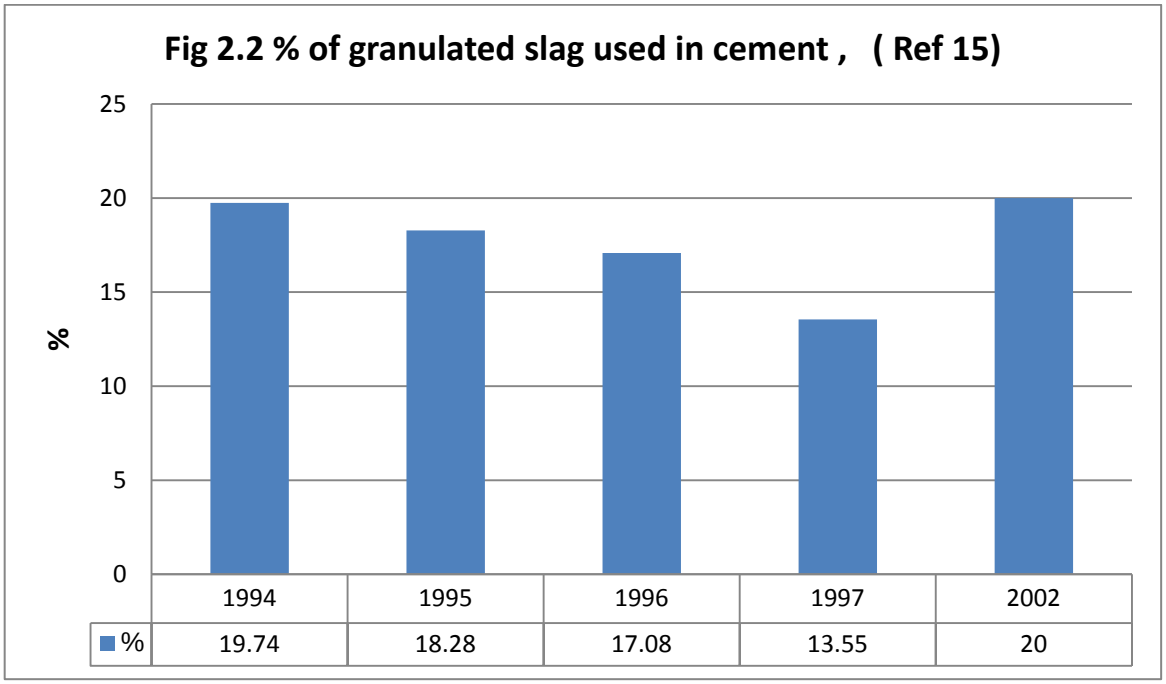

2.2.3 Aggregates for concrete:

• The granulated slag can act also as a constituent in the composition of hydraulic concrete. It can be used in conventional concrete sand as active part; either unprocessed or as pre crushed slag.

• The incorporation of granulated slag in classical concrete as natural aggregates, replacing all or part of the sand, contribute to an increase of the strength (at constant cement mix). The mixing and implementing cause attrition fines hydraulic whose action has be combined with that of the binding cement paste - granulated slag sand (both products are hydraulic and have a mutual affinity). For against, the rheology of mixtures can be affected, the concrete becomes rough and loses its handling, dosing water constant.

The use of slag granulated or crystallized EL HADJAR as aggregate in concrete has remained at an experimental stage, As part of our study, the use of slag in the fabrication of the filled concrete, we have structured this chapter in two parts:

The first part will be devoted to methods of processing and treatment of slag the second part will deal with slag crystallized, its characteristics and its use in concrete.

2.3 PROCESSING AND TREATMENT OF SLAG

2.3.1 Introduction:

Slags are by-products of the metallurgical industry and consist mainly of lime and calcium–magnesium aluminosilicates. The most common slags produced are from the iron and steel industry, called blast-furnace slag [5], which is defined as the glassy granular material formed when molten blast-furnace slag is rapidly chilled as by immersion in water [23–10]. Fast cooling results in minimum crystallisation and converts the molten slag into fine aggregate sized particles (smaller than 4 mm), composed of predominantly noncrystalline material [23].

Due to its high content of silica and alumina in an amorphous state, ground blast-furnace slag shows pozzolanic and binding properties in an alkaline medium [23]. Blast-furnace slag has been widely utilized as an ingredient in cement or concrete [52].

2.3.2 SLAG TREATMENT

Depending on the product and especially the structure we wish to obtain from the molten slag is used the corresponding cooling method.

. Granulated slag

Granulation was originally used as a means of fragmentation of slag to facilitate handling. It was done very simply by pouring the liquid jet of slag into a basin filled with water]. It later becoming latent hydraulic properties of granulated slag thus obtained.

Crystallized slag

A slow cooling leads to crystallization of slag. This gives a solid material in the form of large aggregates after crushing and classification by granular fractions. It can be used as an aggregate for road construction and a concrete aggregate component.

Use of crystallized slag

Crystallized crushed, slag can be used as gravel with natural sand rolled in a binary mixed concrete yields a slag concrete. In addition, when the sand used in concrete is a granulated milk (raw or pre-ground), we talk about any concrete slag.

2.4 THE USE OF SLAG IN CONCRETE

The use of slag in its two forms granulated and crystallized as aggregate in concrete is uncommon in the world. Few studies have been made and little work has been devoted, for several reasons:

- Most of the production is granulated for use in cement.
- Crystallized slag is used exclusively in road foundations.
- Ignorance of crystallized slag as aggregate.

According to M.Behim [6-44] The use of crystallized slag in concrete, still at the experimental stage in laboratories, only few result has been in papers and seminaries. Its low price and availability are factors should encourage manufacturers to focus on its integration into the composition of concrete.

It is well known that the granulated slag is a hydraulic; it can be used in its gross assets as sand in the composition of hydraulic concrete. Also crystallized slag aggregate is available that can be used as aggregates in concrete which is then called slag stone concrete SSC.

The most recent experimental tests made on the performance of slag stone concrete were made by Mr. Behim [44]

In this studies a series of test were carried out to estimate the compressive strength, splitting tensile and gas permeability of SSC, and then compared with results test obtained from an ordinary aggregate concrete.

Only strength results are presented in this section.

For the purpose of this test four samples were prepared two ordinary; aggregate concrete and SSC, then part of the natural sand which is too fine (fineness modulus = 1.54) in the first mix was substituted by granulated slag sand more larger (fineness modulus = 2.85) to give an improved concrete aggregate, and in SSC some of the granulated slag sand has been replaced by natural sand this mixture of the two types of sand allowed the correction of the sand fineness.

Ordinary aggregate concrete: natural sand + ordinary gravel

Improved aggregate concrete: natural sand + granulated slag + ordinary gravel

Slag Stone Concrete: granulated slag **+** Crystallized slag

Improved Slag Stone Concrete: natural sand **+** granulated slag **+** Crystallized slag

For each mix, six samples were tested:
Four in simple compression and two in tensile splitting.

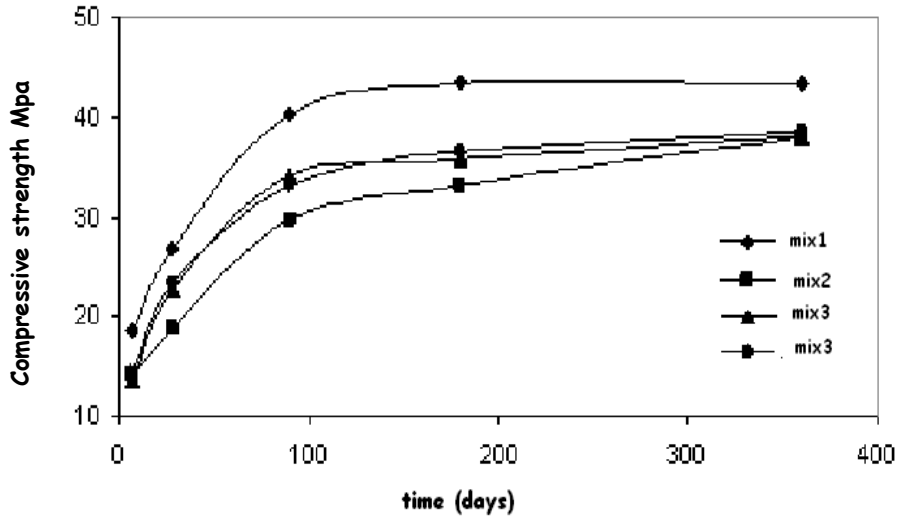

Fig 2.3. Evolution of the Compressive strength

2.4.1. Compressive strength

The evolution the Compressive strength in the time of the four concretes is presented in Figure 4. A first exploitation of the results shows kinetic hardening slightly different between the slag concrete (mix1, mix3 and mix4) in relation to concrete mix1. However the evolution of the compressive strength of slag increases with time. Rather than concrete mix1 tends to be stable from 180 days.

2.4.2. Tensile strength by splitting

The behaviour of tensile strength of concrete by splitting slag is different from their behaviour in compression. The increase of tensile strength of concrete by splitting mix2, mix3 and mix4 is faster than that of concrete mix1 (Figure 5). The mix3 concrete and mix4 composed predominantly by slag (granulated and crushed) give the best tensile strength by splitting to 360 days. This behaviour shows the positive influence of the nature of the aggregates on aggregate links - cementations matrix that determine the tensile strength in general. The slopes of the curves clearly show hardening speeds stronger mix 2, mix3 and mix4 concrete compared to that of mix1 concrete.

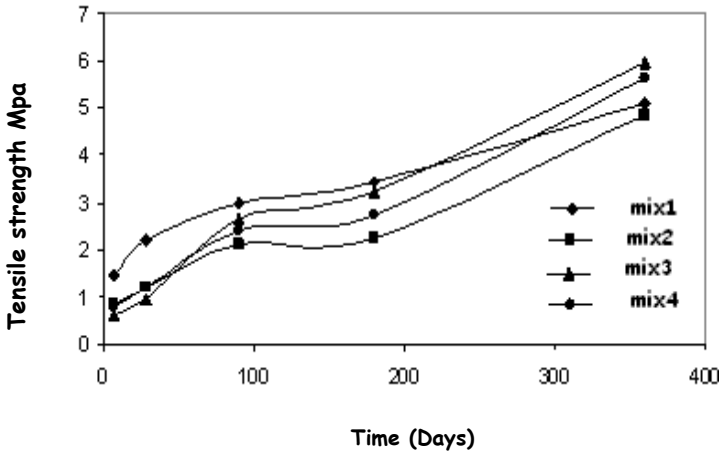

Fig 2.4 Evolution of the Tensile Strength

2.5 CONCLUSION

The substitution of a portion of natural sand by sand granulated slag in mix2 concrete, contribute not only to fix the module to a finesse value of 2.5 corresponds to a medium sand, but also to improve some characteristics of concrete, including the tensile strength by splitting that takes full scale long term.

The substitution of natural aggregates (sand and gravel) by the aggregate slag (granulated and crushed) in mix 4 and mix4 concrete is even more interesting because the results are better than those obtained with concrete BII. Presumably crushed slag aggregate strengthens links - cementations matrix, which resulted in a marked increase in tensile strength by splitting in mix3 and mix1concrete.

The use of slag as a cement component or concrete aggregate contribute not only to the environmental aspect but the test showed that we can obtain a most cheaper construction material with better resistance.

CHAPTER 3

CONCRETE-FILLED STEEL TUBE, RESISTANCE ISSUE

3 CONCRETE-FILLED STEEL TUBE, RESISTANCE ISSUE

3.1 INTRODUCTION:

Interest on the use of Composite construction in steel and concrete has increased dramatically in recent years, composite structure stands for elements using more than one materials such as steel and concrete this combaination is currently used in the concrete-filled steel tube structure and has many advantages manely resistance (strenght) , fire resistance, and economy.

There are three types of Composite colums fig 2.1, 2.2 and 2.3

- PartiallyConcrete encased clumuns
- Totaly Concrete encased clumuns
- Concrete filled tubular colums

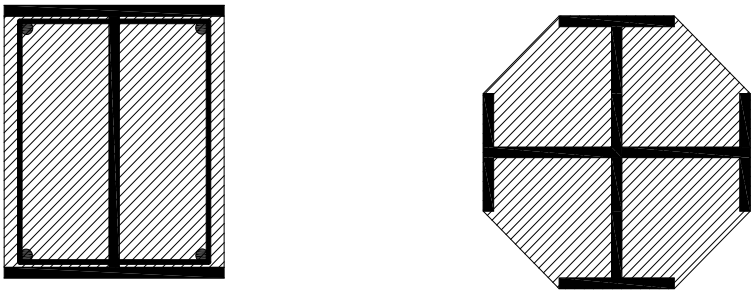

Fig. 2.1 Partially concrete encased columns

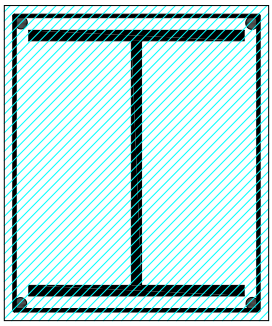

Fig. 2.2 Totally concrete encased columns

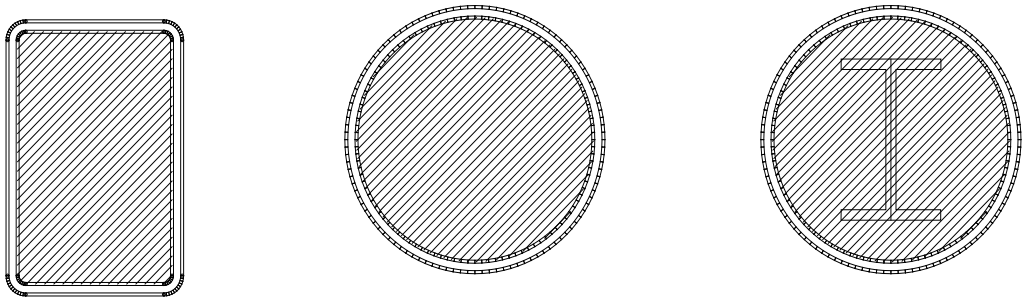

Fig. 2.3 Filled Concrete Columns

Concrete-filled steel tube structural members have a number of distinct advantages over comparable steel, reinforced concrete, or steel-reinforced concrete members [35]. The steel lies at the outer perimeter, where it performs effectively in resisting flexure as well as axial tension and compression, while the concrete forms an excellent core to help withstand compressive loading.

Composite concrete-filled steel tubes (CFTs) have been used increasingly as columns and beam–columns in braced and unbraced frame structures. Their use worldwide has

ranged from compression members in low-rise, open-floor plan construction, using cold-formed steel circular or rectangular tubes filled with precast or cast-in-situ concrete, to large diameter cast-in-situ members used as the primary lateral resistance columns in multi-story braced and unbraced frames.

Concrete filled steel box columns, fabricated from welded steel plates, and concrete-filled steel fabricated circular pipes have been used in some of the world's tallest structures. In addition, concrete-filled steel box columns are commonly used as bridge piers concrete, or steel-reinforced concrete members. Steel members have the advantages of high tensile strength and ductility, while concrete members have the advantages of high compressive strength and stiffness. Composite members combine steel and concrete, resulting in a member that has the beneficial qualities of both materials. The steel tube serves as a form for casting the concrete, which reduces construction cost. No other reinforcement is needed since the tube acts as longitudinal and lateral reinforcement for the concrete core. In addition, the placement of longitudinal steel at the perimeter of the section is the most efficient use of the material since it provides the highest contribution of the steel to the section moment of inertia and flexural capacity. The continuous confinement provided to the concrete core by the steel tube enhances the core's strength and ductility. The concrete core delays local buckling of the steel tube by preventing inward buckling, while the steel tube prevents the concrete from spalling.

3.2 Light steel structure Building

Building systems based on cold-formed steel profiles, gypsum plasterboard and mineral wool is gaining ground in many countries. It started in the US and the inspirationcame from timber framed buildings. In the US and also in Australia and Japan light steel framing has substantial shares of the residential market. The most common systems have load-bearing walls and the floors may be of lightweight steel profiles or concrete. The load-bearing studs are lipped channels typically of thickness 1–3 mm. In the US, it is common to assemble the building on site (stick building) usually by welding. This system is used for as tall buildings as eight storeys.

In Europe, similar systems have been developed but they are usually not used for as high buildings as in the US.

In Sweden and Finland, the energy prices are much higher than in the US and the climate is quite cold. This means that energy conservation is an important concern. In order to reduce the cold bridge created by the steel, thermally efficient studs with slotted webs have been developed.

This kind of studs can be used in curtain walls and also in load-bearing walls up to three or four storeys. The slotting of the web reduced the resistance of the stud especially for shear. Design methods for slotted studs have been developed but they are not yet codified.

3.3 Recent research and developments on Composite concrete-filled steel tubes:

Composite structure have been used widely as they speed up construction by eliminating formwork and have high load carrying capacity[1] and the use of thin steel wall thickness is more economic.

Experimental research on concrete filled tubular metallic columns has been ongoing throughout the world for many years, with significant contributions having been made particularly by researchers in the past few years.

- 1969 Neogi et al. [48] investigated numerically the elasto-plastic behaviour of concrete filled tubular metallic columns pinned at both ends, loaded either axially or with some eccentricity about one axis. Complete interaction between the steel and concrete was assumed so triaxial and biaxial effects were not considered. To compare the experimental results with the numerical solution eighteen eccentric loaded columns were taken. They found good agreement between the experimental and theoretical behaviour of columns with L/D ratios greater than 15. Moreover they also inferred that triaxial effects were small for such columns, whereas for columns with smaller L/D ratios there was a gain in strength due to the triaxial effect.

- 2000, A series of tests were carried out by O'Shea and Bridge [50] to study the behaviour of circular thin-walled concrete filledsteel tubes having D/t ratio ranging between 55 and 200. These tests were conducted on bare steel tubes, tubes with unbounded concrete with only the steel section loaded, tubes with concrete infill with the steel and concrete loaded simultaneously and tubes with concrete infill loaded alone. The obtained load carrying strengths were compared with the strengths calculated using the design standards and specifications. The results showed that the concrete infill for the thin-walled circular steeltubes has little effect on the local buckling strength of the steel tubes.

- 1996, O'Shea and Bridge [51] also tried to estimate the strengthof CFTs under different loading conditions. The loading conditions examined include axial loading of the steel only, axial loading of the concrete only, and simultaneous loading of the concrete and steel both axially and at small eccentricities.All the tested specimens were short with a L/D ratio of 3.5 and D/t ratio between 60 and 220. The used concrete had a compressive strength of 50, 80 and 120 MPa. From these experiments, O'Shea and Bridge concluded that the degree of confinement offered by a thin-walled circular steel tube to the internal concrete is dependent upon the loading condition. The confinement effect was highest when only the concrete was loaded axially and the thin-walled steel was used as pure circumferential restraint. They also concluded that Eurocode 4 can be used for the design of thin-walled steel tubes filled withvery-high-strength concrete if care is taken in the formulation of the design equations.

- 1997, Kilpatrick et al. [21,22] also examined the applicability of Eurocode 4 for the design of CFTs which use high strength concrete and compared 146 columns from six different investigations with Eurocode 4. The concrete strength of the columns ranged from 23 to 103 MPa. The mean ratio of measured/predicted column strength was 1.10 with a standard deviation of 0.13. The Eurocode safely predicted the failure load in 73% of the columns analysed.

- 1998, Brauns [4] declared that the confinement effect exists at high stress level and when structural steel acts in tension and concrete in compression and that the ultimate limit state of material strength was not attained for all parts simultaneously.

In his study of the constitutive relationships for material components, the stress state in composite columns was determined by considering the dependence of the modulus of elasticity and Poisson's ratio on the stress level in concrete.

- 2004, recently the behaviour of circular concrete-filled steel tubes (CFT) with various concrete strengths under axial load was also presented by Georgios Giakoumelis and Dennis Lam [17]. In their study they examined the effects of steel tube thickness, the bond strength between the concrete and the steel tube, and the confinement of concrete. Measured column strengths were compared with the results predicted using Eurocode 4, Australian standards and American codes. All three codes predicted lower values than that measured during the experiments. Eurocode 4 gave the best estimation for both CFT with normal and high-strength concrete. They also found that the effect of concrete shrinkage was critical for highstrength concrete and negligible for normal strength concrete.

- Very few experiments have been performed on cold formed welded steel sections filled with concrete or recycled materials such as slag stone concrete (SSC). The latter has been tested by J. zeghiche [34--39] under direct compression and was used as a filling material to overcome the undesired effects of imperfections in built up cold formed sections. The gain in strength was found to reach a value of up to 2 and decreased linearly with the tube height[6-7].

- Results from an experimental program conducted by V.K.R.Kodur [56] on the behaviour of high strength concrete-filled steel hollow structural section (HSS) columns were presented for three types of concrete filling. A comparison was made of the fire-resistance performance of HSS columns filled with normal strength concrete, high strength concrete, and steel fibre-reinforced high strength concrete. The various factors that influence the structural behaviour of high strength concrete-filled HSS columns under fire conditions were also discussed. It was demonstrated that, in many cases, addition of steel fibres into high strength concrete improves the fire resistance and offers an economical solution for fire-safe construction

- A theoretical study of the local and post-local buckling of thin-walled circular steel tubes that contain a rigid infill was presented M.A. Bradford, and al [43]. This generic approach was calibrated against test data, and a cross-section slenderness limit was proposed that delineates between a fully effective cross-section and a slender cross section. A simple prescriptive equation was proposed for the buckling strength of the steel cross section that is consistent with many design codes, and illustrates that the presence of an infill may enhance the cross-sectional strength, not only by the added strength of the infill itself, but by delaying the buckling of the steel tube. An experimental and theoretical[10] treatment of coupled local and global buckling of concrete filled steel columns was presented. The work was concluded with comparisons of design recommendations for the strength evaluation of slender composite columns with thin-walled steel sections.

- Results of tests conducted on 27 concrete-filled steel tubular columns were reported by Brauns J [4]. The test parameters were the column slenderness, the load eccentricity covering axially and eccentrically loaded columns with single or double curvature bending and the compressive strength of the concrete core. The test results demonstrate the influence of these parameters on the strength and behaviour of concrete-filled steel tubular columns. A comparison of experimental failure loads with the predicted failure loads in accordance with the method described in Eurocode 4 Part 1.1 showed good agreement for axially and eccentrically loaded columns with single curvature bending whereas for columns with double curvature bending the Eurocode loads were higher and on the unsafe side. More tests were reported to be needed for the case of double curvature bending.

- Thirty-six specimens, including 30 stiffened stub columns and six unstiffened ones, were tested by Zhong Taoa [63] and al, to investigate the improvement of ductile behaviour of stiffened composite stub columns. The parameters investigated were stiffener height, stiffener number on each tube face, using saw-shaped stiffeners, welding binding or anchor bars on stiffeners, and adding steel fibres to concrete. It has been found that adding steel fibres to concrete is the most effective method in enhancing the ductility, while the construction cost and difficulty is not significantly increased.

- The behaviour of self-consolidating concrete (SCC) filled hollow structural steel (HSS) stub columns subjected to an axial load was investigated experimentally by Lin-Hai Hana and al, [25]. A total of 50 specimens were tested. A mathematical model was developed and a unified theory was described whereby a confinement factor was introduced to describe the composite action of the steel tube and the concrete infill. The predicted load versus deformation relationship was in good agreement with the test results. The theoretical model was used to investigate the influence of important parameters that determine the ultimate strength of the composite columns. The parametric and experimental studies provided information for the development of formulae for the calculation of the ultimate strength and the axial load versus axial strain curves of the composite columns. Comparisons were made with predicted stub column strengths using the existing codes.
- An experimental study on the behaviour of short concrete filled steel tubular columns (CFT) axially loaded in compression to failure was presented by Muhammad Naseem Baig and al, [46]. A total of 28 specimens (16 filled with concrete and 12 hollow) with different cross-sections were tested to investigate the load capacity. The length-to-diameter ratios of these columns were between 4 and 9. Parameters for the tests were tube shape and diameter-to-thickness ratio. Some of the concrete filled columns had internal bracing of #3 deformed bars. The test results are compared with the theoretical results and previous studies. The results showed that the confinement effect on concrete does play a role in increasing the compressive strengths, in some cases by almost 60%. Based on the test results, an equation to estimate the ultimate axial compressive loading capacities was also proposed for square CFT columns.

- A series of tests were performed by M. Mouli, H. Khelafi [47] to consider the behaviour of short composite columns under axial compressive loading, two rectangular hollow steel sections (RHS) were used in these tests, (120 × 80 × 5 mm and 150 × 100 × 5 mm). The sections were filled with normal and lightweight concrete with natural pouzzolan as the lightweight aggregate. The main objectives of these tests were to clarify the performance of the lightweight aggregate-concrete filled steel specimens compared with those manufactured from normal concrete. The experimental investigations included tests on short steel and short composite columns.

The experimental failure load was seen to be adversely affected when the height of the specimen was increased from 100 to 200mm. The results of this investigation showed that the contribution of lightweight aggregate concrete to the failure load was important.

- Thirty specimens., including 24 recycled aggregate concrete filled steel tubular (RACFST) columns and 6 normal concrete filled steel tubular (CFST) columns, were tested by Zhong Taoa and al, [63] to investigate the influence of variations in the tube shape, (circular or square), concrete type, (normal and recycled aggregate concrete) and load eccentricity ratio, (0 to 0.53) on the performance of such composite columns. The test results showed that both types of filled columns failed due to overall buckling. Comparisons were made with predicted ultimate strengths of RACFST columns using the existing codes. The theoretical model for normal CFST columns was used in this investigation for RACFST columns. The predicted load versus deformation relationships were in good agreement with test results.

- P.K. Gupta and al 2006 [65] conducted an experimental and computational study on the behaviour of circular concentrically loaded concrete filled steel tube columns till failure. Eighty-one specimens were tested to investigate the effect of diameter and D/t ratio of a steel tube on the load carrying capacity of the concrete filled tubular columns. The effect of the grade of concrete and volume of flyash in concrete was also investigated. The effect of these parameters on the confinement of the concrete core was also studied. Diameter to wall thickness ratio between $25 < D/t < 39$,and the length to tube diameter ratio of $3 < L/D < 8$ was investigated. Strength results of Concrete Filled Tubular columns were compared with the corresponding findings of the available literature. Also a nonlinear finite element model was developed to study the load carrying mechanism of CFTs using the Finite Element code ANSYS. This model was validated by comparison of the experimental and computational results of load–deformation curves and their corresponding modes of collapse. From the experimental and computational study it was found that for both modes of collapse of concrete filled tubular columns at a given deflection the load carrying capacity decreases with the increase in % volume of flyash up to 20% but it again increases at 25% flyash volume in concrete.

3.4 Conclusion and scope:

Various parameter has been studiesed which affect the resistance of composite structure or the load carrying capacity of the concrete filled tubular columns, such as , the shape and the dimension of the cross section or the tube shape, (circular, rectangular or square), also the hight of the stubs, the resistance or strenght of the steel and the filler materials exp normal and lightweight concrete, in adition to the loading type and nature However, More test results are needed for thin cold formed steel tubes filled with non conventional concrete such as slag stone concrete to investigate the effect of weld fillet location and the stub height on the failure load. The present work is a contribution to the understanding of the behaviour of SSC filled cold formed thin short steel tubes subjected to axial compression.

3.5 Experimental behaviour of concrete filled steel stubs.

3.5.1 General

In the present work, results of tests conducted on thin welded rectangular steel-concrete stubs are presented. The stub section was made from two U shaped cold formed steel plates welded to form box whose dimensions were: 100x70x2mm. The main parameters studied were: stub height (50-500mm), effect of the concrete infill and the weld fillet location. The tests were carried out 28 days after the date of casting the concrete infill under axial compression up to failure. A total of 28 stubs were tested, 14 were empty and 14 filled with concrete made with crushed crystallized slag aggregate. The object of the study was to investigate the failure load of composite sections and the use of crushed slag instead of conventional aggregate. From test results it was confirmed that the length of stubs had a drastic effect on the failure load and resulted from local buckling. It appeared that the location of weld fillets had only a slight effect on the failure load for empty steel stubs and was insignificant for composite stubs.

3.5.2 Introduction.

Composite columns have been used widely as they speed up construction by eliminating formwork and have high load carrying capacity1 and the use of thin steel wall thickness is more economic. The major difficulty encountered is however the local buckling of the

steel wall especially in the case of stocky columns [37-38]. Very few experiments workes have been performed on cold formed welded steel sections filled with concrete or recycled materials4-5 such as slag stone concrete (SSC).

To study the behaviour of SSC filled cold formed steel tubes 28 specimens were prepared. All had cross sectional dimensions of 100x70x2 mm. The main parameters studied were the stub height, infill concrete and weld fillet location. Steel coupons were prepared to investigate the tensile yield steel strength and concrete cylinders were tested under direct compression after 28 days. 14 hollow steel tubes with stub heights from 50 to 500mm were tested under axial compression, 7 with the weld on the short side and 7 with the weld on the long side. The tests were repeated with tubes filled Concrete mix as shown in Table 3.1.

Cement content	350. kg/m^3
Water-cement ratio	.50
10mm crushed slag stones	1200. kg/m^3
Sand of crushed slag 2/5	600. kg/m^3
Slump	70. mm
Compressive strength at 28days	20. MPa
Ec	21. GPa

Table 3.1: Slag stone concrete mix properties

Fig 3.1 Samples of filled Stubs

3.5.3 Materials and fabrication

The crushed stone and sand aggregate was replaced with 10mm crushed crystallized slag supplied by the iron manufacture ELHADJAR-ALGERIA. The use of such artificial stone instead of natural stone would contribute to environmental protection by the recycling of industrial waste. The 28 days compressive strength of SSC was 20 MPa and the steel yield strength was 300.MPa with a Young's modulus of 205.GPa. During casting, concrete was vibrated externally with a shaking table for 2 to 3 minutes. All composite specimens were left in the curing room for a period of 28 days. Both, top and bottom faces of composite stubs were mechanically treated to remove surface irregularities and to ensure that both steel and concrete were loaded during the tests.

Fig 3.2 Samples of filled Stubs

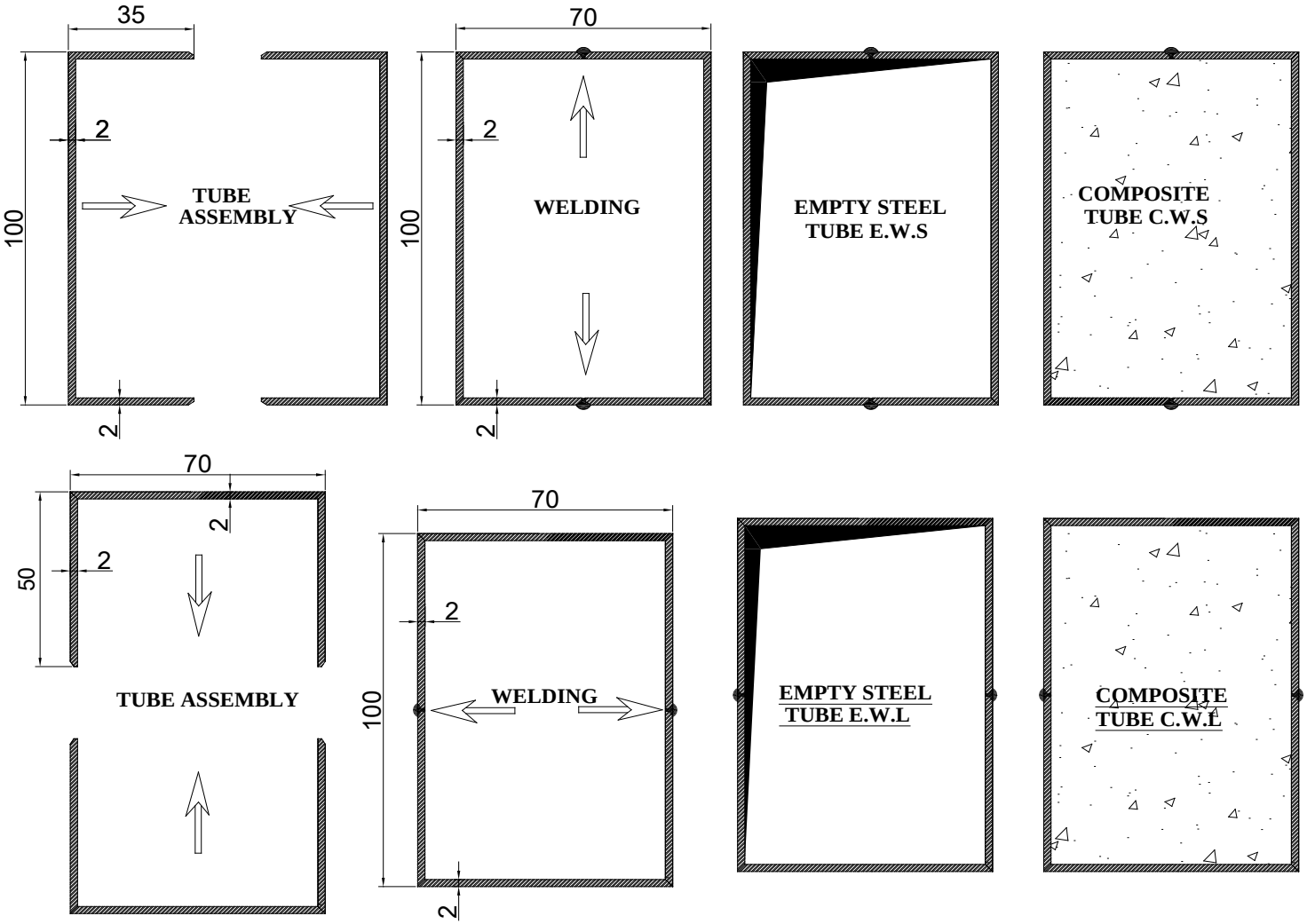

Fig 3.3 Tube manufacture cross section

3.5.4 Test rig and procedure

All specimens twenty eight stubs were tested in a 1000kN compression machine with an absolute accuracy of 0.5%. Special attention was given to verifying the correct position of the stubs before any loading. After the first load increment, a complete check of strains and load was carried out. Several loading and unloading cycles were performed at this stage. When the results were satisfactory, the loading proceeded to failure.

Fig3.4. Test arrangement for concrete filled tube testing.

3.5.5 Results of stub tests

Tables 3.1 and 3.2, show the results for hollow steel tubes and composite tubes respectively. The nomenclature used was as follows:

- EWS hollow steel tubes welded in the middle of the short sides
- EWL hollow steel tubes welded in the middle of the long sides
- CWS composite steel/concrete tubes welded in the middle of the short side
- CWL composite steel/concrete tubes welded in the middle of the long side.

The main feature of failure of the empty thin wall steel tubes was the local buckling that took place in all samples with a small attenuation for longer tubes. Long and short sides buckled inwards and outwards respectively. The decrease in failure load with the stub height increase is shown in Fig.3. It was found that failure load increased when the weld fillet was located in the long sides.

The results of the composite group clearly show the benefit of composite steel-concrete stubs. The load ratio (composite/hollow) had an average value of 1.80 for CWS samples and 1.75 for CWL samples, the ratio for the 50mm stub being much higher, a consequence of tri-axial stress state. It can also be seen from Table 3 and Figure 3 that the long side welded samples had a slightly higher load ratio than the short side weld samples. Both, large and small sides of the composite section buckled outwards significantly with attenuation for the longer samples. The carrying capacity of empty steel tubes with the weld fillet on the short sides varied from 160. to 140. kN and for tubes welded on the long side from 183 to 145 kN.

Table 3.2 Results for hollow stubs.

Stub n°	**HxBxt (mm)**	**Steel Area A_s (mm^2)**	**Height L (mm)**	**Failure load Nsq(kN)**	**test load (kN)**
EWS50	102X68X2	664	50.	199.	**160.**
EWS100	102X68X2	664	100.	199.	**159.**
EWS150	102X68X2	664	150.	199.	**156.**
EWS200	102X68X2	664	200.	199.	**148.**
EWS300	103X68X2	668	295.	200.	**146.**
EWS400	104X68X2	672.	395.	201.	**141.**
EWS500	104X68X2	672.	490.	201.	**140.**
EWL50	98X75X2	676.	50.	202.	**183.**
EWL100	98X74X2	672.	100.	201.	**180.**
EWL150	98X74X2	672.	149.	201.	**174.**
EWL200	96X74X2	664.	198.	199.	**169.**
EWL300	94X72X2	648.	295.	194.	**154.**
EWL400	96X74X2	664.	395.	199.	**150.**
EWL500	98X75X2	676.	490.	203.	**145.**

. The mean load carrying capacity increase when the weld is on the long sides of the section is about 13% for samples with height 50 to 200 mm and about 5% for samples with height of 300. to 500. mm, Fig.3. For composite samples, test loads varied from 500. to 245. kN with weld fillet on the short sides and from 490. to 260. kN for weld fillet on the long sides. The mean load carrying capacity increase is approximately 5% when the weld fillet is on the long sides, Fig.3. The mean test load ratio (filled / empty) for sections longer than 50mm was 1.80 for CWS and 1.75 for CWL. The 50mm sections had load ratios 3.12 and 2.67 respectively. This expresses well the advantage of filling cold formed and welded steel tubes with concrete. Knowing steel and composite test loads, concrete loads can be calculated by subtracting the test steel load from the composite test load. Hence, the average normal stress for the concrete can be approximately calculated[6]. Fig.4. Calculated mean failure loads for both empty and composite stubs were 200. and 270. kN respectively. Test results are shown in Fig.5, it can be seen that the experimental ultimate failure loads diverge from the theoretical value for empty steel stubs, this reflects the drastic effect of stub height on the axial load carrying capacity. Local buckling failure mode took place in all empty samples irrespective of the weld position. For the composite sections the experimental ultimate loads were greater than or close to the calculated composite failure load. This result was not reported in a previous work[6] where it was observed that composite test ultimate axial loads were lower than the theoretical failure load after 28 days curing. The difference between the experimental and theoretical values was found to decrease with composite samples where the concrete had been cured for 3 years. It is believed by the authors that the use of crushed slag stone and sand aggregate contributed in reaching the composite failure load level.

The in-fill concrete reduces local buckling as the steel walls are restrained from deforming outwards and the concrete core is contained by the steel envelop leading to a confined stress state which allows the concrete to withstand stresses greater than the 28 day cylinder strength. This explains the high values obtained for both composite samples CWS50 and CWL50. With the stub height increase, the confining effect of the steel is reduced but failure loads remained close to the theoretical.

Table 3.2 Results for filled stubs.

Stub n°	HxBxt (mm)	Steel A_s (mm^2)	Concrete A_c (mm^2)	Height L (mm)	Squash loads Nsq(kN)	test loads (kN)	Load Ratio Composite/ Hollow
CWS50	102X69X2	668	6370.	50.	273.	**500.**	**3.1**
CWS100	102X68X2	664	6272.	100.	270.	**290.**	**1.8**
CWS150	104X68X2	672	6400.	150.	274.	**285.**	**1.8**
CWS200	102X68X2	664	6272.	200.	270.	**270.**	**1.8**
CWS300	103X68X2	668	6336.	300.	272.	**265.**	**1.8**
CWS400	102X67X2	660.	6174.	400.	268.	**250.**	**1.8**
CWS500	102X67X2	660.	6174.	500.	268.	**245.**	**1.8**
CWL50	98X72X2	664.	6392.	50.	272.	**490.**	**2.7**
CWL100	98X74X2	656.	6256.	100.	268.	**310.**	**1.7**
CWL150	98X73X2	668.	6486.	150.	274.	**300.**	**1.7**
CWL200	95X74X2	660.	6370.	200.	270.	**290.**	**1.7**
CWL300	95X74X2	660.	6370.	300.	270.	**270.**	**1.8**
CWL400	95X75X2	664.	6461	400.	273.	**265.**	**1.8**
CWL500	97X75X2	672.	6603.	500.	276.	**260.**	**1.8**

Failure loads for both composite series CWS and CWL were close, confirming that the weld fillet location did not affect significantly the composite axial load carrying capacity. All composite samples failed by local buckling where the steel envelop deformed outwards. Photographs of some failed composite samples are shown in Fig.7..

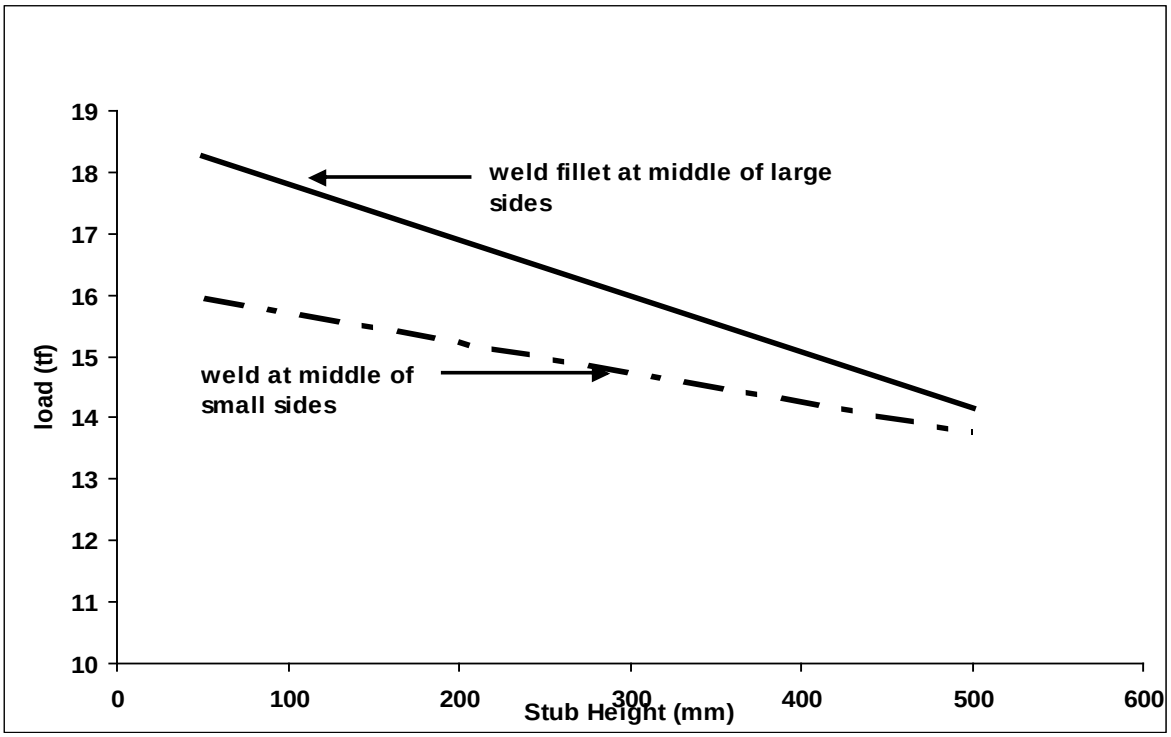

Fig.3. Experimental failure loads for hollow steel tubes with different weld fillet locations

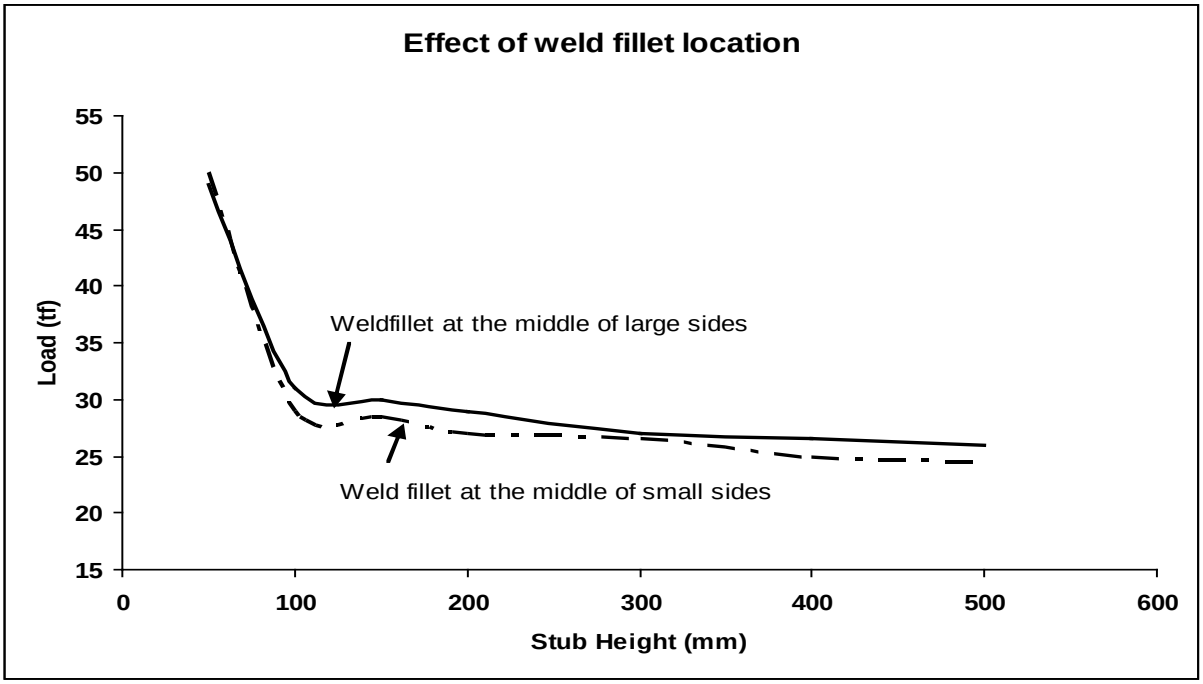

Fig.3. Experimental failure loads for composite tubes with different weld fillet locations

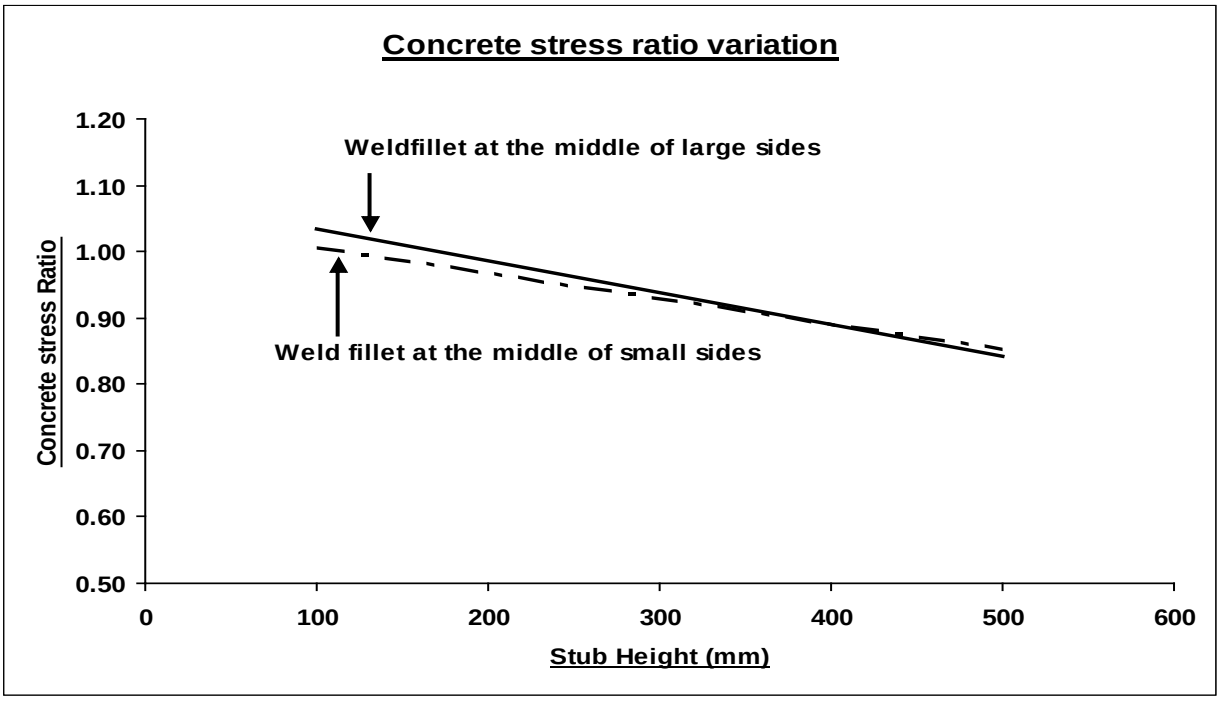

Fig.4. Concrete mean stress variation

3.5.6 Discussion

As no experimental evidence could be found on the effect of the welding location on the axial load carrying capacity it was decided to test empty and composite cold formed steel tubes with different weld fillet locations. The experimental results presented in Table.3. and Fig.3. for empty steel tubes show a slight increase of the axial load carrying capacity of 5 to 13%.when the weld fillet is in the middle of the long sides of the steel cross section. The main feature of the failure of empty stubs is the local buckling that took place in all samples. Long and short sides deformed inwards and outwards respectively. Ultimate test loads were below the corresponding theoretical failure load, a consequence of the high H/t ratio which was 50. for all samples. Composite samples reached experimental loads beyond or close to the theoretical composite failure load. The infill concrete played a major role in increasing the load carrying capacity and hence delaying the local buckling of steel walls. From the experimental results shown Table.3. and Fig.3., the weld fillet location did not significantly affect the axial load carrying capacity of composite stubs. Samples with height of 50 mm CWS50 and CWL50 had failure test loads approximately twice the theoretical failure load. This is believed to be a result of the concrete core being in a confined stress state allowing it to reach approximately 3 times the 28 days concrete compressive strength. The failure mode of tested composite stubs was a local buckling mode where all steel walls deformed outwards. No sign of weld fillet failure was reported for any sample.

Fig.3.5. Experimental failure loads comparison

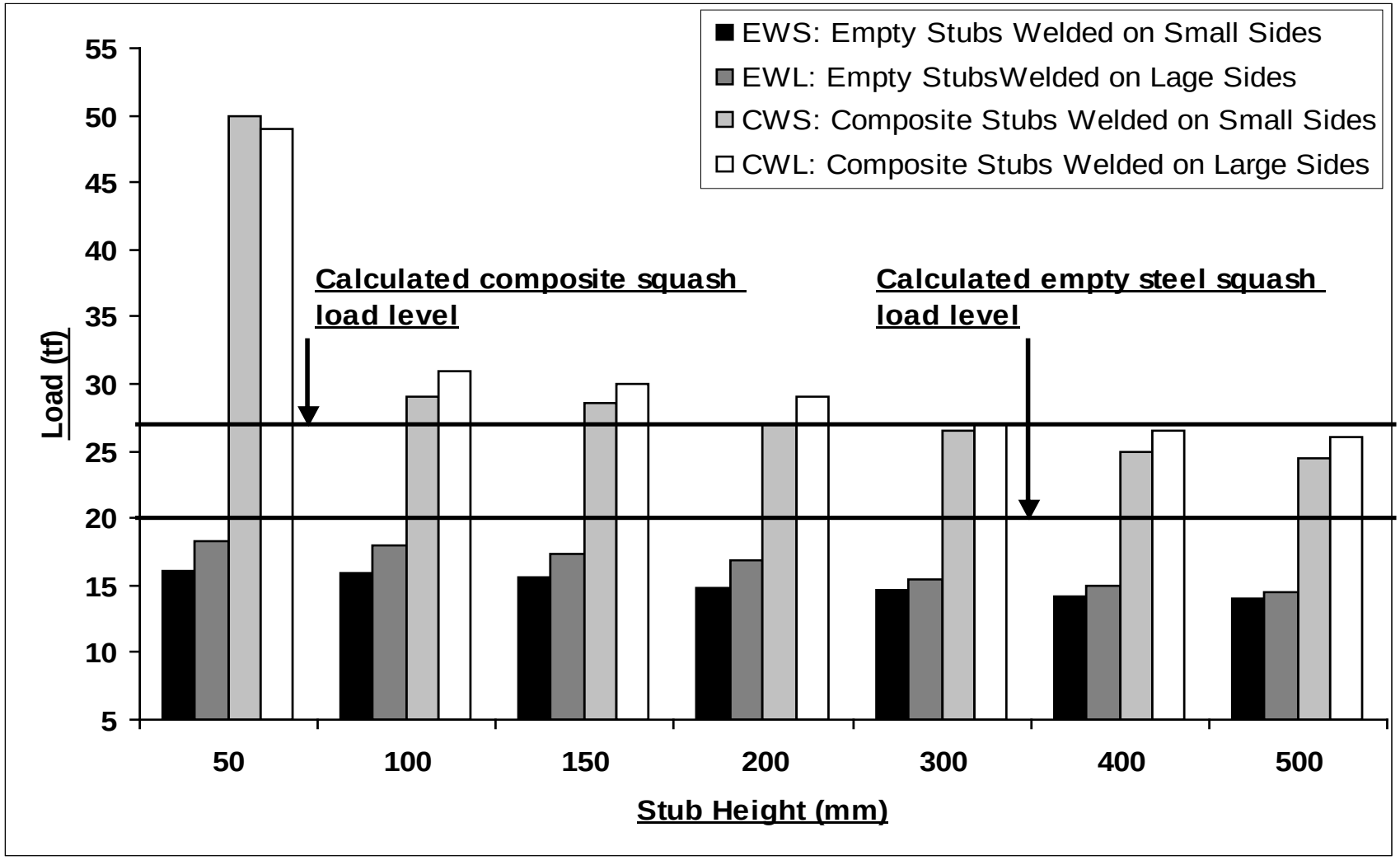

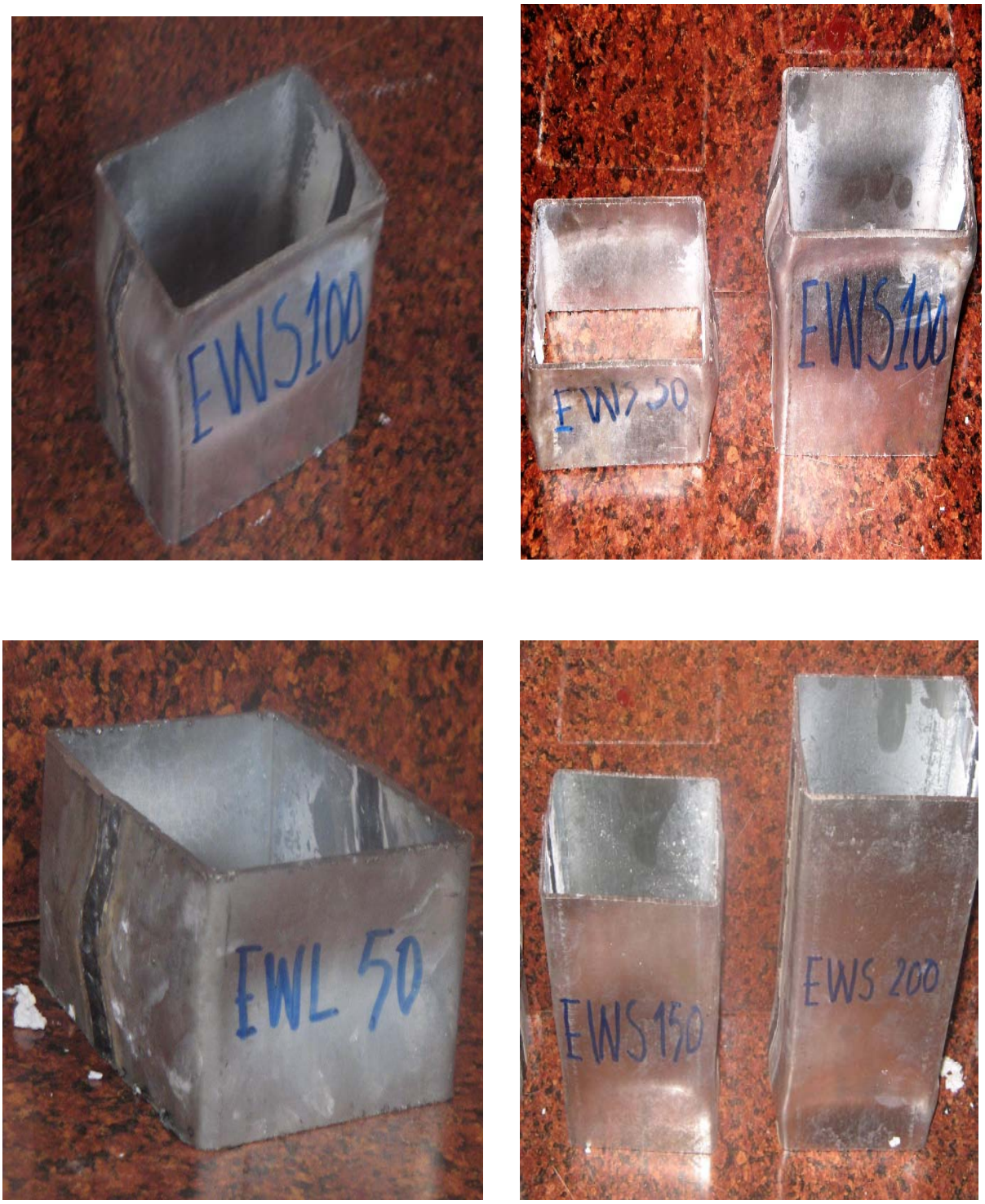

Fig 3.6 Emplty stubs after test

Fig 3.7 Filled stubs after test

3.5.7 Conclusion

Empty cold formed and welded steel tubes with a H/t ratio of 50 suffered drastically from local buckling and reached loads below the theoretical steel failure load and increased from 5 to 13% when the weld fillets were located at the middle of the long side of the steel cross section. Composite stubs tested 28 days after casting, behaved well and reached maximum loads beyond or close to the corresponding theoretical failure load. This is a clear indication of the effect of the concrete core and composite steel-concrete action. The weld fillet location did not significantly affect the axial load carrying capacity in composite tubes. The failure mode of the samples was a typical local buckling mode with yielding of the steel and crushing of the concrete. No weld failure was reported in any samples. To understand the post-failure behaviour of the stubs cyclical loading was carried out and results of these tests will be presented in a future work.

.

CHAPTER 4
THERMAL PERFORMANCE OF LIGHT STEEL STRUCTURE. (EXPERIMENTAL APPROACH)

4. Thermal performance of light steel structure.

4.1 Introduction:

There are increasing demands for improvements in standards of construction quality, comfort and performance in building internationally. The building industries in many countries are looking for new and improved methods for construction.
Light steel structure provide alternatives to traditional forms of construction, but the future growth of steel structure will depend on the ability of the industry to provide high quality, economical steel structure systems which meet the needs of the builder and the home owner. Any evaluation of a construction method must look not only at the structural requirements but also at the total performance of the building. Structural requirements for buildings using cold formed steel sections are covered by various standards and design manuals. Load bearing tables and all information that designers and building officials need are generally available from steel manufacturers.

Increasingly, energy efficiency issues have come much more important in the assessment of a construction system. In particular, the ability to provide the required thermal performance so that excessive heating or cooling are avoided, and comfort is maintained. Furthermore, concerns over global warming have led to an international commitment to reduce emissions of global warming gases.
Due to the high thermal conductivity of steel and concerns about possible corrosion, conventional rules used for designing construction to achieve good thermal performance may not be appropriate when light steel construction is used. In particular, moisture control and thermal bridging need to be examined closely. Particular attention must be paid to the type, amount and location of thermal insulation within the assembly in order to prevent excessive heat loss, condensation and dust streaking on the interior. Also, consideration must be given to the detailing around junctions and openings.
The condensation resistance of wall and roof assemblies is a function of the type of construction used, including the type, amount and location of thermal insulation and vapour control layer; the internal design temperature; indoor climate of the building

and the external conditions. Analysis of condensation resistance can be based both on mathematical modelling and on full-scale testing.

Increasingly, building codes require that steps are taken to control air leakage across the envelope of the building. This is important to reduce heat losses from air leakage which becomes more significant in well insulated dwellings, and to ensure that air movement through the envelope assemblies does not compromise the insulation and moisture resistance qualities of the envelope. Increasingly, thermally insulated wall and roof assemblies are constructed so that they include an air barrier system to provide a continuous barrier to air leaking in or out of the building. Steel frame assemblies need to be designed to include air barrier systems.

Thermal capacity may be an issue in some climates to avoid overheating especially in the Algerian climate. It can also be used to reduce the size of heating or cooling plant.

Figure 4.1 *typical light steel structure assemblies.*

4.2 Light steel Structure

Light steel structure is being used successfully for housing in many countries. In the USA, Japan, Canada, Sweden, and Australia, increasing numbers of light steel structured houses are being built. In the UK several systems are now available and significant numbers of schemes are being built. The reasons for this are the inherent quality and durability of light steel structure when compared to the alternatives, and its suitability for the design of well insulated dwellings. Concerns about the volatility of the timber market, the declining quality of structural timber, environmental issues such as sustainable forestry practices and quarrying for clay used for bricks and aggregates used in concrete blocks, have affected the use of these materials. The American Institute of Architects, in its Environmental Resource Guide, recommends that steel may be considered less environmentally harmful than many other alternatives because many steel products are made totally or partially from recycled scrap.

Light steel structures typically comprise of C, U and Z shaped, galvanised cold-formed steel sections, usually 0.9 mm to 3.2 mm thick that are produced by roll forming. The technology has developed from specific applications such as purlins and lintels to the wider building market. Construction on site can use individual light steel components or sub frames; often prefabricated welded, bolted or riveted panels are assembled on site using self tapping screws to create whole building structures. Increasingly, there is interest in volumetric production using whole room or even whole house pods with internal finishes and services fitted in the factory.
Steel is manufactured to tight specifications and does not suffer from twisting, warping or movement due to changes in moisture content. This results in easier fixing of linings and higher quality finishes, avoiding problems such as opening up of cracks around architraves around doors due to movement. Steel components are lightweight and easy to lift and carry. Wall panels can be moved around by two men; only about 2.5 to 3 tonnes of steel is required for a typical house in the UK. There is little waste in production, fabrication or assembly and benefits can be gained from off-site prefabrication in controlled conditions in a workshop. This minimises inefficient and disruptive work on site and improves quality control. Useable roof spaces and clear

span internal spaces can be easily created without the need for internal load bearing walls, allowing for future adaptability and change.

4.3 Scope of the Section.

The objective of this Section is to increase the understanding of how light steel structure (tube) construction should be designed to ensure that buildings using this technology can achieve excellent comfort conditions and be used in an energy efficient manner with special reference is given to cold formed steel stubs filled with slag stone concrete. This will allow the industry to address market concerns and design light steel structure buildings which are comfortable to live in, achieve energy efficiency requirements, and result in low greenhouse gas emissions.

Thermal properties of concrete slag stone concrete samples are measured, a review and description of the measurement methods is given, a model for the estimation of the heat transfer through a composite elements are developed based on thermal network methods and a review of simplified calculation of thermal resistance of wall with light steel structure is given.

The Chapter also provides a review of computer simulation design tools and identifies how these can be used to define and improve the detail design of light steel framing. It discusses the most appropriate computer simulation tools which can provide a detailed analysis of the thermal and hygroscopic performance of light steel framing envelopes. These tools provide the opportunity to optimise the location and thickness of insulation and vapour control layers to avoid excessive thermal bridging and the risk of condensation. They also allow the assessment of the impact of alternative strategies for incorporating more thermal capacity into buildings.
This Section reviews simplified calculation methods for calculating the thermal resistance of light steel structure assemblies, and looks at the effect of junctions and details on the whole wall thermal resistance. The last part discusses various issues of detail design to ensure that light steel frame assemblies provide a high level of thermal resistance, and make best use of the installed insulation. Also the role of

thermal capacity is considered and finally a reviews of alternative ways of integrating thermal capacity in light steel structure.

4.4 Review of experimental methods of measuring thermal properties of construction materials

4.4.1 Introduction

The thermo physical characteristics of construction materials are the ability of heat to spread through a body or to be stored.

In order to introduce the internal materials thermo physical characteristics, it is necessary to define some basic notions on the propagation of heat in solids and then some measurements methodologies of thermal coefficients properties are presented.

Thermo physical quantities studied are:

- The thermal conductivity
- Thermal diffusivity
- Specific heat0

4.4.2 The thermal conductivity:

Is the most thermo physical properties used for construction materials. In steady state, and in the simplest case of one-dimensional flow of heat through a wall of a uniform thickness e and uniform temperature

and T_2, the heat flux φ in W is given by:

$$\varphi = \frac{\lambda}{e} \ (T_1 - T_2)A$$

Where: A is the wall face area m^2.

Thermal conductivity measures the ability of heat to pass through a body. It depends on the nature of the body and its temperature. Equation (1.1) implies that the process of transfer of thermal energy is a statistical phenomenon. In reality, propagation of energy is not simply from one end to the other end following a straight line, but the

energy diffuses into the sample through successive collisions. This is the statistical nature of the process that brought the temperature gradient and a mean free path in the expression of heat flux. In the case of thermal insulation of buildings, the aim is to minimize this transfer.

4.4.3 Thermal diffusivity

When the medium temperature is a function of time and that the conductivity depends on temperature and spatial coordinates, Fourier's equation is written as:

$$\rho C_p \frac{\partial T}{\partial t} div(\lambda . \text{gradT})$$

When the thermal parameters are independent of temperature, the above relationship becomes:

$$\frac{\partial T}{\partial t} = \frac{\lambda}{\rho C_p} \Delta T$$

With

$$\Delta T = \frac{\partial^2 T}{\partial x^2} + \frac{\partial^2 T}{\partial y^2} + \frac{\partial^2 T}{\partial z^2}$$

This relationship shows that $a = \frac{\lambda}{\rho C_p}$ represents the thermal diffusivity of the medium.

We can write:

$$\frac{\partial T}{\partial t} = a \, \Delta T$$

Thermal diffusivity, when set is linked to the thermal conductivity, heat and mass density. It characterizes the speed of the propagation of a wave in a body which in fact very relevant in the thermal inertia of materials.

4.4.4 Specific Heat

The calorimetric classical equation: $\varphi = mC_p(T_2 - T_1)$ shows that the amount of heat absorbed by a body of mass m when the temperature increases from T_1 to T_2 is proportional to the specific heat C_p of the considered solid.

Practically, the specific heat C_p of a body corresponds to the amount of heat needed to rise its mass unit temperature by one degree. This underlines the importance of the specific heat for all calculations of storage or transport of heat.

4.4.5 The main methods of thermo physical properties measurement

The thermal conductivity λ, specific heat C_p, the thermal effusively E and the thermal diffusivity a are the most important thermo physical parameters in the study of heat transfer in buildings materials, so they are essential at processes of drying, heating, cooling and when thermal building behaviour is concerned.

These parameters can be measured by various methods, it should be noted that the determination of any two of them leads to the calculation of the other using the relations:

$$a = \frac{\lambda}{\rho C_p} \qquad \text{And} \qquad E = \sqrt{\rho C_p \lambda}$$

The measurement of thermal conductivity is of great importance when the study of heat transfer in a system is considered. Many methods have been used to determine the thermal conductivity of different materials. Some of them develop theories based on equations of heat conduction.

The methods for measuring the thermal conductivity can be classified into two categories: steady-state and dynamic methods.

4.4.5.1 The steady-state methods.

These methods require a long handling time and the variation of moisture over time

can lead to results affected by errors. But among these, the method used by (Ingran and Avery, 1976) which gives satisfactory results, but it requires long time especially for materials with low thermal conductivity.

The static measures imply the use of Fourier equations in the steady-state. It is necessary to determine the current density of heat and the temperature gradient along the normal to the sample. The system allows for permanent measures the obtention of precise results, however, the time it takes a very long time to reach equilibrium if the conductivity is very low.

Among the steady state measurement methods that most used are:

- Method of the guarded hot plate.
- Method of boxes.

4.4.5.1.1 Guarded hot plate Method

The method of the guarded hot plate was developed for measuring low thermal conductivities materials (Gustafson et al 1981, Pradhan et al 1991).

The experimental principle is to maintain a temperature difference ΔT between two plates, A and B planes, respectively parallel and constant temperatures T_A and T_B. A sample of material to study is placed between the two plates (Figure 4.2).

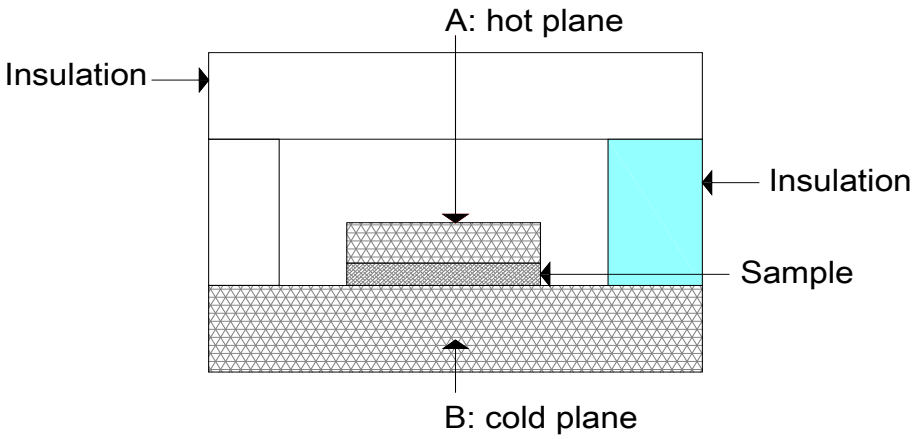

Fig 4.2; Cross Section of the hot plate dispositif

If e is the sample thickness and φ the steady state heat flux transferred from one plate to another. The thermal conductivity λ of the material is then given by:

$$\lambda = \frac{\varphi e}{\Delta T}$$

With $\Delta T = T_A - T_B$

To avoid the edge phenomena, the plate A is surrounded by a ring at the same temperature TA. The interval between the ring edges of plate A is small enough to avoid too much disturbance of heat flow on the edges of the plate. The measurement precision depends on the quantities contained in equation (2.3). As well as corrections made to this relationship which does not take into account several thermal aspect? However For materials with relatively large requiring samples for measurement, such as construction insulation, this technique is very suited and most often used.

4.4.5.1.2 Method of boxes

The principle of this method, developed by the Laboratory of Solar and Thermal Studies of the University Claude Bernard in Lyon, is illustrated in

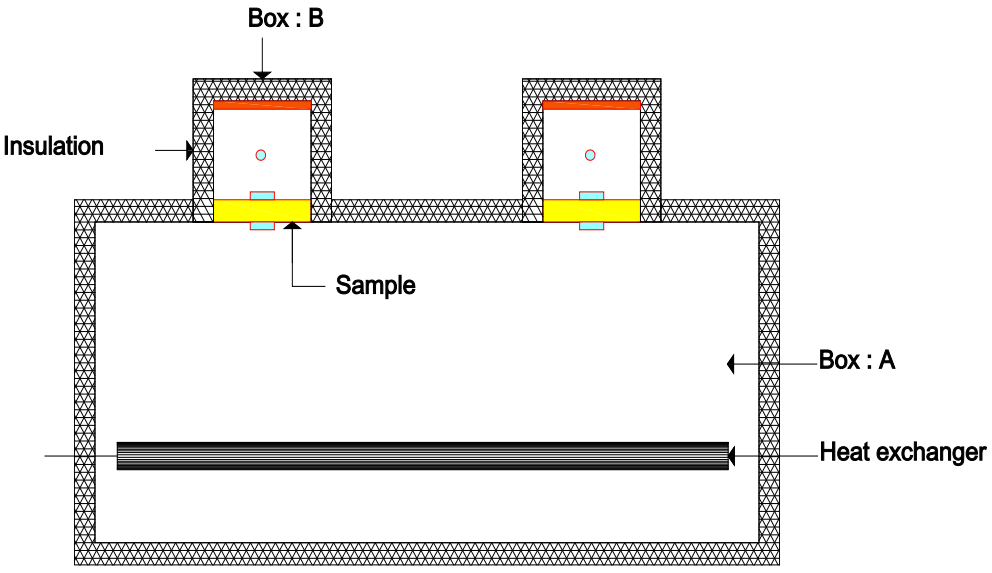

Fig 4.3 Cross section of boxes dispotif

The volume A is maintained at a lower temperature than the two boxes, with a low temperature heat exchanger R. The hot plates C situated in the boxes create a temperature gradient across the sample E.

- In Steady state, the measurement of the heat flux emitted by C and temperatures on the upper and lower sides of E are used to calculate the thermal characteristics of the sample.

- The heating system is maintained for a certain period. The temperatures changing TC and TF of hot and cold sides of the sample are recorder.

The steady state is reached when these temperatures stabilize (variation of 1/10th of a degree in an hour)
This usually takes 4 to 7 hours after the mounting of the sample, if the cooling system was not stopped after the previous test. At this point, three fluxes are to be considered in the energy balance of the "local box":

The Joule effect produced by the heating element C is:

$$\varphi_j = \frac{V^2}{R}$$

The heat loss through the box B:

$$\varphi_d = C_1 (T_B - T_A)$$

The heat flux by conduction through the sample:

$$\varphi_c = \frac{\lambda_e A}{e}(T_c - T_f)$$

The heat φ_d will componsate the heat by conduction φ_d and the the heat lossφ_c, thus,
$\varphi_d = \varphi_d + \varphi_c$
So the sample thermal conductivity can be calculated as:

$$\lambda_e = \frac{e}{A(T_c - T_f)}\left[\frac{V^2}{R} - C_1\,(T_B - T_A)\right]$$

4.4.5.2 The non steady-state methods

These methods also known as dynamic methods are most often used for biological materials which generally are heterogeneous with high humidity level. The hot wire method is one of these. They require
a complete differential equation of the heat flow (Carlos and Jagger 1959).

Based on the work of Jannot (2003), on the different methods of measuring thermo physical properties by the hot wire and hot plan procedure. The most used dynamic methods for measuring the thermal conductivity are presented as follow:

4.4.5.2.1 Method the hot plate Method with sinusoidal excitation.

This method is based on the hot plate plan. .Figure 4.4 represents a schematic diagram of the method.
The principle of this method is that, a periodic thermal signal is generated on the underside of the samples, while at the same time the temperature of the upper face is kept constant, with a cold water cooling plate.
This signal is produced by an intermittent heat flux in the hot plate. When the periodic state is established, the signals of temperature and heat flux can be expressed by Fourier series, giving sinusoidal signals as well as the electric generator.
These sinusoidal terms are in fact the diffusivity and the thermal effusivity. It should be noted that the choice of the period of the signal depends on the thickness and the material to study. In general, this choice is made so that the assumption of constant temperature of the upper surface of the pair of samples is to be verified, while avoiding to have a negligible signal. For a given material, the period of the signal increases with the thickness.

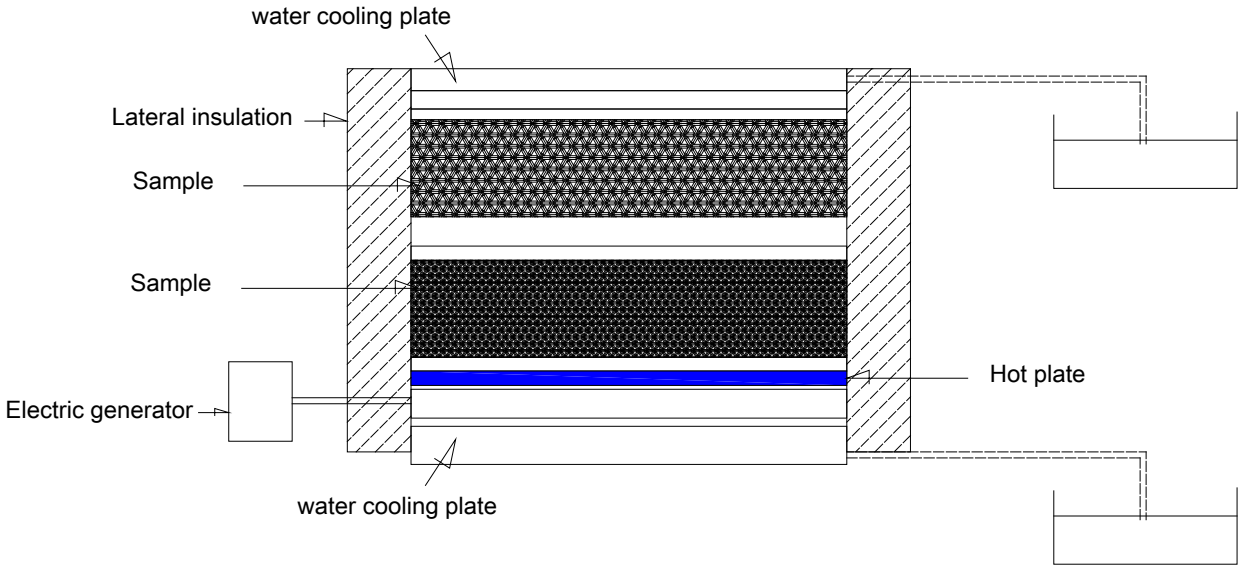

Fig4.4. Signal device for thermal conductivity mesure

- **Mathematical Modelling**

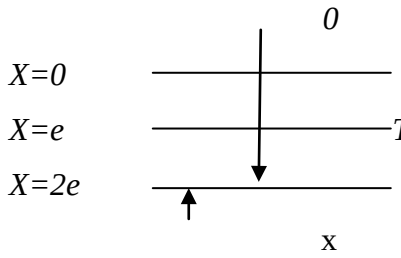

$T(0, t) = T_1$

$T(e, t) = T_2 + |T_2|\sin(\omega t - \Gamma)$

$T(2e, t) = T_3 + |T_3|\sin(\omega t)$

$\varphi(2e, t) = |\varphi|\sin(\omega t + \psi)$

The heat transfer is assumed to be unidirectional due to the sample symmetry, and the lateral insulation. Thus, the following Laplace equation can be written:

$$\frac{\partial T(x,t)}{\partial t} = \alpha \frac{\partial^2 T(x,t)}{\partial^2 x^2}$$

With the boundary conditions: $T(0, t) = T_1 = constante$

$T(2e, t) = T_3 + |T_3|\sin(\omega t)$

The interface temperatures can be written as:

$$T(2e,\ t) = T_3 + |T_3|\sin(\omega t)$$

T_1, $T2$ and T_3 are the temperatures at points ($X=0$, $X=e$ and $X=2e$), respectively.

$\omega = \frac{2\pi}{T}$, T is the period and t is time

The heat flux applied on the underside is:

$$\varphi(2e,\ t) = |\varphi|\sin(\omega t+\psi)$$

We put ;

$$Z = 2e(\frac{\omega}{2\alpha})^{1/2}$$

The thermal diffusivity a can be calculated as;

$$a = \frac{(2e)^2\pi}{Z^2 T}$$

And the thermal emissivity E can be calculated as;

$$E = (2e)Z\sqrt{T\pi}$$

4.4.5.2.2 Thermal characterization using physical probes:

4.4.5.2.2.1 Hot plan method for thermal effusively Measurement:

This measurement is performed using a plane heating resistance on which a thermocouple is placed. At time t = 0, and during the measurement a constant voltage is applied to this resistance, placed between two blocks of the sample to characterize. Thus, a constant heat flux through the sample is imposed by Joule effect. The Modelling of this heat transfer allows an estimate of parameters such as:

- The Material Thermal effusively (E)

- The probe Thermal capacitance.
- The contact resistance, at the interface probe / sample (R_c);

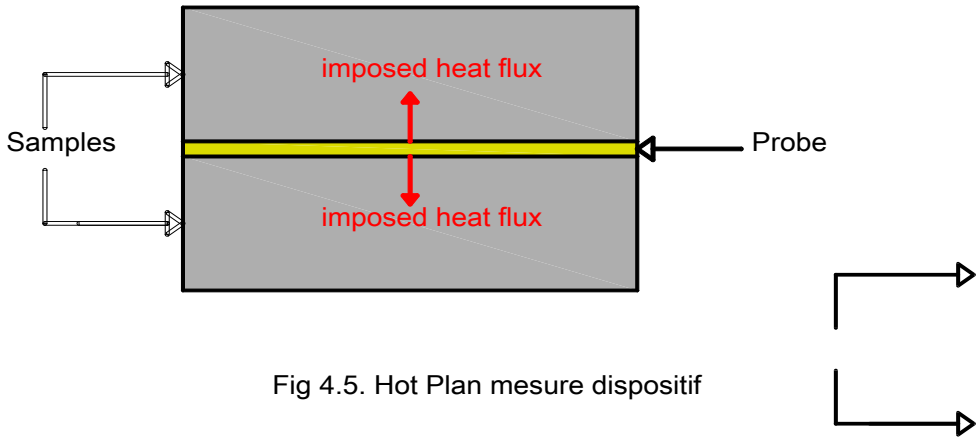

Fig 4.5. Hot Plan mesure dispositif

In order to model the hot plane this assumption are made;

- The heat flux imposed by the probe is perpendicular to the plane ;
  The sample is a semi-infinite. I.e. that the disturbance induced by the imposed flow does not reach the outer surface of the sample.

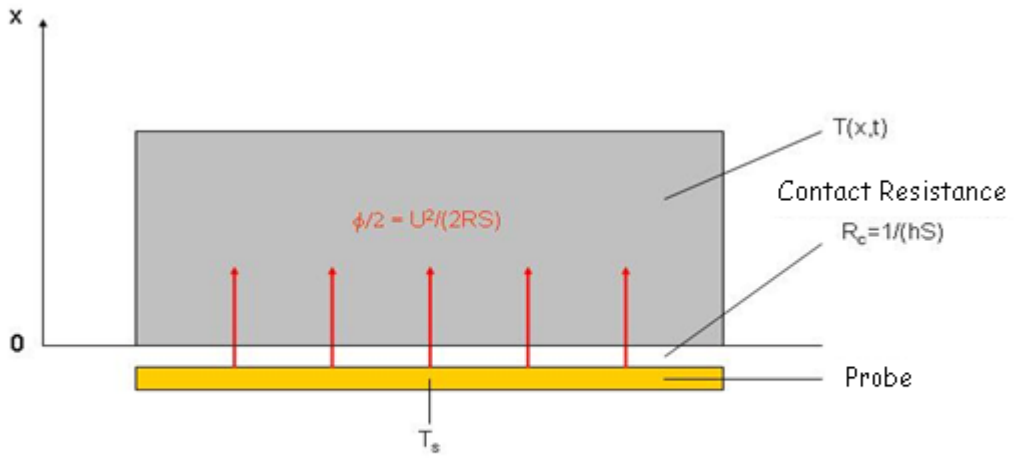

Fig 4.5 The Hot Plan Notations.

The equation of the heat trough the sample may be written as

$$\frac{\partial^2 T}{\partial x^2} = \frac{1}{a}\frac{\partial T}{\partial t} \qquad \text{(a)}$$

With the boundaries conditions:

- $T(x,0) = T_s(0) = T_i$ (b)
- $T(\infty, t) = T_i$ (c)
- $h[T_s(t) - T(0,t)] = -\lambda \frac{\partial T(0,t)}{\partial x}$ (d)
- $\frac{\phi S}{2} = m_s c_s \frac{dT_s}{dt} + hS[T_s(t) - T(0,t)]$ (e)

The expression (d) is the heat conservation within the contact surface sample /probe, the relation (e) gives the heat conservation within the probe.

As : $\overline{T} = T - T_i$

Then : $\frac{\partial \overline{T}}{\partial x} = \frac{\partial T}{\partial x}$, $\frac{\partial^2 \overline{T}}{\partial x^2} = \frac{\partial^2 T}{\partial x^2}$ and $\frac{\partial \overline{T}}{\partial t} = \frac{\partial T}{\partial t}$. The relation became:

$$\frac{\partial^2 \overline{T}}{\partial x^2} = \frac{1}{a}\frac{\partial \overline{T}}{\partial t} \qquad \text{(a)}$$

- With the buanderies conditions :

- $\overline{T}(x,0) = 0$ (b)
- $\overline{T}(\infty, t) = 0$ (c)
- $h[\overline{T}_s(t) - \overline{T}(0,t)] = -\lambda \frac{\partial \overline{T}(0,t)}{\partial x}$ (d)
- $\frac{\phi S}{2} = m_s c_s \frac{d\overline{T}_s}{dt} + hS[\overline{T}_s(t) - \overline{T}(0,t)]$ (e)

The Laplace transformation of the equation (a) leads to:

$$\frac{d^2\theta}{dx^2} - \frac{1}{a}[p\theta - \overline{T}(x,0)] = 0$$

Then; $\theta(x, p) = Ae^{-qx} + Be^{+qx}$ with $q = \sqrt{\frac{p}{a}}$.

But the temperature has a defined value when x is undefined, then B=0, we deduce

$$\theta(x, p) = Ae^{-qx} \text{ With } A = \theta(0, p)$$

Laplace transformation of the equations (d) and (e) may be written as:

- $h[\theta_s(p) - \theta(0, p)] = -\lambda \frac{\partial \theta(0, p)}{\partial x} = \lambda \sqrt{\frac{p}{a}} \theta(0, p) = E\sqrt{p}\theta(0, p)$
- $\frac{\phi S}{2} = m_s c_s p \theta_s(p) + hS[\theta_s(p) - \theta(0, p)]$

With the elimination of $\theta(0, p)$ between the two equations, we get the temperatures variation at the probe centre as:

$$\theta_s(p) = \frac{\phi S}{2p} \frac{1 + R_c ES\sqrt{p}}{m_s c_s p + [R_c m_s c_s p + 1] ES\sqrt{p}}$$

By Laplace inverse transformation using the Stefhest method, the probe temperature change can finally be calculated using the formula:

$$\overline{T}(0,0,t) = \frac{\ln(2)}{t} \sum_{j=1}^{n_L} V_j \theta_s\left(0,0, \frac{j \ln(2)}{t}\right)$$

The unknown parameters are E, Rc and mcs that are estimated by minimizing the difference between the probe temperature measured during the experiment and the calculated temperature by inverting the Stefhest formula.

4.4.5.2.2.2 Hot Disk Method

The aim of the Hot Disk method is to impose a uniform heat flux in a plane between two samples of symmetric extension "infinite."

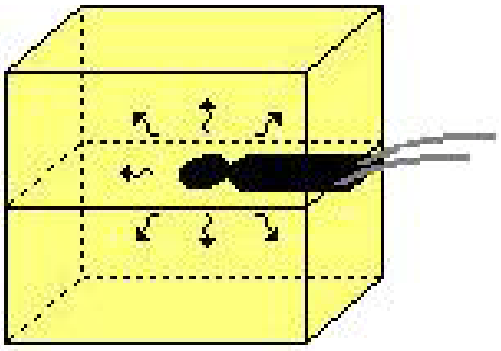

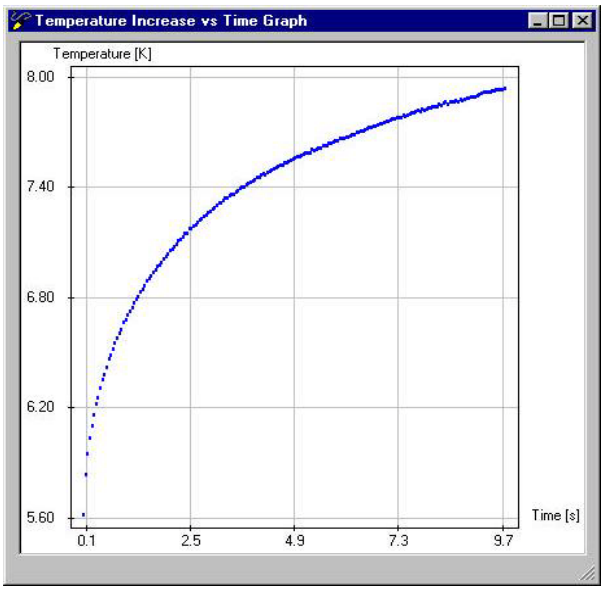

Figure 4.6 Hot Disk experimental principal

Figure 4.7 : Hot Disk out put

The probe serves as a heat source and capture for dynamic measuring, the increases in the probe resistance is registered (which corresponds to the increase in temperature).

If the Hot Disk is heated electrically, the increase in resistance as a function of time can be expressed by:

$$R(t) = R_0 \{ 1 + \alpha . [\Delta T_i + \Delta T_{ave}(\tau)]\}$$

R_0 the disc resistance at t = 0, α is the thermal coefficient of resistance, ΔT_i is the temperature difference that develops almost instantly on the thin insulating layers covering both sides of the field sensor Hot Disk which makes Hot Disk an appropriate capture. ΔT with (τ) which makes Hot Disk Sensor appropriate.

From the equation (1) we obtain the temperature rise recorded by the sensor:

$$\Delta T_{ave}(\tau) + \Delta T_i = 1/ \alpha * (R(t)/R_0 - 1)$$

ΔTi is a measure of the thermal contact between the sensor and the surface of the sample. ΔTi is equals zero when the "thermal contact" is perfect, produced by a thin layer deposited (PVD or CVD) or a sample insulator against electricity.

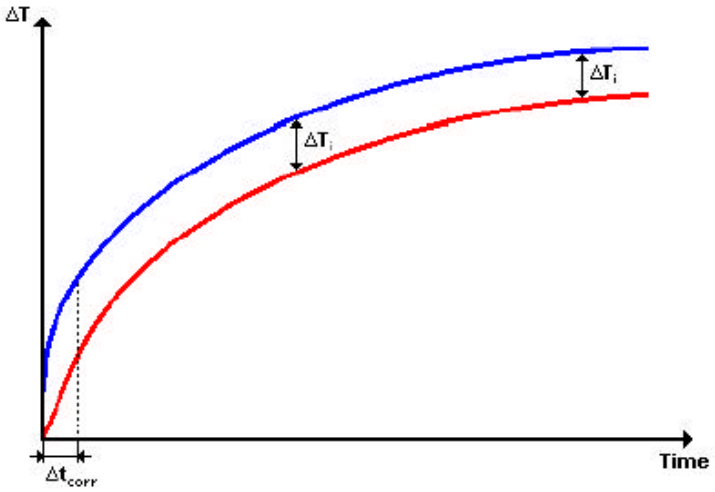

Figure 4.8: The blue curve shows the temperature increase of the sensor itself and the red curve shows the increase in surface temperature of the sample.
ΔT_i after a while become constant, Δt_i, can then estimated as :

$$\Delta t_i = \delta^2 / K_i$$

Where δ is the thickness of the sample and K_i its diffusivity.

The temperature increase is a function of time and can be expressed by:

$$\Delta T_{ave}(\tau) = P_0/(\Pi\text{^}(3/2) \,.\, a \,.\, \Lambda\,) \,.\, D(\tau)$$

Where P_0 is the capture power, a disc radius, Λ *is the thermal conductivity of the sample and* $D(\tau)$ *is a function which depends on time and given by:*

$$\tau = \sqrt{(\, t / \Theta\,)}$$

In this equation, t is the time measured from the beginning of the transitional registration and Θ is the characteristic period defined by:

$$\Theta = a^2 / K$$

Where K is the thermal diffusivity of the sample.

Then in the thermo gram in terms of $D(\tau)$, we get a straight line where the increase in temperature between the beginning and the end point is ΔT_i (we read on

the ordinate) and the slope is $P_0/(\Pi\text{^}(3/2) \cdot a \cdot \Lambda)$, for experimental durations much longer than Δt_i.

As K, and thus Θ are not known before the experiment, the final line from which the thermal conductivity is calculated is obtained through iterations. Thus it is possible to determine both the thermal conductivity and thermal diffusivity from a single recording.

- **THE MEASURING DEVICE**

The Complete Hot Disk device in the figure below:

Figure 4.9 : The Complete Hot Disk device

In order to estimate thermal property, the Hot Disk dispositive requires:

A probe of appropriate size,
A sample (optional)
A Wheatstone bridge,
A data acquisition system with two Keithley (feed and measure),
The software Hot Disk Thermal Constants Analyzer,
PC (for calculations).

Probes

The probes are designed to fit between two pieces of the sample. They consist of a double spiral of nickel 10 microns thick taken between two sheets of insulation (Kapton Mica or depending on the temperature of use**).**

The different existing ray's sizes are: 0.492, 2.001, 3.189, 6.403, 9.719, 9.908, 14.610, 29.4 mm.

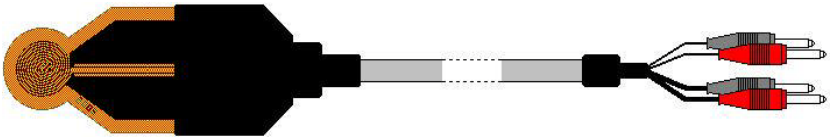

Figure 4.10 : Hot Disk Kapton Probes (500 K)

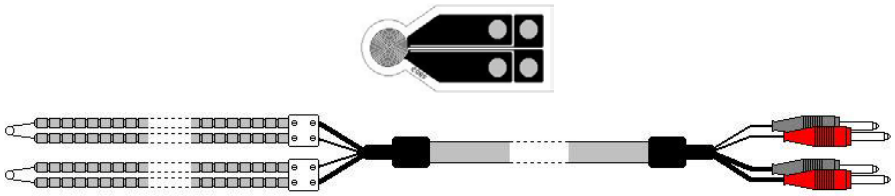

Figure 4.11 : Hot Disk Mica probe (1000 K)

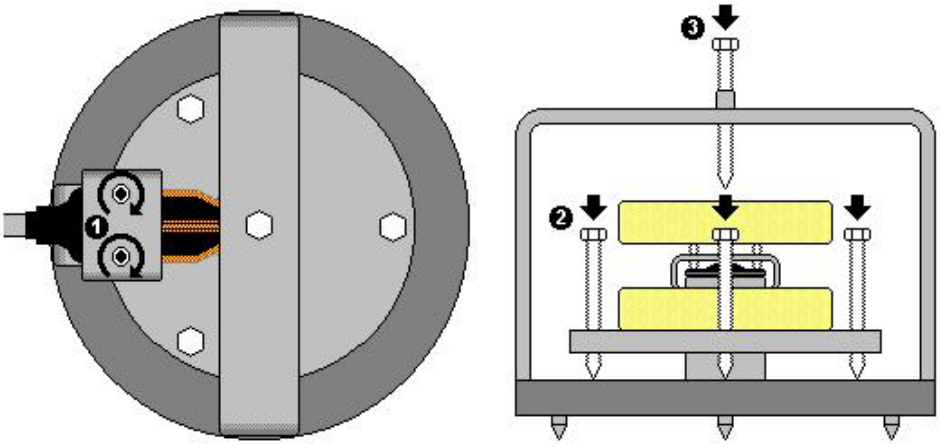

Figure 4.12: Hot Disk

The out put of the hot disk are :

• Thermal conductivity,
• thermal diffusivity,
• heat capacity..

4.4.5.3 Conclusion

The method of hot disk is a method of thermal characterization based on a complex model to obtain reliable results and can be implemented for a relatively low cost. The probe type described above can characterize a wide range of materials including local building materials.

In an experimental measure, the objective to achieve is the accuracy and the reliability of the results. The choice of measurement method will depend on several factors which are:

- reliability of the results and duration of measurement,
- the cost of acquisition and maintenance of equipment and its robustness,
- Equipment availability.

Measurements of thermo physical properties in the present work have been performed using the devices available at the laboratory TREFLE INSAT de Bordeaux which is the hot disk.

4.5 Experimental programme.

4.5.1 Introduction.

Lightweight concrete can be obtained by replacing totally or partially standard aggregate by low weight and preferentially low cost components. The interest is of course to decrease the volume of load-bearing elements but also to get better thermal properties with regard to conventional concrete. This last point is especially relevant with regard to the new regulations that aim at reducing energy consumption in buildings. Achieving both the thermal insulation and the bearing structure with a unique material is indeed an attractive idea, which would allow in particular the suppression of thermal bridges present in conventional buildings techniques. The difficulty is to find a material that fulfils a priori contradictory requirements: a low thermal conductivity- for which the presence of void is suitable – and a high mechanical strength – for which matter instead of void is needed.

Among the various types of lightweight concretes that have been proposed in the past decades, those obtained by mixing high performance cement with millimetre-size expanded polystyrene (EPS) spheres [1,2] are particularly interesting for various reasons. First, it is expected that structural elements in EPS concrete can be fabricated on construction site. This is an important advantage with respect to other materials such as autoclaved cellular concrete, whose fabrication process is rather complex. In addition, it is possible to tailor the properties of EPS concrete by varying material parameters such as EPS sphere size and volume fraction. For this purpose an accurate knowledge of the relationship between the composition and the properties of this material is required. Such relationship can be deduced from series of experiments, but modelling is expected to be fruitful to provide general trends and reduce the experimental effort.

The aim of this section is thus to characterize the thermal properties of the **concrete made with crushed crystallized slag aggregate** and to investigate the possibility of predicting these properties of concrete-filled thin welded cold formed steel stubs through modelling approaches and simplified calculations.

The crushed stone and sand aggregate was replaced with crushed crystallized slag supplied by the iron manufacture ELHADJAR-ALGERIA. The use of such artificial stone instead of natural stone would contribute to environmental protection by the recycling of industrial waste and an alternative way to obtain a Lightweight concrete with better thermal properties with regard to conventional concrete.
It should be noted at this stage that, any work concerning the thermal charaterition of **concrete made with crushed crystallized slag aggregate** has been made so no information are available on the thermal proprieties of SSC, therefore it has been decided first to realize some measurement of thermal proprieties of SSC, for this purpose four series of samples with different compositions (aggregate dimension) have been fabricated The 28 days compressive strength of SSC measured at the laboratories of Genie civil UBMA was around 20 MPa for all series their thermal properties have been measured at the laboratory TREFLE (ENSA of Bordeaux) using hot disk technique as described in the last section of the work.

4.5.1 Materials and fabrication,

4.5.2.1 Slag Concrete properties

Slag Concrete of design strength of around 20 MPa was produced using commercially available materials with mixing using vibrators and simple curing techniques. The mix design for the four series is shown in Table 1. These grades of concrete are designated as controlled concrete. Standard cube tests were used to determine the compressive strength of the SSC which was around 20 MPa.

Table 4.1. Slag stone concrete mix properties

Cement content	350. kg/m^3
Water-cement ratio	.50
crushed slag stones	1200. kg/m^3
Sand of crushed slag 2/5	600. kg/m^3
Slump	70. mm
Compressive strength at 28days	20. MPa
Ec	21. GPa

The only changed component was the dimension of the Crushed slag stones as follows :

- First mix **SM1** used 10 mm crushed slag stones
- Second mix **SM2** used 12 mm crushed slag stones
- Third mix **SM3** used 15 mm crushed slag stones
- Fourth mix **SM4** used 20 mm crushed slag stones

Fig 4.13 sample befor test

Fig 4.14 Hot disk Test Processing

Fig 4.15 Probe disposition between samples.

For each mix, three 50 mm _ 50 mm _ 150 mm samples were prepared, also for each mix two more (150 mm _ 150 mm _ 150 mm) cubes were prepared and tested after 28

days in order to assess the Compressive strength at 28 days which was around 20MPa.

4.2.5.2 Testing procedure.

The thermal conductivity of each mix has been measured using the Hot Disk method this transient method is based on the measurement of the temperature increase at a defined distance from a linear heat source (hot wire) embedded between two samples of the tested material.

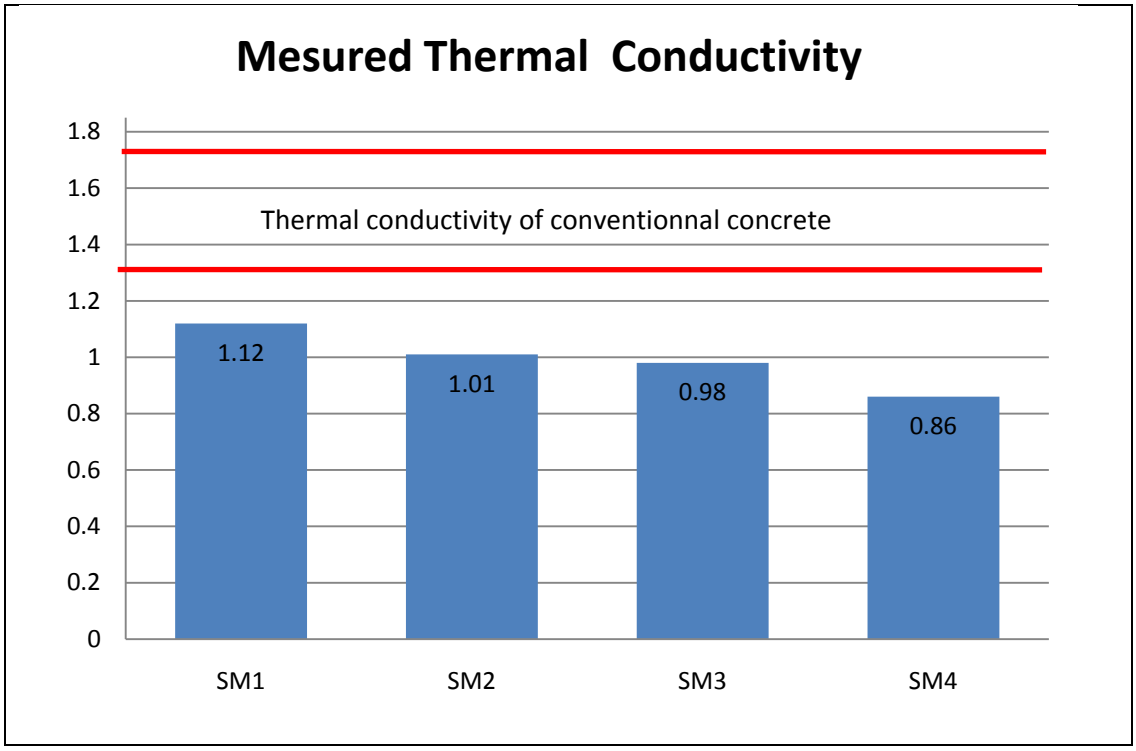

The thermal conductivity of conventional concrete 1.28 -1.75 w/mk
The thermal conductivity of steel 46 w/mk.

4.5.3 Results and discussion

For each mix, three specimens have been measured. Table 1 presents the average values of thermal conductivity. As expected, the conductivity is increasing with decreasing aggregate as the void ratio decrease. Values between 1.12 and 0.86 W m−1 K−1 have been found. These value still below the conductivity of the conventional

concrete, as there a gain of between 48% which is very important in the total calculation of heat loss through the whole building.

Tabe 4.02 Hot Disk Out put.

Mixte	Sample notation	Measured Thermal conductivity	average
SM1	**SM1.1**	1.13	1.12
	SM1.2	1.11	
	SM1.3	1.12	
SM2	**SM2.1**	1.04	1.01
	SM2.2	1.00	
	SM2.3	0.99	
SM3	**SM3.1**	1.03	0.98
	SM3.2	0.96	
	SM3.3	0.95	
SM4	**SM4.1**	0.94	0.86
	SM4.2	0.84	
	SM4.3	0.80	

As a conclusion the SSC an fill-in material for light steel tubs, contribute not only to the sustainable development by the use of recyclable materials but also contribute in the decreasing of the heat loss through these elements which may reduce the overall energy consumption in buildings.

It is not possible with the hot disk dispositive to measure the thermal conductivity of the studs, as the thermal conductivity of both materials are known, it is possible to calculate the thermal resistance of the filled stub by using either simplified calculation or simulations modelling.

Which is the aim of the next section which starts with a review and comparison of the current used methods then the heat transfer through these elements are modelled using of thermal network then a simplified calculations methods are presented.

CHAPTER 5
THERMAL PERFORMANCE OF LIGHT STEEL STRUCTURE (THEORETICAL APPROACH)

5. Thermal resistance calculations.

5.1 COMPUTER MODELLING AND STEEL FRAMED BUILDINGS

5.1.1 Introduction

The use of sophisticated computer modelling tools, such as dynamic thermal simulation to predict overall energy use and internal conditions, has become widespread over the last decade. In parallel with increasingly affordable and available computer processing power, such software has become more accessible to the practitioner working in the design field and is no longer purely in the domain of academic researchers. The introduction of accessible graphic user interfaces, such as virtual reality displays, means that a detailed knowledge of computing is no longer necessary to build a model and achieve useful results as long as the modeller has a good understanding of the relevant fundamental principles.

The range of software tools available to assist designers of buildings and their services is now quite wide, and includes the following overall classifications:

- Computational fluid dynamics (CFD): for detailed prediction of air flows (temperatures, velocity vectors) within internal spaces. Used, for example, to model room air temperature distributions and local flow vectors resulting from varying layouts of air inlets and outlets in both mechanically and naturally ventilated buildings, and to model smoke spreading in fire applications.

- Lighting design software: use techniques such as ray tracing to predict daylight factors in buildings and often produce photo-realistic output showing internal views at different times of day.

- Heat transfer modelling tools: for detailed modelling of steady state or transient heat transfer processes within individual construction elements, such as walls and windows, or within whole rooms. This building physics software uses techniques such as finite difference conduction analysis to predict

- temperature distributions, heat flows and properties such as equivalent thermal resistance (R) or U-value. Both 2D and 3D tools are currently available.
- Dynamic thermal simulation: whole building simulation software which enables a building, or part of a building, to be modelled geometrically, assigned thermal properties relating to the thermo physical properties of the materials in each element of its construction, and to be subjected to real recorded weather data over the course of a year. Ventilation can be set at a certain rate, or many packages now enable variable wind and temperature dependent ventilation rates for naturally ventilated buildings to be modelled by use of a linked multi-zone bulk air movement facility. These modelling tools can be used to compare different design options, for example glazed area, and their effect upon both energy use and internal comfort conditions.

Computational fluid dynamics and lighting design software is dependent more upon geometry (layouts of spaces, windows, and inlets/outlets) than construction method, and as such will not be dealt with in more detail here. More information on all these software tools is available elsewhere ref 38. However, methods of heat transfer analysis programs based on thermal net work are considered, as they apply to steel-framed buildings.

5.1.2 Heat transfer modelling tools

Overview

Computational heat transfer modelling can be used to assess all heat transfer processes (conduction, radiation and convection) occurring within a structure or space. In practice, conduction analysis is the most commonly used technique, with radiation and convection processes being modelled in relation to cavities within a structure.

Calculation methods

Conduction can be modelled numerically using finite difference techniques to compute temperature or heat flow through discrete nodes. Conduction is a highly

predictable process, and hence possible to model with a high degree of accuracy if the thermo-physical properties (thermal conductivity, specific heat capacity and density) of the materials are known. The object to be analysed is represented as a nodal network or mesh, for which it is assumed that each node has a uniform temperature dictated by the temperature of surrounding nodes (steady state conduction) or by the temperature of surrounding nodes at the previous time step (transient conduction). Equations for nodal temperature are derived using the energy balance technique that can be found in most heat transfer text books. These equations are solved to give a temperature for each node, either in the steady state or at each chosen time step for transient heat transfer problems. When radiation and convection heat transfer is also modelled (such as in a cavity), other techniques are used in parallel. The radiative heat transfer component is determined as a function of all relevant view factors in the enclosure and surface emissivities. Convective heat transfer is evaluated using non-linear empirical equations linking natural convective heat transfer coefficients and enclosure air and surface temperatures.

The heat balance equations.

At each node a heat balance equation is written using an explicit or implicit formulation. Explicit methods have the advantage that future temperatures can be predicted at each time interval. This means that computation of each node's temperature requires little computational power and can be done using a hand calculator. The major disadvantage is that stability is a function of the time step used and the solution may require extremely short time intervals and consequently a large number of calculations for one day simulations.

Implicit methods of solutions result in a series of simultaneous equations describing the whole network with the future temperatures at each node being the unknowns. As there is one equation for each unknown temperatures simultaneous solutions of the equations results in the calculations of all unknown temperatures. This method requires the ability to solve a large number of simultaneous equations and store the matrix of coefficients at each time step. Thus greater computational capacity is required but the solution is inherently stable.

In the most complex formulation each node will have thermal capacity and there will be conduction or convection and radiation to other nodes. Solar radiation may fall on a node or there may be environmental plant which passes heat to or from the nodes. For each the energy balance may be written:

$$Heat_{in}^{t} - Heat_{out}^{t} = Change\ in\ stored\ enegy^{t}$$

Where the superscript t refers to the time over which the energy flow occurs.
For a single node heat transfer (ϕ) may be conduction, convection or radiation, and the equations describing the heat transfer are:

a) Conduction

In the Hypothesis of mono-dimensional transfers, the heat conduction may be written, in the form references [18, 28, and 41]:

$$\frac{d^2T(x,t)}{dx^2} = \frac{1}{a}\frac{dT(x,t)}{dt}$$

In a no homogenous two layers case with low thickness (Δx_n), the conduction equation in discrete form is written as:

$$\frac{T(x+(\Delta x_1),t)-T(x,t)}{R_1} - \frac{T(x+(\Delta x_2),t)-T(x,t)}{R_{21}} = C\frac{(dt(x,t))}{dt}$$

The layers are characterized by their Resistance, R and its thermal capacity C:

$$R = \frac{\Delta x}{\lambda} \quad \text{and} \quad C = \rho C_m \Delta x_n S \quad Or \quad C = \rho C_m V$$

For a single node heat transfer ϕ to other nodes the equation describing the heat transfer by conduction is:

$$\phi_{cond} = \frac{A\lambda\Delta T}{x} \quad \text{Or} \quad \phi_{cond} = \frac{A\Delta T}{R}$$

b) Convection

The convective heat flow exchange between a wall surface at temperature T and an air volume at temperature T_a can be expressed with Newton equation reference [40]:

$$\phi_{conv} = h_c A(T - T_a)$$

For convective resistance is:

$$R = \frac{1}{h_r}$$

The convective heat transfer coefficient h_c depends on the thermal proprieties of the fluid and the state and the geometry of the flow. For natural convection which is our case the CIBS reference [11] recommended the following values:

Inside building

Walls to air 3.0 W/m²K
Ceiling to air 4.5
Floor to air 1.5

Outside Building: For surfaces the value of h_c is a function of the wind speed across the surface and the expression commonly used reference [11] is:

$h_c = 5.8 + 4.1\ v$ where v is the air speed across the surface [m/s].

Three standard conditions are defined for external convective coefficient:

Severe v=9.0 m/s, exposed site, 5th floor suburbs, 9th floor city.
Normal v=3.0 m/s, up to 4th floor suburbs, country, 4-8th floor city.
Sheltered v= 1.0 m/s up to 3rd floor city.

And the heat flow by Convection can be expressed by:

$$\phi_{conv} = \frac{A\Delta T}{R_{conv}}$$

c) Long wave radiation

The external surfaces of the walls exchange LW radiation with the sky and the external environment. The heat flow can be written in a linear form reference [15]:

$$\phi_{rad}^{ext} = h_{r_{vc}} A(T - T_c) + h_{r_{env}} A(T - T_{ext})$$

If we represent the sky by means of a half-sphere and the external environment by a horizontal plane, the radiative heat transfer coefficients are respectively:

$$h_{r_{vc}} = 4\varepsilon\sigma \frac{1 + cos\beta}{2} \left(\frac{T + T_c}{2}\right)^3$$

$$h_{r_{env}} = 4\varepsilon\sigma \frac{1 + cos\beta}{2} \left(\frac{T + T_{ext}}{2}\right)^3$$

Inside the building, there are several methods, which evaluate, in a more or less approximate way, radiatives exchanges between surfaces references [15, 18]. We retain a linear equation expressing the radiative flow between a wall and all the others walls:

$$\phi_{rad}^{int} = h_r A(T - T_m)$$

The value of h_r depends on the mean temperature of the walls T_m:

$$h_r = 4\varepsilon\sigma T_m^3$$

Typical values of h_r are: 5.70 for T=20°C (293°K)
4.61 For T=0°C (273°K)

The radiative resistance is:

$$R_{rad} = \frac{1}{h_r}$$

And the heat flow by radiation can be expressed by:

$$\phi_{rad} = \frac{A\Delta T}{R_{rad}}$$

The similarity of the equations of these three modes in that heat transfer is directly proportional to a simple temperature difference for a given area leads to the description of heat flow by conduction, convection or radiations between nodes in the form:

$$\phi = K_{ni}\,\Delta T$$

Where: K_{ni} is the thermal conductance between the nodes n and i.

The units of conductance are W/°C or J/s°C and it can be thought of as the heat flow per unit temperature difference per second.

As a result of heat flow to the node, the node may change in the temperature. This change is determined by the thermal capacity associated with the node, thus for a heat flow ϕ (J/s) into a node for a time t seconds the energy balance may be written as:

$$\phi = V\rho C\frac{T_t - T_0}{t}$$

Where V is the volume associated with node, ρ is the density of the surrounding material, C is the specific heat, T_t is the temperature of the node after t seconds, and T_0 is the initial temperature of the node, this equation may be written:

$$\phi = C_n(T_t - T_0)$$

Where: C_n is the capacitance of node n which has the same units as conductance W/°C.

In addition to heat transfer between nodes solar energy may cause heat transfer to a node. This will obviously depend on whether the node is seen by the sun, and its magnitude will depend on the presence of attenuating surfaces such as windows which reduce the solar input.

d) Examples

Consider a three internal node system (1), (2) and (3) with another node (a) to represent the outside air temperature. The most complex heat exchange pattern may be represented by a network shown in **figure 5.1.**

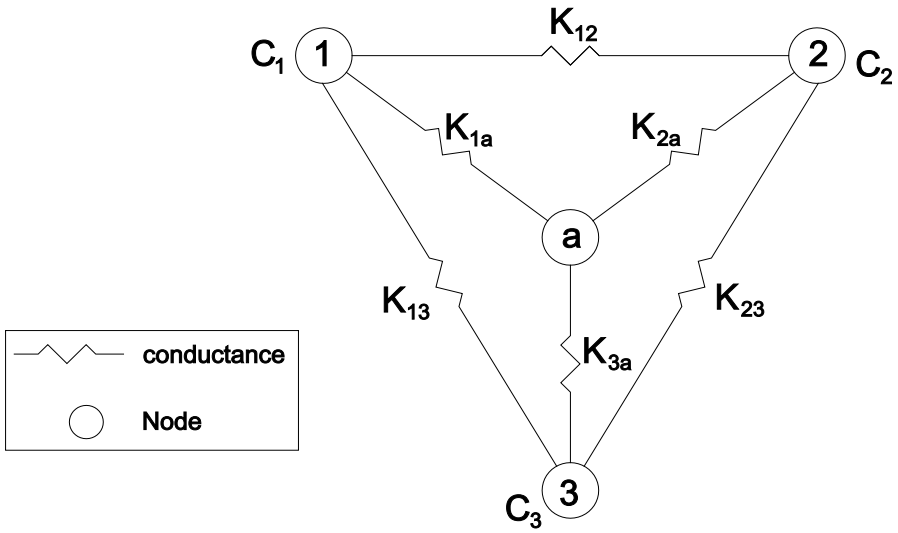

Fig 5.1. Network Representating the Heat exchange between
Three internal nodes (1,2,3) and an ouside air temperature node (a)

The temperature T_1, T2 and T_3 can represent the node temperature at the time t or at the time t+∂ where ∂ is the time step employed in the simulation.

If they are the temperature at the time t it assumed that they are all known and an explicit from of the heat balance equation results with the only unknown temperature being T_1 at time t+∂. As has been already noted the implicit formulation is to be preferred and the energy balance for node 1 may be written as follows.

$$K_{12}(T_2-T_1)+K_{13}(T_3-T_1)+K_{1a}(T_a-T_1)+Q_{s1}= C_1(T_1-T_1^t)$$

Or

$$T_1(K_{12}+K_{13}+K_{1a}+C_1)+T_2(-K_{12})+T_3(-K_{13}) =T_1^t(C_1)+T_a(K_{1a})+Q_{s1}$$

Where Ta is the air temperature and Qs1 is the solar radiation absorbed by the node 1 during a time interval ∂.

In this form the unknown nodal temperature and the known solar radiation and the air temperature are at the time t+∂. The only superscript variable T^t is the known node temperature at the time t. similar equations may be written for the others nodes:

$$T_1(-K_{12})+T_2(K_{21}+K_{23}+K_{2a}+C_2)+T_3(-K_{23}) = T_2^t(C_2)+T_a(K_{2a})+Q_{s2}$$

$$T_1(-K_{31})+T_2(-K_{32})+T_3(K_{31}+K_{32}+K_{3a}+C_3) = T_3^t(C_3)+T_a(K_{3a})+Q_{s3}$$

These nodal equations may be rewritten:

$$B_{11}T_1 + B_{12}T_2 + B_{13}T_3 = D_1$$

$$B_{21}T_1 + B_{22}T_2 + B_{23}T_3 = D_2$$

$$B_{31}T_1 + B_{32}T_2 + B_{33}T_3 = D_3$$

Where:

$$B_{ni} = C_n + \sum K_{ni} + K_{na} \qquad \text{for } n=i$$

$$B_{ni} = -k_{ni} \qquad \text{for n not equal to i}$$

$$D_n = C_nT_n + K_{na}T_a + Q_{sn}$$

These equations may be solved for the unknown nodal temperatures using standard procedures for solving simultaneous equations.

5.1.3 Simulations procedure

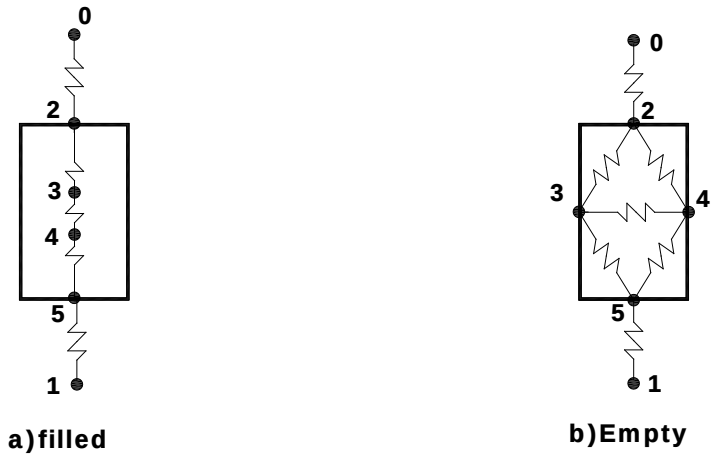

Fig 5.2 Sub network representing the heat exchange throught an empty and Filled stubs

Empty stub: the heat exchange inside the stub is more complex and represents the combination of convection and radiation, so there is convection plus radiation between the surfaces.

Filled stub : the heat exchange inside the stub is only by conduction through the Slag Stone Concrete.

Six heat equations for each case are set and then solved for the unknown temperature as far as the thermal conductivity, and thermal capacitance of each materials are known, Thermal resistance between any nodes can be then calculated.

The results gives a thermal resistance of 0.28 for filled stubs and 0.36 for empty stubs, however, there is an increase of thermal capacitance of the filled stubs caused by the slag stone concrete, this gain in the thermal capacity, gives the filled stub greater ability to absorb heat when ambient temperatures are high and cool down slowly when ambient temperatures are cool, whereas the empty stub with a low thermal capacitance has a quick respond to the temperature change.
In order to evaluate the overall thermal response of the wall and to show in more details the influence of the thermal capacitance on the temperature swing a heat transfer modelling of a part of wall with both cases has been made (see figures 2.00 and 2.00), and simulation of the both models over an entire days are realised, two typical days are chosen summer and winter days results are summarized in graphs fig 2.1. these show clearly that the wall with empty stubs has a more quick response to the temperature change and the internal temperature swing are similar to the external temperature, whereas in the case of the wall with filled stub, the temperatures swing is very different from the first case and also slightly different from the external temperature and this is caused by the higher thermal capacitance of the SSC which gives the whole wall greater ability to absorb heat when ambient temperatures are high and cool down slowly when ambient temperatures are cool which is very relevant in the Algerian climate characterize by a very great temperature difference within a day which may reach 12°C.

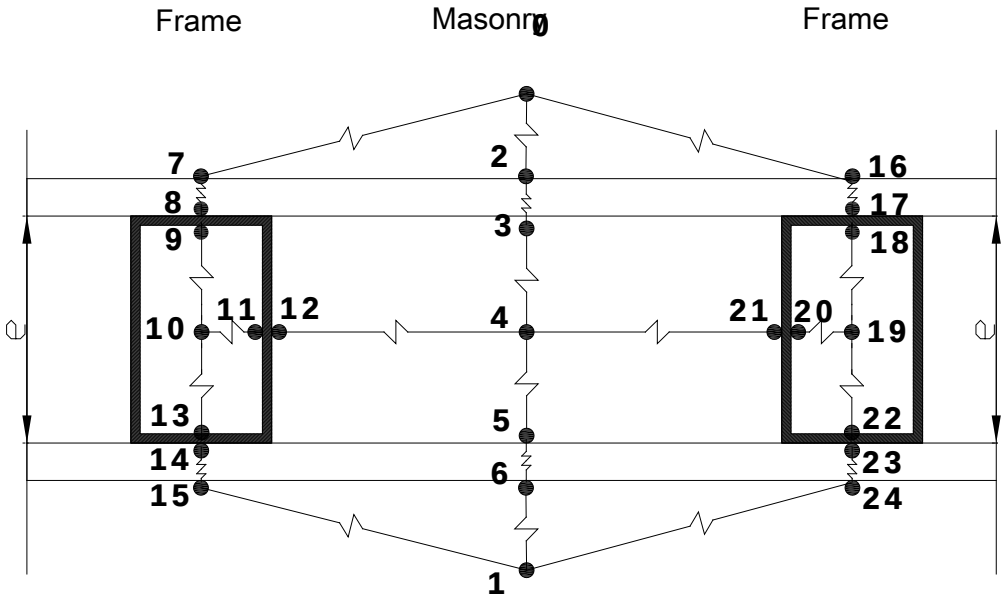

Fig 5.3 Thermal network representing the heat exchange throught a wall with filled stubs

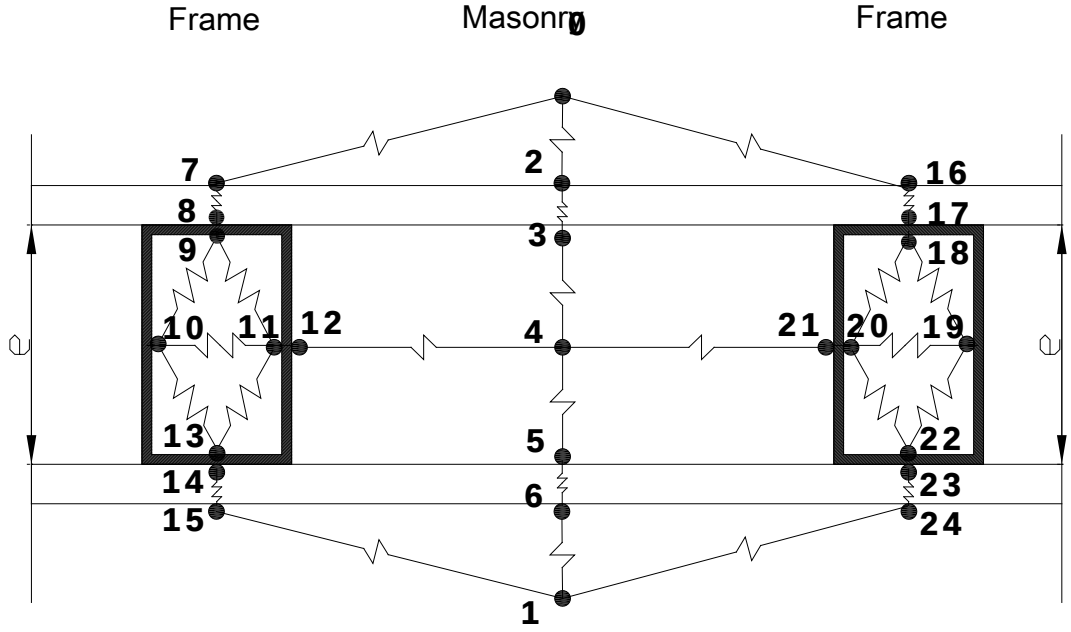

Fig 5.4 Thermal network representing the heat exchange throught a wall with emplty stubs

5.1.4 Conclusion.

The use of SSC as in filled material for the steel , contribute not only to the thermal resistance compared to ordinary concrete made with conventional aggregate, but the thermo characterization of sample of SSC has shown that conductivity of SSC is less by 48% than ordinary concrete.

Hot disk measurements and calculations using finite difference modelling has been carried out simultaneously have shown good correspondence between measured and simulated values. Such computer models are now becoming increasingly available but require some specialist knowledge and training to use and are time consuming.

5.2 Simplified thermal resistance calculation of a wall with steel stubs:

This section reviews various proposed simplified methods for calculating the thermal resistance of a light steel structure assembly. These are often used for design purpose as they are simple and easy for use gives very good results.

The resistance to heat flow through the envelope of a building is usually quantified by the thermal transmittance (U-value) or thermal resistance (R-value). Based on the geometries and the proprieties of the materials used, these values can be measured for a given materiel by tests as it was shown in the last section. Alternatively, accurate predictions can be also made using 2 or 3 dimensional finite difference or thermal net work modelling (see last section).

Simplified methods for calculating an approximated U-value for an assembly of the building envelope have been developed. The basis for simplified heat loss calculations through building elements is the apparent thermal conductivity, λ, of a material measured in W/mK. From this basic material characteristic, the thermal resistance of any uniform homogenous layer is calculated as follows:

$$R = \frac{\lambda}{e}$$

Where λ is the material thermal conductivity in W/mK

e is the thickness of the layer in m.

For structures comprising of several layers, the R-value is found simply by summing up all the individual R-values of each layer as follows:

R total =Rt = Rsi + R1 + R2 + R3 + …….Rn +Rse (m2 K/W)

The resistance of the internal and external surfaces to heat flow (Rsi and Rse) must be included to find the total resistance. The total thermal transmittance (U-value) is calculated by:

U-value = 1 / Rt (W/m2K)

This procedure is accurate if the real construction is merely a set of homogenous layers. However, many structures are more complex and often contain layers that do not consist of one homogenous material. For example, in light steel or framed construction, the framing material is often interspaced with masonry including insulation all in the same "layer" of the material. Other examples include air gaps between insulation, mortar between blocks in masonry construction and fixings through cavities.

5.2.1 Light steel structure

In light steel structured construction, the space between the steel elements is often filled with masonry (brick wall and insulation or air gap). Together, this forms one layer. Although, the steel web usually forms less than 0.5% of the area of the wall, the steel has a thermal conductivity which is very higher than the material type on either side. It has been shown that ignoring the effect of the steel within this layer can lead to an overestimation of the thermal resistance of the construction by up to 50%, depending on the details of the construction.

5.2.2 Review of Simplified calculation methods

There has been considerable debate over simplified methods for U-value calculations that can accommodate the effects of non-homogenous layers and thermal bridges. Generally, two approaches have been proposed:

- Parallel Path method
- Isothermal Planes method

Parallel Path method

The *Parallel Path method*, which is described in the ASHRAE 1997 Handbook - Fundamentals3, assumes simple one dimensional heat flow perpendicular to the face of the element, i.e. that heat flow through the thermal bridge is parallel to the heat flow through the masonry and there is no lateral distribution of heat between the framing material and the masonry. Thus, the thermal resistance through the framing element is calculated and a separate thermal resistance through the masonry is calculated. These are then area weighted for the total element, depending on the proportion of framing material to clear wall.

Fig 5.5 Parallel flow method

R parallel path = Rpp =1/(Aframe / Rframe) + (A insulated / R insulated) (m2K/W)
Where R frame is the thermal resistance calculated through the steel frame and
R masonnery is the thermal resistance of the assembly calculated through the mesentery part of the assembly. A frame is the fractional area of the frame (ep/L) and A massonery is the fractional area of masonry (1-ep/L).

Isothermal Planes method

The *Isothermal Planes method* (ASHRAE 1997 Handbook - Fundamentals) ref [ ] assumes that the temperature is uniform at each plane parallel to the face of the element, i.e. that heat flow through the structure is completely redistributed at each layer (isothermal plane) and there is no resistance to lateral heat flow. This is representative of assemblies with highly conductive panels. Thus, the area weighting is applied to each layer individually, and the R-value of all the layers is summed to give the total thermal resistance.

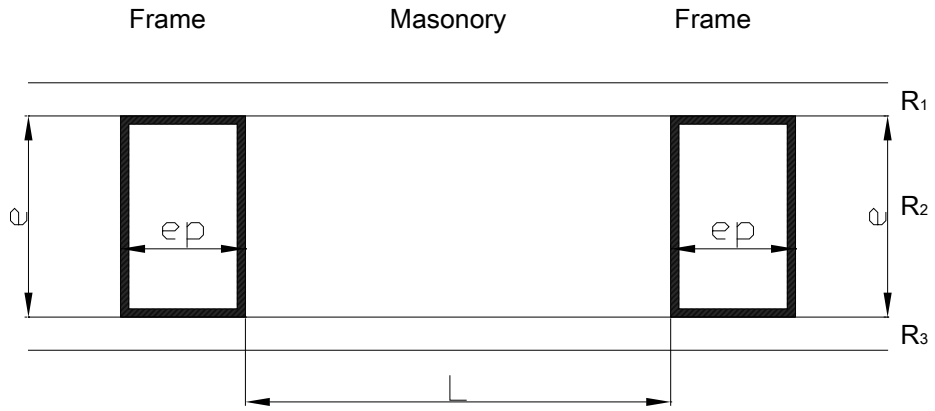

Fig 5.6 Isothermal plane method

R isothermal plane = Rip = Rsi + R1 + R2 + R3 + Rse (m2K/W)
Where R1 is the thermal resistance of layer 1 and R2 is the thermal resistance of layer 2 and is calculated as follows:
R through bridged layer = R2= 1/[(Aframe/Rsteel) + (A masonry/Rinsulation)] (m2K/W)

And R3 is the thermal resistance of layer 3.

The EN ISO 6949:19964 has described the parallel path method as the upper limit to total thermal resistance and is likely to be optimistic, while the isothermal plane method is described as the lower limit to total thermal resistance and is likely to be rather conservative. The ASHRAE Book of Fundamentals suggests that the two provide an upper and lower limit and a true examination of the construction will usually reveal whether a value closer to the higher or lower calculated value should be used. When highly conductive layers that enhance lateral conduction are present, as occurs in steel framing, a value closer to the isothermal planes method may be more appropriate. It should be noted that these are calculation procedures.
They have been found to be useful tools, but they are not necessarily a correct description of what is happening to the heat flow.

The thermal performance of construction assemblies using light steel structure, where the steel components form thermal bridges through part or all of the insulation layer, may not be suitable for assessment using the above simplified models. The main issue centres around the implicit assumptions within the models being at odds with the huge difference in thermal conductivity of the steel and the insulation material. Several variants on the above calculation procedures have been developed to improve the accuracy of prediction for steel frame constructions.
These are reviewed below:

5.2.2 .1 Averaging of parallel path and isothermal planes

EN ISO 6946:19964 presents a method for calculating the thermal resistance and thermal transmittance of building elements using an averaging of the parallel path and isothermal planes methods (50/50 rule). Thus:

R total = Rt = (Rpp + Rip) / 2

Where Rpp is the total thermal resistance of the element using the parallel path method, and Rip is the total thermal resistance of the element using the isothermal planes method.

This averaging (50%/50%) of the two extremes has been found to correspond well with measured guarded hot box test results for various construction types. Comparisons carried out by a joint project between BHP and Dofasco5 found that, by using the method of least squares analysis on test and calculated data of steel framed assemblies, the following proportions were found:

R total = Rt = 0.45 Rpp + 0.51 Rip

This is very close to the 50/50 averaging rule and within the accuracy of the data available. This project found that the 50/50 rule gave a prediction within 10% of tested data for most assemblies, with a greater inaccuracy only for wall stubs 150 mm deep, and with no external thermal sheathing. It was found that similarly increased inaccuracies occurred for timber as well as steel-framed assemblies.
However, the text of ISO 6946 does exclude this method for use when "an insulation layer is bridged by a metal". Nevertheless, the 50/50 rule has been used for light steel frame structures and is recommended for use in some countries.

5.2.2 .2Danish Standard DS418

When using a combined isothermal plane/parallel path method, as suggested in EN ISO 6946, it is possible to adjust the weightings to suit empirical data. It has been found that the 1:1 weighting best represents wood frame construction and masonry construction. However, a weighting of 2:1 (isothermal plane: parallel path) has been suggested from various test data to better represent the performance of light steel frame construction. The Danish standard DS418 use this method for steel framed construction, and it was initially proposed by the Canadian Model National Energy Code6 thus:

R total = Rt = (Rpp + 2 Rip) / 3

Research by Oak Ridge National Laboratory, together with Enermodal Engineering [30], showed that the 50/50 rule, as recommended in EN ISO 6946:1996, gives greater accuracy for typical steel frame assemblies used in North America. However, the 2:1 weighting was found to provide more conservative and more consistent results, with less variation from specimen to specimen.

5.2.2 .3 Canadian Model National Energy Code

The Canadian Model National Energy Code7 (MNEC) contains prescriptive requirements for the thermal performance of envelope assemblies. For timber framed elements, the use of the parallel path calculation method is recommended for calculating thermal resistance. However, since no single method for light steel frame assemblies had widespread acceptance in North America, further research was undertaken to develop a methodology[31].
This consisted of reviewing existing measured data and carrying out further tests of the thermal resistance for ten full-scale (2.44 m x 2.44 m) wall specimens built with steel stubs using a guarded hot box. Separate measurements were undertaken of the thermal properties of the materials used to construct the test specimens so that these accurate figures could be used when refining the calculation method.
The measured and calculated results were then compared and the accuracy of the calculation method was investigated. The project also evaluated the effects of alternative sheathing, stub spacing and stub gauge.

It was proposed that the model code should use a combined method using both the parallel path and isothermal planes method and weighing the two values appropriately. The weighing of the two values was to be determined empirically using the data from the guarded hot box tests. Analysis of the tests and other recent work on this subject suggested that the weighting could vary depending on the configuration of the construction. Initially a weighting of 2:1 (isothermal plane: parallel path) was investigated.

It was found that the most accurate calculated predictions were achieved when the weightings were varied depending on the details of the construction. Thus, in the final proposal for the Model National Energy Code, the following method is used:

Total thermal resistance Rt = (K1 x Rpp) + (K2 x Rip)
Where Rpp is the thermal resistance of the element calculated using the parallel path method
Rip is the thermal resistance of the element calculated using the isothermal planes method.
The constants K1 and K2 are as follows:

Table 5.1 *Weighting factors used in the Canadian MNEC method for calculatin U-values*

Frame Spacing	**K1**	**K2**
< 500 mm without insulating sheathing	1/3	2/3
< 500 mm with insulated sheeting	2/5	3/5
> 500 mm in all cases	1/2	1/2

These weightings gave agreement within +7.5% in all cases.

5.2.2 .4 The Modified Isothermal Planes method

A joint New Zealand/Australian standard for determining the thermal resistance of building components and elements, DZ 4214, is currently under development. The proposed calculation method is a modified, one dimensional, isothermal planes method which was developed by the Building Research Association of New Zealand (BRANZ)[4]. The method was developed, in particular, to deal with steel framing and has been calibrated against actual measurements using guarded hot box equipment.
In this calculation method, a steel stub is replaced by a notional rectangle with the same overall width and depth (Figure 5.7) as the stub. However, the thermal conductivity used in the calculation is the conductivity of steel multiplied by the ratio of the web thickness to the flange width (Figure 5.7). The justification for this is that

the thermal conductivity of the steel is so high that even a very thin cross-section offers little resistance to the transfer of heat. A 50 mm depth of steel will have a thermal resistance of only 0.001 m2 K/W. Thus, in general, steel frames have very small temperature gradients along the steel web and effectively approach an isothermal state. Thus, the temperature on the outer flange is almost the same as that on the inner flange. Therefore, the shape of the steel component is not important and can be replaced by a notional equivalent solid rectangle with a modified conductivity.

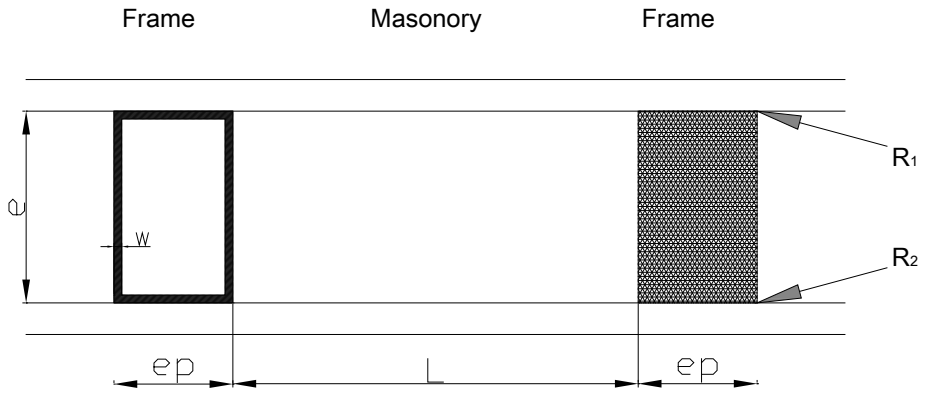

Fig 5.7Transformation of stud into a notional equivalent solid rectangle

Furthermore, from measurements with the hot box, BRANZ found that for steel framing calculations, it is important to allow for contact resistance (see next section) between the stub and the cladding or lining, and to include the important real world aspects such as cavity ventilation and the influence of fixings. The contact resistance is particularly relevant for light steel framing, due to the low thermal resistance of steel. Building materials, when assembled, never fit together perfectly and a thermal contact resistance exists between them. A typical value for building materials may be only 0.02 to 0.06 m2K/W, and this may only contribute 0.1% to a typical R-value and is of little significance in most constructions. However, when contact resistances of 0.03 m2K/W occur in series at each face of a steel component which may have a resistance of only 0.04 m2K/W, the contact resistances become a significant part of the overall R-value of 0.1 m2K/W.

Thus, to calculate the effective thermal resistance through the steel frame component the BRANZ method adds the contact resistances Rc1 and Rc2to the thermal resistance of the steel, follows:

Rsteel = [(d / k) x (w / t)] + Rc1 + Rc2 (m2K/W)

The Rsteel value is then applied in the normal isothermal plane calculation outlined earlier.

Note that the implication of the transformation into an equivalent solid rectangle is that the sectional shape of steel is not very significant. BRANZ [4] have measured the variation with shape to be within 3%. Figure 2.4 compares guarded hot box measurements with calculations made using the BRANZ modified isothermal planes calculation method. The test wall was a brick veneer system, with the bricks left in place and frame changed from wood to steel and insulated with either foil, glass-fibre blankets, expanded polystyrene, or combinations of the three types. The calculated figures for steel frame constructions are within 0.2 m2K/W of measured values for 87% of cases.

The calculations for light steel framed walls over a considerable range of R-values are no less accurate than those for timber framed walls. This suggests that any inaccuracies are likely to be due to the aspects of the construction that have not been allowed for, such as cavity venting and the effects of ties, etc. rather than an inherent bias in the calculation method. The calculations are always within 10% of measurements and generally within 5%.

5.2.2 .5 The Modified Zone Method

The Modified Zone Method (MZM) is based on the Parallel Path Method and the ASHRAE Zone Method [1]. The only difference between the three methods is the way in which the area of wall affected by a thermal bridge is accounted for. The parallel path method assumes the zone affected by the thermal bridge is only the actual geometric area of wall where the bridge is present. The zone method accounts for the fact that a thermal bridge acts over a larger area than the geometrical area of thermal bridge itself. It takes into account the geometric dimensions of the stub flange and layers of material between the flange and the wall surface to calculate a wider

area of wall affected by the thermal bridge. This improves accuracy, but further improvements can be achieved by considering additional factors including:

- Ratio of resistivities of cavity insulation and sheathing material.
- Thickness of sheathing material.
- Stub depth.
- Stub flange size.
- Stub metal thickness

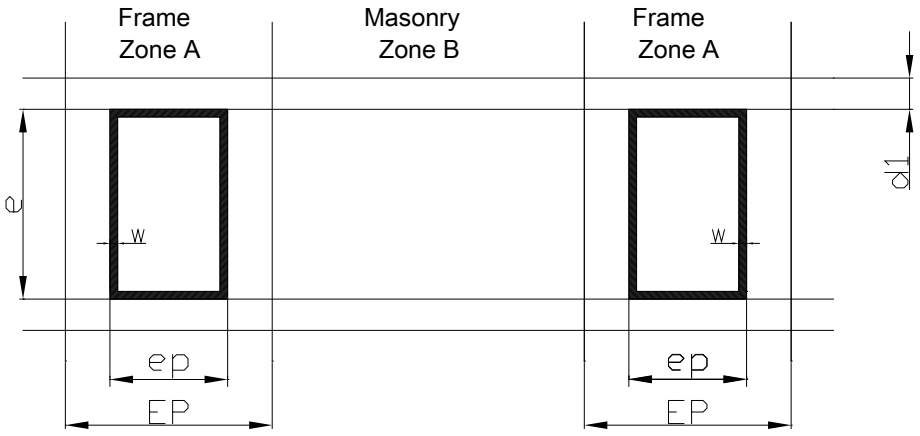

Fig 5.8 Zones for the modified zone method

When calculating thermal resistance using the parallel path method, the wall is divided into zones. In Figure 5.8, zone A is the part of the wall with the steel framing and is affected by the thermal bridge and zone B is assumed not to be affected by the thermal bridge. The width EP of zone A, is used to calculate the area of the zone affected by the stub. For simple parallel path calculations, the width of zone A is assumed to be the thickness of the stub web ep. And a distance doubles that from the wall surface to the steel flange surface d1. Thus, the width w of zone A is given as follows:

For Parallel path w = EP
ASHRAE zone method w = EP + 2d1

The work to improve the accuracy of the ASHRAE zone method for light steel framing was undertaken at Oak Ridge National Laboratory (ORNL) and the National Association of House builders (NAHB) Research Centre in the USA.[30]A total of 23 hot box tests were carried out on 2.44 m x 2.44 m specimens and the results were used to calibrate a finite difference thermal modelling programme.
This was used to carry out over 1,000 two-dimensional computer simulations on metal frame walls. R-values calculated using the ASHRAE zone method was compared with the results of simulations. These indicated that, for most configurations, the ASHRAE zone method over predicted the impact of the thermal bridge on the overall R value whiles the parallel path method under predicted the impact of the thermal bridges.

The effect of all the wall design parameters was estimated by means of a parametric analysis and a new, more precise, modified zone method of predicting the thermal impacts of steel stubs in walls, and was developed. To more accurately reflect the impact that zone A has on the overall thermal resistance, the modified zone method introduces a zone factor Zf. This is a variable parameter used to adjust w, the width of zone A. Thus:

For modified zone method w = L + Zf d1

In effect, for the ASHRAE zone method, the zone factor Zf = 2,
And for the parallel path method Zf = 0.
As a result of the parametric study, it was shown that the zone factor is mostly affected by the:

- Ratio between the thermal resistivity of the sheathing material and the cavity insulation.
- Size (depth) of the stub.

- Thickness of the sheathing material

The value of the zone factor Zf is taken from Figure 5.2. These curves were generated from the comparison of simulated and calculated data.

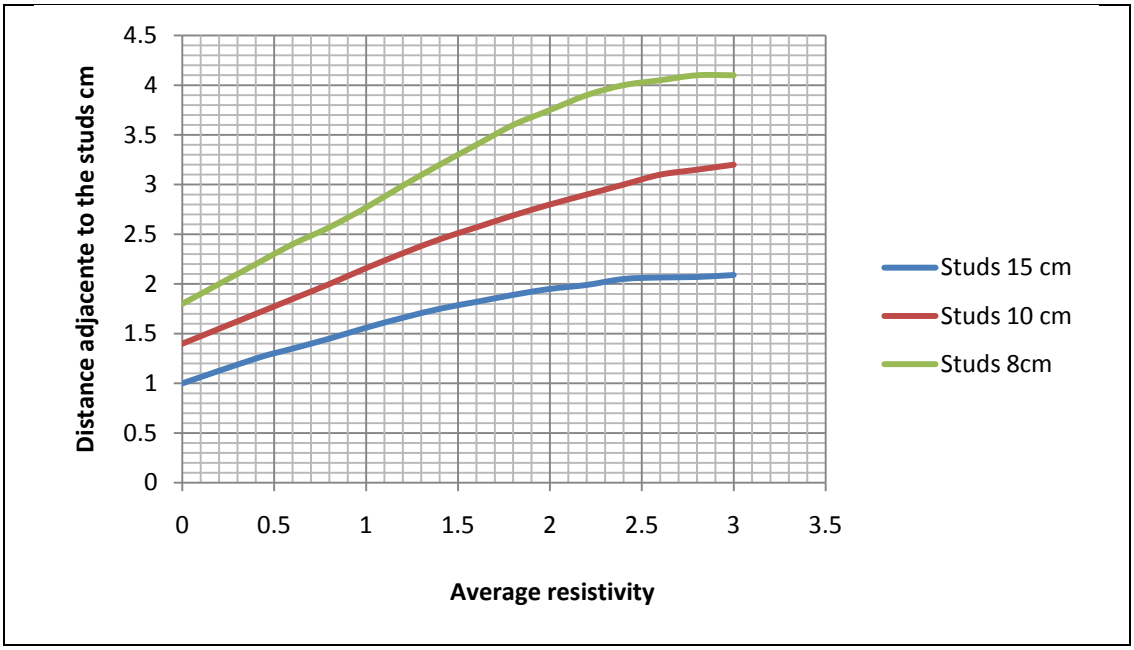

The accuracy of the modified zone method was verified for over 1000 simulated cases of metal frame walls. The discrepancy between the simulated and calculated results were within the range – 4% to + 14%. In addition, hot box tests of 15 metal stub walls were compared with the modified zone method calculation. The average error was found to be only 6.5%; the largest error was 13.3%. The modified zone method is one of the methods recommended by the ASHRAE book of
Fundamentals 1997 for R-value calculations for steel stub walls.

5.2.2 .6 Comparisons and conclusion

Comparisons have been carried out of some of the above simplified calculation methods to assess how they compare to measured results or simulated figures, using finite difference analysis, for light steel framing. In general, these have concluded that the 50/50 method proposed in EN ISO6946:1996 and the modified zone method provides the most accurate results.

Investigations carried out by BHP with Dofasco5, compared 39 timber and light steel assemblies and concluded that the 50/50 rule provides the most accuracy and is equally applicable to steel and timber framed assemblies. It was also found that the BRANZ modified isothermal plane method provides a good approximation of measured data, but requires a greater understanding of how to apply the method to obtain good results.

A joint Enermodal Engineering and ORNL study11 also concluded that if testing or simulation using finite difference modelling is not possible, then the 50/50 method should be used and will generally provide results within 10% of measured figures.

It found that the 2:1 rule used in Denmark provides more consistent results, but is less accurate overall. It also concluded that the modified zone method provides good predictions and is easy to adapt to a spreadsheet (it is now available on the internet).

However, the Canadian MNEC proposals were developed and refined after the above comparisons were carried out and seem to be a further refinement of the 50/50 approach. Comparisons between the 50/50 method and the MNEC proposals (which vary the weightings between the PPM and IPM depending on the composition of the assembly) have found that accuracy can be improved for some constructions by using the more refined MNEC method. Table 2.3 presents a comparison of test data with the predictions of R-values using:

- EN ISO 6946 method (50/50 rule)
- MNEC method (Canada)
- Modified Zone method (ORNL)

This shows that in most cases there is no difference between the MNEC and the 50/50 method proposed by EN ISO 6946. However, where the worst discrepancies occur, in the case where stubs are at centres less than 500 mm, accuracy is improved. The modified zone method also provides good predictions although the error range is slightly greater than for the MNEC method.

5.2.2 .7 Contact resistance

In general, building materials, when assembled, do not fit together perfectly and a thermal contact resistance exists between them. A typical value for building materials may be only 0.02 to 0.06 m2K/W. This may contribute only 0.1% to a typical R-value and is of little significance in most construction assemblies.
However, the ASHRAE Handbook - Fundamentals suggests that contact resistances can be important where highly conductive materials, such as steel, are used and suggests a range of values from 0.01 to 0.1 m2K/W can occur. A typical value of 0.035 m2K/W has been suggested. When contact resistances of 0.035 m2K/W occur in series at each face of a steel component that may itself have a resistance of only 0.04 m2K/W, the contact resistances become the major part of the overall R-value of 0.11 m2K/W.

An investigation of the effect of contact resistances was carried out at the Building Research Association of New Zealand (BRANZ). A 1.9 m2 wall panel constructed with a simple 80 mm deep steel stub wall assembly was used with foil faced gypsum board on the inner face, hardboard sheathing on the exterior side and the gap between filled with mineral wool or sheep wool bats. The gap between the gypsum board and the steel was varied from 0.5 mm to 3.0 mm.

The hot box tests found that the contact resistance varied between 0.02 m2 K/W for a 0.5 mm gap to 0.1 m2K/W for a 3.0 mm gap, as shown in Figure 5.3 Thus, the total R-value of the wall panel varied from 1.3 m2K/W to 1.51 m2K/W, depending on the gap between the steel and gypsum board. This is a variation of 16%. If a similar variation were assumed for the contact resistance between the steel and the external sheathing board, the overall R-value could vary by over 30%, depending on the contact resistance.

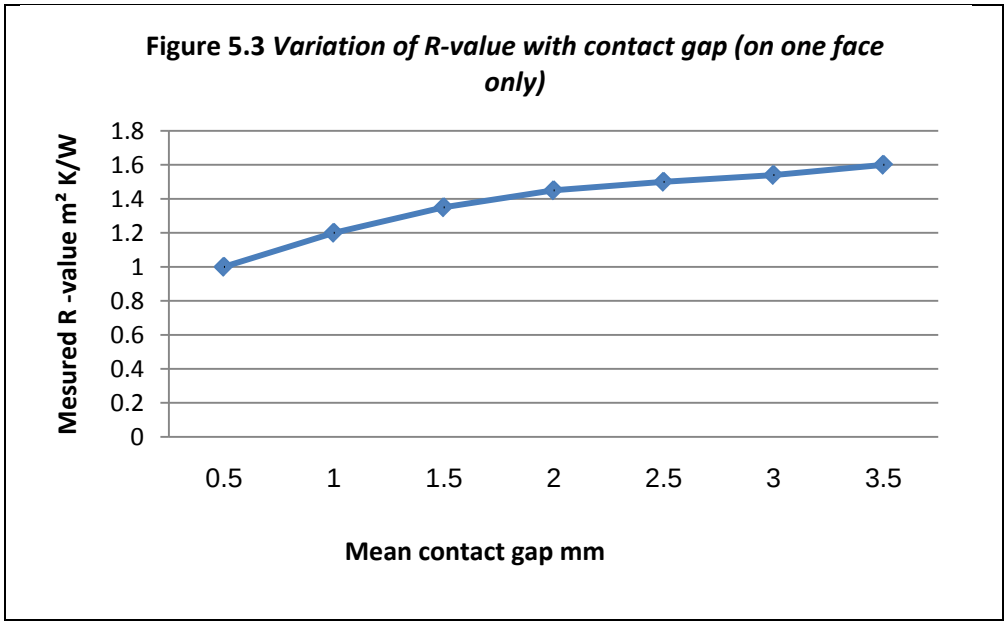

This is most relevant for light steel framing assemblies where there is no insulating sheathing board outside the steel frame. In cases where insulating sheathing is used, the thermal resistance through the steel and sheathing is greater, and so the contact resistance is less relevant.

The variation in R-value depending on contact resistance can explain why otherwise identical panels have shown significant variations in measured thermal resistance.

A study by Enermodal Engineering11 concluded that when carrying out finite difference simulation, the inclusion of typical contact resistances of 0.035 m2K/W, can improve the accuracy of predictions. Table 2.4 shows that for 6 assemblies, the average difference between simulated and tested results were reduced from -4.7% to +0.8% when including contact resistances. Overall, by including the contact resistances in the calculation procedure, the R-value increases by between 3% and 9%.

Ref	Simulated R-value (m2K/W)				
	Tested R-value (m2K/W)	No contact Resistance	% difference from test	With contact resistance	% difference from test
A1	1.38	1.23	-10.2%	1.35	-1.7%
A2	2.24	2.06	-6.3	2.15	-2.7%
A3	2.44	2.36	-3.0%	2.44	+0.1%
B1	1.68	1.56	-7.4%	1.72	+1.9%
B2	2.49	2.45	-1.3%	2.59	+3.3%
B3	2.77	2.77	0%	2.88	+4.0%

Table 5.4 *Comparison of test and simulated thermal resistance with And without contact resistances included*

In most U-value calculations and simulations, contact resistances are not considered. This may account for some of the differences between tested, simulated and calculated R-values. However, the Modified IPM proposed by BRANZ8, does require that contact resistances be included in the calculation.

5.3 DETAIL DESIGN OF LIGHT STEEL STRUCTURE - THERMAL ISSUES

This section reviews some of the most significant variables that affect the thermal performance of light steel frame construction.

5.3.1 How much insulation on the outside of the structure

Due to the high thermal conductivity of steel, creating a thermal break between the steel stub and the cold side of the building envelope is essential in most climates. The thermal break is usually achieved by adding board-type insulation to the cold side of the stubs with variety of approaches or rules.

A variety of rules have developed in different areas of the world about how much insulation is necessary on the outside of the steel framing:

- Some manufacturers in the USA advocate minimum of 25% of the overall R-value should be outside the steel frame.
- In Canada 30% to 40% of the thermal resistance outside the steel frame is sometimes quoted.
- In the UK and France it is generally felt that 50% to 60% of the overall Rvalue should be outside the steel frame.
- Typically, 12 mm of EPS insulating sheathing is used in New Zealand.
- Thermal sheathing is not generally used in Australia.
- In Algerian climate, more attention should be given to increase the thermal capacitance of stubs with low conductive materials, and this is achieved in our case by the use of slag stone concrete as …...

In general, it is difficult to assess the basis of these rules. A careful assessment of the necessary amount of insulation on the cold side of the frame, in various climatic conditions, would provide a useful tool for the steel industry, and a more reliable way to ensure that condensation problems do not occur.

5.3.2 Thermal impact of the shape of the steel stubs

Due to the high thermal conductivity of steel, even a thin steel section can transmit a large amount of heat. This means that the temperature difference between the inner and outer flange of the steel is generally very small. Some efforts have been made to design stubs with a thermal break to increase thermal resistance. However, in the case of a normal section, it is expected that the shape of the steel stub does not make a significant difference to overall performance. Furthermore, the relevance of the stub design will reduce if insulating sheathing is added to a wall construction.

5.3.3 Thermal impact of stub spacing

Clearly, if the distance between the stubs is reduced, thermal bridging will occur in a larger proportion of the area of the envelope and this is likely to reduce the overall thermal resistance of the assembly. The precise effect of reducing stub spacing depends on the location of insulation. In 'warm frame' construction, where all the insulation is on the outside of the frame, there will be very little affect on stub spacing. However, as the proportion of insulation that is located between
The steel framing elements increases, so the impact of reducing stub spacing will increase.
Testing and modelling at ORNL16 has shown that when increasing the stub spacing from 400 mm to 600 mm, the R-value of the assembly increases by up to 25%.
The largest increases are observed for walls with no external insulation outside the steel. Smaller increases of about 15% were observed for walls with 25 mm of EPS sheathing (see Figure (5.6).

Figure 5.6 ***The effect of stud spacing on R-value***

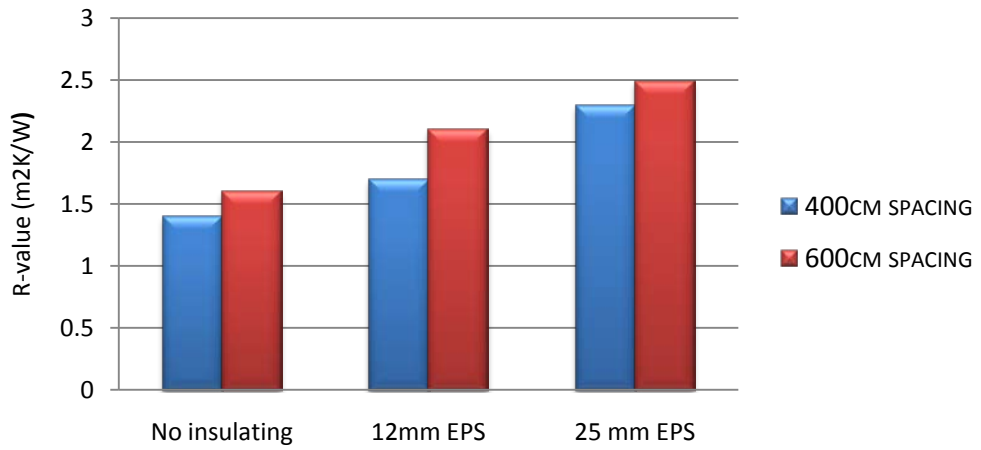

Hot box tests in Japan17 on a light steel frame wall using 89 cm deep steel stubs with mineral wool bulk insulation between, showed that stub spacing for a wall with no insulated sheathing is the most significant of a range of variants tested.

These tests compared the thermal resistance of three walls with stub spacing of 300 cm, 450 cm and 900 cm. It was found that the thermal resistance of the wall with stubs at 300 cm centres was 23% lower than the wall with stubs at 450 cm centres and 56% lower than a wall with stubs at 900 cm centres. Generally, from a thermal point of view, it is advantageous to reduce the amount of framing in the envelope by increasing the stub spacing.

5.3.4 Thermal impact of the steel thickness

Increasing the thickness of the light steel structure elements within a light steel assembly increases the size of the potential bridge. This may lead to an increase in heat loss. BRANZ compared the thermal resistance of two constructions which were identical, except for the thickness of steel used in the light steel structure18. A change of steel thickness from 1.2 mm to 0.8 mm, resulted in an increase in the effective thermal resistance of the steel from 0.041 m2K/W to
0.059 m2K/W. The overall measured wall thermal resistance shown in Table 5.7 indicates that, due to the high conductivity of the steel, there is little impact when reducing the steel thickness. The BRANZ isothermal planes R value calculation method overestimated the impact of steel thickness.

Steel Thickness	**Measured R-value (m2K/W)**	**Calculated* R-value (m2K/W)**
1.2 mm thick steel	1.32	1.26
0.8 mm thick steel	1.34	1.39

Table 5.7 *Comparing the effect of steel thickness*

In Japan, comparisons were carried out of the thermal resistance of walls with stubs of varying steel thickness for a simple steel stub wall with only bulk insulation and no insulating sheathing. Figure 3.2 presents the results of hot box tests.
The results indicate a variation in thermal resistance of up to 11%, depending on the steel thickness used in the stub. However, there is little change in thermal resistance

for thickness from 0.6 mm to 1.4 mm. However, the thermal transmittance increases more significantly when steel thickness is increased from 1.4 mm to 3 mm.

Figure 5.8 ***comparing the heat transmittance of walls assemblies with steel studs of varying steel thickness***

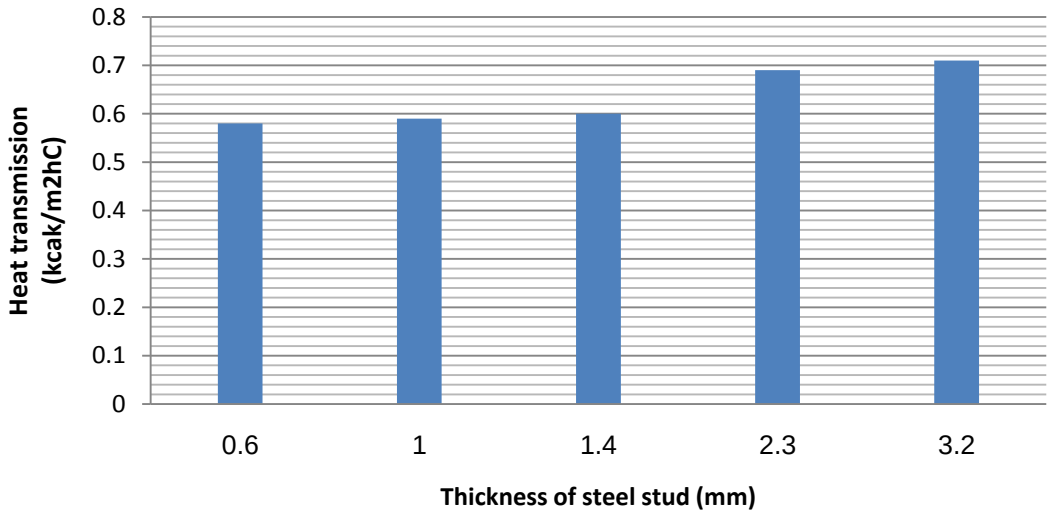

5.3.5 Insulation efficiency

In a variety of tests of thermal resistance of wall with light steel structure it has been found that the addition of an insulating to the assembly results in an increase in measured thermal resistance. For example, Brauns J [30] found that when a 25 mm extruded polystyrene (XPS) sheathing with a nominal thermal resistance of 0.88 m2K/W was added to a steel stub assembly, the overall thermal resistance increased by 0.99 m2K/W. Similarly, when 50 mm thick XPS with a thermal resistance of 1.76 m2K/W was added, the overall thermal resistance of the assembly increased by 1.87 m2K/W.

However, an envelope assembly must be considered in its entirety as a system working together to provide thermal insulation, air tightness and control of moisture (as well as a variety of other functions). The quality of the installation of thermal insulation in a light steel construction envelope assembly is an important factor which

will determine its in-situ performance. A variety of problems can occur due to inappropriate design or incorrect site practices. A poorly designed and built assembly can lead to:

- Increased local internal surface temperatures leading to local condensation and mould growth.
- Increased local heat loss.
- Air movement within or through a structure, possibly leading to interstitial condensation and increased heat loss.
- Convection currents within the assembly due to temperature differences.

5.3.6 ALTERNATIVE ENVELOPE DESIGNS

In all light steel structure construction, it is important to consider the structural elements as a thermal bridge through the construction. Traditional structural assemblies have tended to put thermal insulation in the masonry between the framing elements which then act as a thermal bridge from the inside to the outside of the wall. This leads to areas of reduced thermal resistance and increased heat loss through the structure.

Steel has a far high thermal conductivity, so the impact of the thermal bridges is too great.

The thermal conduction through the stub will cause cold spots to occur on the inner surface of the wall close to the line of the structure; surface condensation and mould growth on interior walls can result.

Furthermore, there may be a risk of interstitial condensation within the construction assembly. Research has shown that in hot climates such as Algerian climate, a lack of sufficient thermal breaks can cause the temperature of the stub to drop below the dew point and moisture may condense within the wall. This can occur in both steel and timber walls but it is perceived as a greater problem in light steel structure assemblies.

Thus, in most climates, creating a thermal break between the steel stub and the cold side of the building envelope is a necessary design requirement for light steel structured assemblies. Many systems place some insulation on the outside of the steel stubs, and various rules of thumb have been proposed for how much insulation should go on the outside of the stubs. Clearly, this depends on the local climate, but there seems to be considerable disagreement about this, even in areas of similar external conditions.

5.3.6.1 THERMAL CAPACITY

Buildings react more or less quickly to the input of heat, depending on their levels of thermal insulation and thermal capacity (mass). Elements with high thermal capacity, such as masonry walls and concrete floors, have greater ability to absorb heat when ambient temperatures are high and cool down slowly when ambient temperatures are cool. Thermal capacity is located principally in the structure and envelope of the building. It can significantly affect thermal performance by absorbing and releasing heat. This characteristic can be employed by designers to help control internal conditions and reduce energy use by allowing excess heat gains during the day to be stored in the thermal capacity until they can be usefully used or dissipated to the cooler night air.

Lightweight structures have limited thermal capacity to store heat, while some finishes, such as carpets and dry linings, tend to isolate thermal capacity from the internal environment and reduce its effect. Increased levels of thermal insulation on the external side of the thermal capacity ensure that stored heat can be more usefully used. Thermal capacity is most beneficial in buildings that have a cooling load, to absorb excess heat gains.

Thermal capacity has not generally been regarded as an important issue in residential buildings, except in areas such as the south European countries and areas of the USA where significant summer cooling is required. In these areas, the traditional forms of construction often use thermal capacity to provide cool interiors and there is a preference for more heavyweight forms of construction.

Where heating loads predominate, thermal capacity does not have a great impact on overall energy use in residential buildings. However, variations can occur depending on the pattern of occupancy. Furthermore, the speed at which a building heats and cools is affected by thermal capacity and so suitable heating and control systems need to be selected.
There is an increasing trend in many countries to install mechanical cooling in dwellings which leads to an increase in energy use. This, together with the concerns about the effects of warmer temperatures resulting from global warming, have led to suggestions that Building Codes should advantage construction systems with some thermal capacity.

5.3.6.1.1 Cooling

The benefit of thermal capacity within a building is that it can absorb some of the unnecessary heat gains that occur within the spaces. These are stored within the structure until the air temperature drops sufficiently that they can be given up to the space. In buildings where significant solar or incidental heat gains occur, or in areas where air temperatures are higher than comfort temperatures for significant periods, a thermally massive building fabric can absorb some of the unwanted gains and so reduce air temperatures.
Furthermore, comfort is affected by the mean radiant temperature of the internal surfaces. If these surfaces remain cool they will emit less radiant heat and absorb radiant heat from occupants and the surroundings. They will also cool the air close to them as it moves over the surface and gives up its heat. Often the occupant perceived temperature is close to the Dry Resultant Temperature which is given by:

Dry Resultant Temperature = (mean radiant temperature + air temperature)/2

Therefore, it is possible for occupants to be comfortable at a higher air temperature when the radiant temperature of the walls and ceiling are low.

This has benefits in an area where cooling may be required, by reducing or eliminating the need for mechanical cooling. It is an accepted phenomenon in office buildings, even in climates such as that of the UK. It is more relevant to office buildings since they generally have higher heat gains from denser occupancy by people, office machines, and solar gains through largely glazed facades. In dwellings, the use of thermal capacity for cooling in cooler regions such as northern Europe, has traditionally been seen as unnecessary and comfort conditions could generally be achieved by natural ventilation. In other areas, where the climate in the hot periods is less comfortable, an increasing number of dwellings now have mechanical cooling or full air conditioning installed. This is an additional energy use usually of expensive electricity. As insulation standards increase in dwellings, incidental heat gains are becoming more relevant and overheating is becoming more of an issue, even in cool climates.

5.3.6.1.2 Heating

During the heating period, it is generally thought that some thermal capacity is useful and helps provide a more robust solution in terms of achieving comfort conditions. However, excessive amounts of thermal capacity can result in higher heating loads and long warm up periods, since much of the initial heat is used to warm the building fabric and the air temperature rises slowly. Similarly, when the heating is turned off, the warmth stored in the building fabric is released, slowing down the rate at which the temperature drops.

In lightweight structures such as light steel-framed dwellings, internal temperatures rise quickly when heating is turned on and fall more quickly when heating is turned off. Since most dwellings are intermittently occupied, this has benefits of rapid response to changing patterns of use. The dwelling can be heated to comfortable temperatures very quickly, which saves on the time required and energy needed to heat a space up. Thus, it is not necessary to set a heating programmer to switch the heating on hours before the building is to be inhabited.

In well insulated dwellings, it may be the case that the heating gains from occupants and appliances in a house will be sufficient to heat a space and provide excess heat. This is particularly true in spaces with high heat gains, such as kitchens. Even on cold winter days, it will often be unnecessary to use a heating system in a kitchen, since the activity within it will heat it sufficiently. In such cases, any thermal capacity present will reduce or prevent overheating by absorbing the excess heat and releasing it during cooler periods. In this way, the excess heat may not be wasted but used during other periods, when required. If there is no thermal capacity present, the heat will have to be ventilated away to prevent discomfort and this will usually become a heat loss.

Furthermore, some thermal capacity within a dwelling can reduce the capacity of the heating or cooling system required to maintain comfort conditions. The mass will reduce the rate of heating and cooling of the structure and so smaller amounts of top up heating (or cooling) are necessary.

5.3.6.1.3 Control of overheating

Precautions are needed to ensure that lightweight dwellings do not overheat, as the absence of much thermal capacity will lead to higher temperatures and create discomfort. Overheating can be caused either by excessive solar and other heat gains particularly in the summer months, or by badly controlled heating systems which continue to give out heat after the demand temperature has been reached.

Thus, control of solar radiation incident on glazing in the summer months is important as are responsive heating systems and controls. Control of solar radiation entering the dwelling can be achieved by attention to details such as orientation, positioning of windows, planting, solar shading devices and solar control glazing. If required, the thermal capacity of light steel framed buildings can be increased to suit different patterns of use, by substituting lightweight floor structures with composite or concrete floors and including mass walls at a suitable point within the structure. A ground floor concrete slab will have considerable impact in reducing overheating, particularly in the ground floor rooms, if it is not insulated from the room space. Furthermore, additional layers of plasterboard can provide significant additional thermal capacity.

5.3.6.1.4 Location of thermal capacity

The way in which thermal capacity is distributed in a building is of great importance to its impact on energy use and comfort. Large amounts of thermal capacity that are insulated from the internal spaces are of little benefit. It is necessary for the mass to have good thermal contact with the space. This means that it should have a large surface area exposed to the internal space and ideally, should not be insulated from the space by insulation or insulating finishes such as carpets, curtains and furnishings.

It is often overlooked that the critical factor governing how much heat can be absorbed by a typical building material is the speed with which the surface can absorb heat (surface resistance to heat transfer). The thermal resistance of concrete and masonry is generally smaller than the thermal resistance of the surface between the masonry and the internal air. Thus, once absorbed, the heat can be dissipated into the material with relative ease. This means that the surface area of the thermal capacity and the degree to which it is distributed around the space, becomes important and a thin layer of mass all around the space may be more helpful than a large concentration of mass in one area.

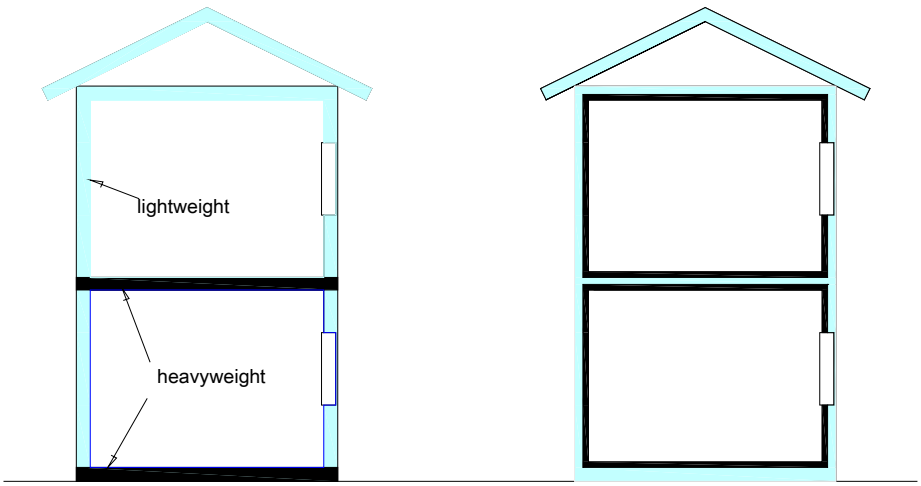

Fig 5.9 Integrate mass into internal walls

5.3.6.1.5 How to integrate thermal capacity

Relatively little analysis has been carried out on the benefits of thermal capacity in steel frame housing. It may be that in many climates, a solid concrete ground floor, plasterboard and furnishings provide sufficient mass. However, there are a number of ways in which thermal capacity can be integrated into light steel framing, when necessary, which may improve performance. These are reviewed below:

5.3.6.1.6 Solid ground floors

Many lightweight steel and timber frame dwellings are built using a solid concrete ground floor. This provides a significant amount of thermal capacity which may be beneficial to comfort and energy use. The detail design of the floor is important, as it is necessary to keep the insulation below the concrete to get full benefit of the mass. Current building practice often places insulation on the top of the concrete ground floor, particularly as suspended pre-cast concrete floors are more widely used. This is detrimental as it insulates the concrete from the space. A floor screed on the insulation will provide some mass but this will be reduced compared with a full concrete slab. There are some limitations to the thermal benefits from solid floors. The positioning of this mass is not ideal as the warmest air will tend to rise to the top of a space, while the cooler air will sink and be in contact with the floor.
Furthermore, the mass is concentrated at the ground floor level and is of little use to spaces in upper floors. Floor finishes are also important and some carpets may create a significant barrier between the space and the mass. A typical 150 mm deep concrete ground floor could provide about 200 kJ/m2K of thermal capacity.

5.3.6.1.7 Solid intermediate floors

Although one of the benefits of light steel framing is that it can provide a dry and lightweight construction process, it is possible to install a concrete floor as an intermediate floor in a dwelling with light steel walls. This provides thermal capacity in the heart of the building with a large exposed surface area from both the top and

bottom. Such a floor can be a composite slab using steel decking with a concrete topping. Alternatively, precast concrete floor units can be used. A typical 150 mm deep concrete floor could provide about 190 kJ/m2K of thermal capacity.
A similar option would be to use a thin steel decking floor supported on light steel floor joists and install a gypsum (or cement) screed of about 75 mm. This is sometimes done to provide a pleasant, more solid surface and to improve acoustic insulation. Such a floor, with a 75 mm thick gypsum screed can provide over 50 kJ/m2K of thermal capacity in the heart of the building.

5.3.6.1.8 Wall linings

The gypsum board lining on walls and ceilings of framed construction provides a significant amount of thermal capacity. A single layer of 12.5 mm gypsum board can provide about 10 kJ/m2K. This is lower than other options, but there is a large area that can be covered generally providing good thermal contact with the space.
Such gypsum boarding can act as an efficient store for excess heat gains. Adding an extra layer of 12.5 mm gypsum board to some walls and ceilings may increase overall available mass significantly. Similarly, using more dense boarding on the floors, such as cement particleboard, can add to the available mass in lightweight construction. Increasingly, Building Regulations now require thicker or double layers of plasterboard for acoustic reasons, particularly on separating and flanking walls. This is helpful in providing increased thermal capacity.

5.3.6.1.9 Phase change material plasterboard

Plasterboards are under development and have been tested which have embedded within them salts which melt when their temperature increases, absorbing heat. On cooling, these "phase change materials" (PCMs) re-crystallise giving off the heat absorbed. Such materials have considerable potential for use in the internal linings of lightweight construction to increase the thermal capacity. In this way, both the benefits of lightweight dry construction and distributed thermal capacity can be realised.

The Japanese WISH house is a light steel frame demonstration building which was constructed as part of an International Energy Agency demonstration scheme37 (see Figure 2.00). It uses PCM thermal storage panels, together with a heat pump to minimise energy use. In this low energy house, 550 kJ of thermal capacity is provided by a 60 m2 of PCM panels with a phase change temperature of 22ºC.
This house has an energy load which is one third of standard dwellings in the same location. This is due to a range of features but the PCM panels are central to the heating strategy for the building.

Unfortunately, PCM gypsum boards are currently not yet widely available.
However, this is a technology which can offer considerable opportunities for the light steel frame industry in the future.

Fig 5.10 The WISH home in Japan

5.3.6.1.10 Integrate mass into internal walls

It is possible to design a dwelling with a lightweight steel frame envelope but to integrate masonry elements with thermal capacity into the internal elements of the

building. Such an approach was taken in the British Steel Demonstration House at the Ebbw Vale Garden Festival in 1992 (see Figure 5.11). This house consists of a light steel frame using the Sure build system with a large south facing conservatory.
To avoid overheating and reduce energy use, masonry walls were included within the insulated envelope as internal partition walls. These walls formed the back wall of the conservatory and also around the fireplace in the living room. They absorb and store excess solar and incidental heat gains. The system was combined with an air to air heat pump and mechanical ventilation to maximise the usefulness of the stored heat.

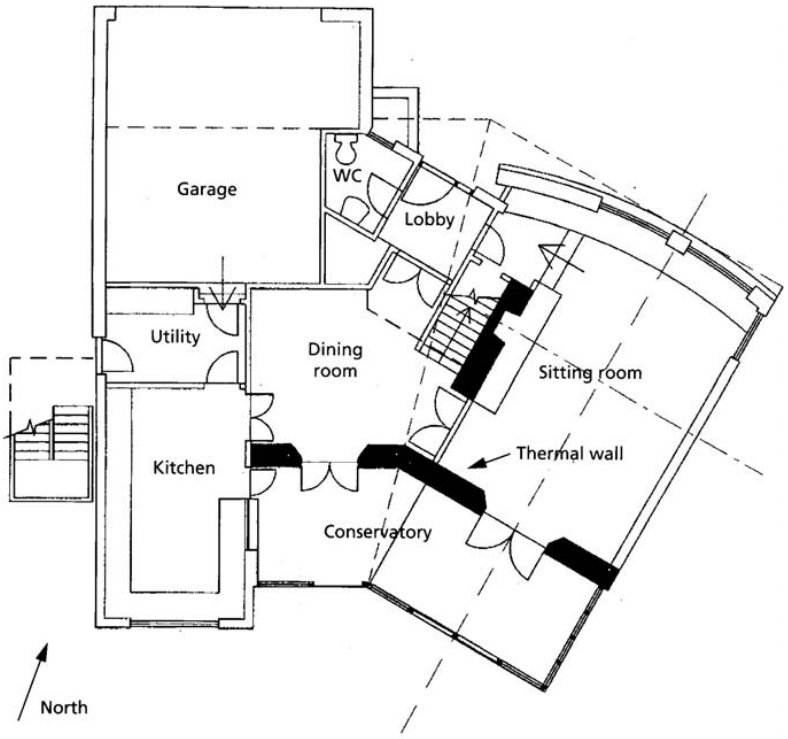

Fig 5.11 The British Steel Demonstration House at the Ebbw Vale Garden Festival with integrated thermal capacity walls in a light steel frame

5.3.6.1.11 Water

Water has considerable benefits as a heat storage medium when compared to building materials such as concrete. It has over four times the specific heat capacity of concrete, which means that it can store considerably more heat per unit of volume.

Furthermore, the convection currents within water mean that the heat can be better distributed within the volume of the fluid. Water can also be easily pumped if necessary so warm water can be moved to a well insulated store for longer term storage.

A recent UK steel house, the "Banham House" in Cambridgeshire by architect Jonathan Ellis Miller, uses a lot of glazing but avoids overheating by incorporating a series of water containers placed in the living space which are warmed directly by solar gains and indirectly by absorbing heat from the space. Thermal modelling apparently showed that the presence of these water containers would avoid overheating in summer, despite considerable solar gains, and reduce energy use for heating in the winter.

Other, similar approaches have been suggested for lightweight houses, including the use of large, oversized radiators which would be full of water and absorb additional heat gains during the summer months. The potential for using water in simple systems is considerable and could readily be modelled using dynamic thermal simulation software.

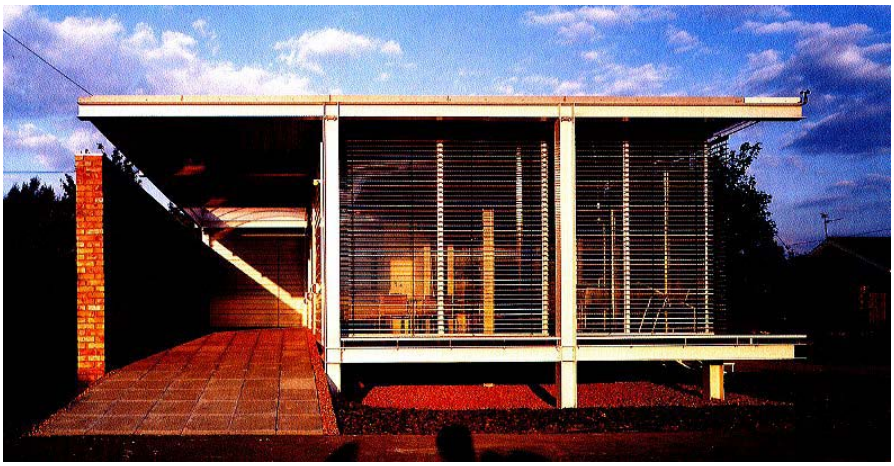

Fig 5.12 The Banham House uses water storage for thermal capacity

Little work has been done to model the performance of the above ideas and to assess their potential for improving the comfort conditions and energy efficiency performance of light steel framing. All the above need comprehensive analysis using dynamic thermal modelling to assess their benefits in various climates, and to optimise their performance.

CHAPTER SIX
CONCLUSION AND RECOMMENDATIONS.

CONCLUSIONS

Empty cold formed and welded steel tubes with a H/t ratio of 50 suffered drastically from local buckling and reached loads below the theoretical steel failure load and increased from 5 to 13% when the weld fillets were located at the middle of the long side of the steel cross section. Composite stubs tested 28 days after casting, behaved well and reached maximum loads beyond or close to the corresponding theoretical failure load. This is a clear indication of the effect of the concrete core and composite steel-concrete action. The weld fillet location did not significantly affect the axial load carrying capacity in composite tubes. The failure mode of the samples was a typical local buckling mode with yielding of the steel and crushing of the concrete. No weld failure was reported in any samples. To understand the post-failure behaviour of the stubs cyclical loading was carried out and results of these tests will be presented in a future work.

There is currently no agreement about R-value calculation methods for light steel framing. The Parallel Path method usually adopted for timber framing is inappropriate for steel framing (it also underestimates the timber frame Rvalue) as it dramatically underestimates the effect of thermal bridging through the steel.

The thickness of steel used in the framing appears to have little impact on the overall thermal resistance of the assembly. However, as the thermal resistance of the assembly increases, for example by fitting insulating sheathing, so the relevance of the steel thickness increases.

The spacing of the steel elements is very important. The greater the spacing the better the thermal resistance. Walls with steel stubs at 600cm centres perform significantly better than those with at 400cm centres. Wider spacing is even more beneficial.

There are still some issues that need attention and careful research if the next generation of light steel framed houses is to be as energy efficient and comfortable as intended. There is therefore much future scope for the use of both heat transfer modelling and dynamic thermal simulation in the optimisation of thermal performance in light steel framed housing design.

Recommendations:

There has been little research into the impact of thermal capacity on comfort conditions and energy efficiency in light steel frame buildings. This is an area of increasing concern due to the increasing use of air conditioners in residential construction. There is potential to improve the design of such buildings by the use of computer simulation techniques to assess the impact of strategically located thermal capacity using, water, gypsum, concrete, masonry or phase change materials.

Airflow within steel frame walls can have very significant detrimental effects to durability and thermal performance. Furthermore, air infiltration through the wall will increase heat loss, risk of condensation and reduce comfort. Increasingly building codes are likely to demand improved standards of air tightness, and questions of durability can legitimately be raised unless air tightness is demonstrated Little research has focused on how best to achieve air tightness in steel framed buildings and the impact of air movement within the construction assembly, including walls, roofs and floors. The air barrier/vapour control layer functions of wall elements need to be considered more closely with service integration and future upgradability

The use of insulating sheathing boards is important to many light steel assemblies. The effect of steel fixings through the insulation needs to be carefully assessed and alternatives considered.

The impact of poorly fitting insulation in steel framing needs to be established, both from the point of view of conduction and convective loops within the wall assembly.

Rules of thumb could usefully be established for different climatic regions about the amount of insulation that should be located on the outside of the steel frame to eliminate the risk of condensation and the risk of ghosting.

References

[1] ASHRAE, 1997. ASHRAE Handbook. Fundamentals American Society of Heating, Refrigerating and Air-Conditioning Engineers, (1997), Atlanta, GA.

[2] B. Chen, J. Liu, Properties of lightweight expanded polystyrene concrete reinforced with steel fiber, Cement and Concrete Research 34 (2004) 1259–1263.

[3] Balcomb J.D, Hedsstrom J.C and Mc Farland R.D (1976): 'Simulation Analysis of Passive Solar Heated Building, Preliminary Results 'Solar Energy', Vol19, (1976) pp277-182.

[4] Brauns J. Analysis of stress state in concrete-filled steel column. J Constr Steel Res 1998;49(2):189–96.

[5] B. Saaba, R.S. Ravindrarajah, Engineering properties of lightweight concrete containing crushed expanded polystyrene waste, Proc. Materials Research Society 1997 Fall Meeting, Boston, 1997.

[6] BEHIM M**.,** « utilisation du laitier de haut fourneau d'El Hadjar en cimenterie », Thèse de Magister, Université d'Annaba – Algérie, 1987, pp 118.

[7] Capderou M.,Atlas Solaire de L'Algerie, Office des Publication Universitaire (O.P.U), Alger 1983.

[8] C. Bonacina, M. Campanale, L. Moro, Analytical and experimental investigations on the heat transfer properties of light concrete, International Journal of Thermophysics 24 (2003) 1407–1414.

[9] CIBSE, Building Energy and Environmental Modelling, CIBSE Applications Manual AM11, Chartered Institute of Building Services Engineers, London, 1998

[10] D.S. Babu, K.G. Babu, T.H. Wee, Properties of lightweight expanded polystyrene aggregate concretes fly ash, Cement and Concrete Research 35(2005) 1218–1223.

[11] CIBS guide A3: 'Thermal properties of building structures' 1980.

[12] D.J. Cook, Expanded polystyrene beads as lightweight aggregates for concrete, Precast Concrete 4 (1973) 691–693.

[13] Djamel Beggas, A passive solar heating model analysis for Algeria, Mphill Thesis (1988) Bath University, United Kingdom.

[14] Djamel Beggas., The use of thermal networks in the thermal analysis of passive solar buildings, proceeding of First U.A.E conference on air conditioning in the Gulf, ACG'96 (1996) p208-215.

[15] F.Allard, C. Inard, A. Roldan., Etude comparative de différentes methods de modélisation des echanges radiatifs de courtes et grandes longueurs d'ondes dans une cellule d'habitations, Annales de l'Institut Technique du Batiment et des travaux publics 442 (1986) 31-60.

[16] F. Blanco, P. Garcia, P. Mateos, J. Ayala, Characteristics and properties of lightweight concrete manufactured with cenospheres, Cement and Concrete Research 30 (2000) 1715–1722.

[17] Georgios G, Dennis L. Axial capacity of circular concrete-filled tube columns. J Constr Steel Res 2004;60:1049–68.

[18] Gilles Fraisse et al: Development of a simplified and accurate building model based on electrical analogy, Energy and building 34 (2002) 1017-1031, Elsevier edition.

[19] H. A. Trethowen & I. Cox-Smith, 1996, Contact resistances in a steel frame wall, Thermal Insulation and Building Environment, Vol.20, October 1996.

[20] H.B. Ji, (2004): A global convergent algorithm for flows in a two-dimensional network, Journal of Computational and Applied Mathematics 167 (2004) 135–146.

[21] Kilpatrick A, Rangan BV. Behaviour of high-strength composite columns. In: Composite construction — conventional and innovative. Innsbruck, Austria; 1997. p. 789–94.

[22] Kilpatrick A, Taylor T. Application of Eurocode 4 design provisions to high strength composite columns. Composite construction — conventional and innovative. Innsbruck, Austria; 1997. p. 561–6.

[23] K.G. Babu, D.S. Babu, Behaviour of lightweight expanded polystyrene concrete containing silica fume, Cement and Concrete Research 33 (2003) 755–762.

[24] K. Miled, R. Le Roy, K. Sab, C. Boulay, Compressive behaviour of an idealized EPS lightweight concrete: size effects and failure mode, Mechanics of Materials 36 (2003) 1031–1046.

[25] Lin-Hai Hana, Guo-Huang Yaoa, Xiao-Ling Zhaob, 'Tests and calculations for hollow structural steel (HSS) stub columns filled with self-consolidating concrete (SCC) ', Journal of Constructional Steel Research 61 (2005) 1241–1269.

[26] Lomas K J, Eppel H et al, Empirical validation of building energy simulation programs, Energy and Buildings 26(3), 1997, 253-276 [27]

[28] J.B Saulnier, A. Alexandre., La modélisation thermique par méthode nodale: ses principes, ses succès et ses limites, Revue Générale de Thermique 280 363-372 (1985).

[29] J. Christian & J. Kosny, 1996, Towards a national opaque wall rating label, Thermal Envelopes VI conference, Florida.

[30] J. Kosny & J. Christian, 1995, Reducing the uncertainties associated with using the ASHRAE zone method for R-value calculations of metal frame walls, ASHRAE transactions, Vol 101, Pt. 2 SD95-5-3.

[31] J. Kosny, J. E. Christian and A. O. Desjarlais, 1997, Thermal Breaking systems for metal stud walls - can metal stud walls perform as well as wood stud walls?, AHRAE Transactions Vol. 103, Part 1, PH-97-5-2.

[32] J. Kosny, T.W. Petrie & J.E. Christian, 1997, Thermal Bridges in Roofs made of wood and light-gauge steel profiles, ASHRAE Transactions, Vol 103, Pt 1, PH-97-5-3.

[33] Kossecka E and Kosny J, Equivalent wall as a dynamic model of a complex thermal structure, J. Thermal Insul. And Bldg Envs, Vol 20, Jan 199

[34] J. ZEGHICHE and K. CHAOUI, 'Experimental behaviour of concrete filled steel tubular columns', Journal of Constructional steel research- Elsevier 2005 /60/1; pp 53-66

[35] J.ZEGHICHE and N. FERHOUNE ‘Experimental behaviour of concrete-filled thin welded steel stubs axially loaded case’, Proceeding of 6th International Conference on steel & Aluminium Structures. 2007, Oxford, UK.

[36] J. ZEGHICHE, ‘Concrete filled steel tubes’, PhD thesis, University of Annaba, Algeria, 2005.

[37] J. ZEGHICHE & all, ‘Résistance des tubes laminés à froid et soudés remplis de béton à base de granulats de laitier’, Séminaire National de Génie Civil, Sidi Belabes, Algeria, 2003.

[38] J. ZEGHICHE, N. FERHOUN,’ Résistance à la compression des tubes laminés a froid et soudés remplis de béton à base de granulats de laitier’, 6éme Séminaire National de la Mécanique, Annaba, Algeria, 2006.

[39] J.ZEGHICHE and N. FERHOUNE ‘Experimental behaviour of concrete-filled thin welded steel stubs axially loaded case’, Proceeding of 6th International Conference on steel & Aluminium Structures. 2007, Oxford, UK.

[40] Ir.L. Balemans., Review of correlations for convective heat transfer from flat surfaces in air. Chaleur et Climats 590 (1987).

[41] Maloney J., Wang T., ChenB. And Thorp J. ‘Thermal Network Prediction of Daily Temperature Fluctuations in Direct Gain Room’. Solar Energy, Vol 29 N°3 pp207-223, 1982.

[42] Mander JB, Priestley MJN, Park R. Theoretical stress–strain model for confined concrete. J Struct Engng ASCE 1988;114(8):1804–48.

[43] M.A. Bradford, H.Y. Loh, B. Uy, ‘Slenderness limits for filled circular steel tubes’, Journal of Constructional Steel Research 58 (2002) 243–252

[44] M. BEHIM. ‘ Sous Produits Industriels et Développement Durable Réactivité, rôle et durabilité des laitiers d’EL HADJAR dans les matériaux à matrice cimentaire’ Thèse de doctorat d’état soutenue en 2005 département de génie civil Annaba.

[45] Mohamed Elchalakania, Xiao-Ling Zhaob,'Concrete-filled cold-formed circular steel tubes subjected to variable amplitude cyclic pure bending', Engineering Structures 30 (2008) 287–299.

[46] Muhammad Naseem Baig, FAN Jiansheng, NIE Jianguo, ‘ Strength of Concrete Filled Steel Tubular Columns’, TSINGHUA SCIENCE AND TECHNOLOGY, Volume 11, Number 6, December 2006, pp657-666.

[47] M. Mouli, H. Khelafi, ‘Strength of short composite rectangular hollow section columns filled with lightweight aggregate concrete’, Engineering Structures 29 (2007) 1791–1797.

[48] Neogi PK, Sen HK, Chapman JC. Concrete-filled tubular steel columns under eccentric loading. Struct Eng 1969;47(5):195–207.

[49] N. Suda, N. Uno, J. Shimizu, R. Kanno & K. Sugita, 1999, Thermal insulation and thermal bridge of steel frame walls, Nippon Steel Technical Report No. 79,January 1999.

[50] O’Shea M, Bridge R. Circular thin-walled tubes with high strength concrete infill. Composite construction in steel and concrete II. Irsee (Germany): ASCE 1996;780–93.

[51] O’Shea MD, Bridge RQ. Design of circular thin-walled concrete filled steel tubes. J Struct Engng ASCE 2000;126(11):1295–303.

[52] R. Le Roy, E. Parant, C. Boulay, Taking into account the inclusions' size in lightweight concrete compressive strength prediction, Cement and Concrete Research 35 (2005) 770–775.

[53] Solha M.S et al ’Solar Building, Science and design’ Pergamon 1986.

[54] S.V SZzokolay' Environmental Science Handbook for Architects and Builders'.Construction Press 1980.

[55] Steel Home Advisor Magazine, published by the American Iron and Steel Institute (www.steel.org).

[56] V.K.R. Kodur, 'Performance of high strength concrete-filled steel columns exposed to fire', Can. J. Civ. Eng. 25: 975–981 ,1998.

[57] T.Y. Chen, A method for the direct generation of comprehensive numerical solar building transfer functions, Solar Energy 74 (2003) 123–132.

[58] W.C. Brown, M.C. Swinton & J.C.Haysom, 1998, A technique for calculating the effective thermal resistance of steel stud walls for code compliance, ASHRAE Transactions Vol. 104, Pt. 2.

[59] www.eren.doe.gove/buildings/tools_directory/software

[60] You-Fu Yang, Lin-Hai Han,' Experimental behaviour of recycled aggregate concrete filled steel tubular columns', Journal of Constructional Steel Research, (article in press, 2006).

[61] You-Fu Yang, Lin-Hai Han, 'Experimental behaviour of recycled aggregate concrete filled steel tubular columns', Journal of Constructional Steel Research 62 (2006) 1310–1324.

[62] Z.M.Bassam and S.G. Emhaidy,' Enhancing Filled-tube Properties by Using Fiber Polymers in Filling Matrix', Journal of Applied Sciences 5 (2): 232-235, 2005.

[63] Zhong Taoa,_, Lin-Hai Hanb,c, Dong-Ye Wanga, 'Strength and ductility of stiffened thin-walled hollow steel structural stub columns filled with concrete', Thin-Walled Structures, 2008.

[64] P.K. Gupta_, S.M. Sarda, M.S. Kumar Journal of Constructional Steel Research 63 (2007) 182–193